Developing and Improving Assays to Detect Autoantibodies in Well Phenotyped Small Fiber Neuropathy and Fibromyalgia Syndrome Patients

Evanka Singh, MSc by Research

St Cross College, University of Oxford

Oxford Autoimmune Neurology Group

Nuffield Department of Clinical Neuroscience

Michaelmas 2026

Table of Contents

Abstract

Small Fiber Neuropathy (SFN) is one of the most cryptogenic etiologies of chronic neuropathic pain and over 40% are said to idiopathic. Recently, Autoantibodies (AAbs) against specific targets have been identified in SFN including those against FGFR3, Plexin D1, TS-HDS, and MX1. More recently, FGFR3 AAbs were found in Fibromyalgia Syndrome (FMS) patients as well, a chronic pain disorder wherein some patients also have small fiber pathology. Assays have been developed to detect these autoantibodies, like Enzyme-Linked Immunosorbent Assays (ELISAs) and Cell-Based Assays (CBAs). This Master's thesis has used a cohort of 72 well-phenotyped SFN patients and 53 FMS patients to detect AAbs against intracellular FGFR3, Plexin D1, and MX1. In terms of assays, ELISAs, CBAs, and a novel concept of "carry-on" CBAs were developed. The "carry-on" CBA expressed the intracellular epitope of FGFR3 outside the cell and the same concept was used for full-length intracellular MX1. The carry-on CBA found 12.5% seropositivity for anti-intracellular FGFR3 IgG in the SFN patient cohort and 13.2% seropositivity in the FMS patient cohort. Lower rates of 6.4% and 3.8% were observed in the ELISA for SFN and FMS patient cohorts respectively. In both cohorts, 0% seropositivity was found for anti-MX1 IgG using the "carry-on" CBA and 0% seropositivity was found for anti-Plexin D1 IgG using the standard CBA. When associated with phenotypes, the significant differences observed in SFN patients seropositive for anti-intracellular FGFR3 were that their symptoms were less chronic (less than 5 years, $p = 0.0238$) and there were fewer seropositive patients with tingling pain that in seronegative patients ($p = 0.0257$). In FMS patients, the only significant difference was that the duration of symptoms was shorter for seropositive patients than seronegative patients ($p = 0.0113$). Thus, a clinically distinct group of SFN and FMS

patients were found who are anti-intracellular FGFR3 IgG seropositive with a shorter duration of chronic pain symptoms.

Chapter 1: Introduction

1.1 Background

Pain

Pain is an adaptive signaling system that acts to protect the organism from severe injury or worsen an already existent injury (Finnerup et al., 2021). Thus, pain is a crucial sensory component of life, without which the human life expectancy is significantly reduced, as is seen in patients with Congenital Insensitivity to Pain and Anhydrosis (CIPA), who in most cases do not live past the age of 25 years (Daneshjou et al., 2012). According to a recent amendment by the International Association for the Study of Pain (IASP) in 2020, the definition of pain is,

"An unpleasant sensory and emotional experience associated with, or resembling that associated with, actual or potential tissue damage".

This pain experience is brought about by a stimulus, which can be mechanical, chemical, or thermal, and activates primary sensory nerve endings called nociceptors that initiate the pain sensation and project to intermediary spinal and medullary dorsal horns for the eventual transmission to the brain for its perception (Sneddon, 2018). Thus, nociception is the detection of such noxious stimuli while pain describes the emotional and subjective sensation resulting from nociception (Mischkowski et al., 2019). There are two major nociceptive fiber types, thinly myelinated A-delta fibers and unmyelinated C fibers (Sneddon, 2018). A-delta afferent fibers are fast conducting and are of two types: high threshold fibers responsive to high-intensity mechanical stimuli (mechanosensitive) and fibers that respond to both mechanical and thermal stimuli (mechanothermal) (Miko and Varga, 2015). These sensory afferents are known to carry fast, sharp pain also known as *first pain* (Miko and Vargas, 2015). On the other hand, C afferent fibers carry slow, dull pain sensations and is also involved in the autonomic nervous system (Kuner and Kuner, 2021). They are polymodal and are responsive to a multitude of noxious

stimuli including mechanical, chemical, and thermal stimuli; they are most often associated with a burning sensation of pain, but it must be noted that not all C fibers are nociceptors (Khalid and Tubbs, 2017; Bennett et al., 2019). These primary sensory afferents have their cell bodies in the dorsal root ganglia (DRG) and thus, this is a key component in the anatomy of pain signaling (Esposito et al., 2019; Kuner and Kuner, 2021). Moreover, the DRG houses the cell bodies of up to 15,000 primary sensory neurons (Esposito et al., 2019). Overall, nociceptors are a vital component of the pain signaling system and the detection of tissue injury.

Neuropathic Pain

When pain occurs long-term it can be debilitating. Such pain lasting over 3 months persistently or recurrently is considered to be chronic pain (Treede at al., 2015). It is said that between one-third and one-half of the United Kingdom population suffers from chronic pain, resulting in a lower quality of life and parallel negative socioeconomic outcomes (Fayaz et al., 2016). Neuropathic pain is a form of chronic pain wherein there is damage or disease to the somatosensory system and is a major issue globally, affecting 3% - 17% of the population, more commonly women as they make up 60.5% of neuropathic pain patients (Baskozos et al., 2023; Finnerup et al., 2021). Treating neuropathic pain with conventional analgesics alone is difficult due to moderate efficacy and adverse effects that limit doses (Thouaye and Yalcin, 2023). Understanding the pathogenesis behind neuropathic pain is important, however, there are some patients with neuropathic pain of idiopathic mechanisms and so there is no gold standard of treatment. Neuropathy, a general term for nerve damage, is a contributor to neuropathic pain but it must be noted that neuropathies do not always lead to neuropathic pain, as damage can occur to non-sensory neurons and sensory nerve damage does not always activate pain pathways

(Jensen et al., 2021). Overall, there is a pressing need to understand the mechanistic causes of neuropathies to develop better therapeutics and diagnostic tools as it is well-accepted that peripheral neuropathies are under-diagnosed (Chaudhary et al., 2021). This under-diagnosis is due to several reasons including a great diversity in the range of symptoms that can be difficult to detect and standardise as well as the complexity of comorbidities since many patients develop peripheral neuropathies as a consequence of other disorders, like diabetes mellitus (Lehmann et al., 2020).

With regards to understanding neuropathic pain as a patient experience, there are signs like allodynia wherein patients feel pain from stimuli that do not normally invoke nociceptive pain, hyperalgesia such that there is a heightened pain experience or lower threshold for pain, and paresthesia which involves a spectrum of pain experiences like tingling, itching, or a loss of sensitivity (Cavalli et al., 2019). These symptoms correlate to the function of sensory afferents in the peripheral nervous system. This dysregulation of the pain experience is collectively termed as pain sensitization due to maladaptive plasticity and can be mediated by the phosphorylation of ligand gated ion channels, like the transient receptor (TRP) channels, that translate a pain signal into an electric current and is induced by inflammatory cytokines (Pinho-Rebeiro et al., 2018; Bennett et al., 2019). Additionally, there can be changes in voltage gated sodium channels, like Nav1.7, that are also key components in relaying noxious stimuli. Pain sensitization is also brought about by transcriptional changes in DRG sensory neurons that upregulate noxious molecular transducers and reduce the activation threshold for action potential firing (Pinho-Rebeiro et al., 2018).

Immune System and Neuropathic Pain: Autoantibodies

It is widely accepted that the immune system can contribute to neuropathic pain, as supported by evidence from preclinical studies (Lacagnina et al., 2024). One arm of this neuroimmune interaction that has gathered recent interest and is supported by both clinical and preclinical observations is that of autoantibodies, in particular those that target antigens within the nervous system (Dawes et al., 2019). Damage to neurons can lead to dysfunction in action potential regulation, resulting in hyperexcitability of neurons to noxious stimuli and a subsequent painful phenotype. With regards to the development of autoantibodies against specific proteins, these targets can be present in functionally significant regions of the neural surface, like myelin, or in other neuron-like cell types such as glia (Farah et al., 2025). Specifically, there are a few key antigen proteins targeted by autoantibodies (AAbs) identified in patients with neuropathic pain, examples include Leucine-rich Glioma-Inactivated 1 (LGI1) and Contactin-Associated Protein 2 (CASPR2) (Farah et al., 2025; Ramanathan et al., 2021; Helyes et al., 2019; Dawes et al., 2018; Irani et al., 2010). In addition to the discovery of autoantibodies against specific protein antigens, there are several points of evidence that support the role of autoantibodies as drivers of neuropathic pain.

a) Immunotherapy

Neuropathic pain has been shown to be reversed when patients are given immunotherapy, like intravenous immunotherapy (IVIg), highlighting the causal influence of these AAbs on neuropathic pain (Finsterer & Scorza, 2022). For example, LGI1-AAb positive patients with predominantly length-dependent pain, showed a marked improvement of pain ratings on questionnaires after treatment with mostly prednisone, a corticosteroid, and IVIg or plasma

transfer (Ramanathan et al., 2021). Additionally, patients with AAbs targeting CASPR2 and Glycine receptors have also shown improvement of disease outcomes upon treatment with immunotherapy, including high dose intravenous steroids and plasma transfer (Cornacchini et al., 2025; Soleimani et al., 2023). This is because such treatments have an impact on the function of these AAbs; as steroids act as immune suppressants, plasma exchange removes and replaces these AAbs with donated plasma, and IVIg acts as not only a replacement therapy but also as an antagonist to clear out AAbs via functions like Fc gamma receptor (Fc$\boldsymbol{\gamma}$R) activation blockage and T regulatory cell surge (Danieli et al., 2025).

b) Passive transfer models and immunisation models

In line with understanding whether autoantibodies are drivers of pathogenicity in neuropathic pain, there is evidence that shows injecting purified IgG from neuropathic pain patients into mice produces a pain phenotype (Farah et al., 2025). For example, the injection of anti-CASPR2 IgG mimicked a significant increase in mechanical hypersensitivity due to a reduction in CASPR2 surface proteins and Kv1.1 ion channel subunits in the axons of peripheral sensory neurons (Dawes et al., 2018). Thus, immunisation models as additional tools to passive transfer models can be used to further validate the pathogenicity of AAbs; for example, injecting patient anti-CRMP5 AAbs into rats resulted in mechanical hypersensitivity and was furthered using a DNA-based immunisation model to produce anti-CRMP5 AAbs, a biomarker of paraneoplastic neurological syndromes, in rats that also resulted in a painful phenotype (Martin et al., 2024).

1.2 Small Fiber Neuropathy

a) Clinical Overview

Small Fiber Neuropathy (SFN) is a type of peripheral sensory neuropathy affecting small, thinly myelinated and unmyelinated fibers, A-delta and C nerve fibers respectively, and is relatively common with a prevalence of 53 – 130 cases per 100,000 people globally (Peters et al., 2013; Bitzi et al., 2021). Pain, especially length-dependent pain, is the hallmark of SFN including paresthesia wherein the pain includes a "tingling" or burning sensation starting at the limbs and is often accompanied with dysautonomia (Devigili et al, 2020). That being said, there can be difficulty in the diagnosis of SFN since a proportion of patients may present with non-length dependent pain or no pain at all, with SFN considered to be significantly underdiagnosed (Terkelsen et al., 2017). Currently, there is no gold standard of diagnosis and thus a combination of two to three techniques are used. These include checking for reduced intraepidermal nerve fiber density (IENFD) of the distal leg assessed using a skin biopsy; clinical examination including family history to rule out genetic etiologies, motor deficits, sensation deficits, deep tendon reflexes, etc.; quantitative sensory testing (QST), which is a psychosocial test of pain thresholds; other questionnaires may be administered such as Douleur Neuropathique 4 (DN4) and Small Fiber Neuropathy - Symptom Inventory Questionnaire" (SFN-SIQ) for pain intensity ratings (Devigili et al., 2020).

Importantly, there are several etiologies of SFN, predominantly metabolic and toxin-mediated, making both the diagnostic criteria and treatment difficult. Diabetes mellitus, both type 1 and 2, is often associated with many different forms of neuropathies due to multisystem dysfunction, wherein at least 50% of patients develop diabetic neuropathy (Feldman et al, 2019; Rosenberger et al, 2020). Genetic etiologies of SFN include those involving mutations to genes for sodium ion channels like SCN9A, SCN10A, and SCN11A (Chan et al, 2023). SFN can also be infectious and autoimmune mediated as seen in SFN cases that are comorbidities from

Sjogren's and sarcoidosis (Raasing et al., 2025; Seeliger et al., 2023). However, about 50% of SFN cases are idiopathic (iSFN) wherein SFN is not secondary to another disorder (de Greef et al, 2018). Recent literature supports that many of these idiopathic cases could actually be autoimmune with the involvement of autoantibodies (Fujii et al., 2021; Antoine et al., 2015). This furthers the need for better diagnostic tools for SFN as those with idiopathic or autoimmune SFN tend to have non-length dependent pain that presents as a patchy, asymmetrical phenotype (Gemignani et al, 2022; de Greef et al., 2018). Moreover, identification of AAb targets in SFN could provide a useful tool to stratify SFN patients who may respond to immunotherapy.

b) Autoantibody targets in Small Fiber Neuropathy

TS-HDS and FGFR3

Prevalence

Trisulfated heparin disaccharide (TS-HDS) is a disaccharide component of glycosylated heparin and is located ubiquitously, 6.5 – 28% of idiopathic SFN patients are positive for AAbs against TS-HDS and have been found in sensory and sensorimotor polyneuropathies as well (Trevino and Novak, 2021; Levine et al., 2019; Pestronk et al., 2012). Additionally, 15 – 17% of idiopathic SFN patients have tested positive for fibroblast growth factor 3 (FGFR3), which is a transmembrane protein with intra- and extracellular components (Murin et al., 2024; Zeidman et al., 2024; Gibbons et al., 2023; Trevino and Novak, 2021; Zeidman and Kubicki, 2021; Zeidman et al., 2021; Levine et al., 2020; Tholance et al., 2020; Levine et al., 2019). Interestingly, TS-HDS functions as a linker of extracellular proteins, including the extracellular epitope of FGFR3,

and contributes to its role in nerve homeostasis (Devigili et al., 2025). FGFR3 has several functions depending on the tissue type its located in, in nerves FGFR3 is involved in axon development and nerve regeneration (Nagarajan et al., 2021).

Correlation to clinical phenotype

Patients with anti-FGFR3 AAbs, specifically the intracellular epitope, tend to have non-length dependent pain (89%) and are predominantly female (74%) (Nagarajan et al., 2021; Tholance et al., 2020; Levine et al., 2019; Antoine et al., 2015). The only study looking at ethnicity found a higher frequency of Brazilians with anti-FGFR3 IgG as compared to Europeans (36% v 13%), marking a need for a more diverse sample to better understand the difference in prevalence in different ethnicities (Tholance et al., 2020). Patients with anti-FGFR3 AAbs have been explicitly stratified to have a 'distinct' clinical phenotype of SFN, with higher neuropathic pain ratings, which was supported by the majority having abnormal sural sensory nerve action potentials (SNAPs), and fewer systemic comorbidities (Salih et al., 2025).

SFN patients with AAbs against TS-HDS have been observed to have a predominantly distal and symmetric sensory nerve function loss and 66% of them had paraesthesia (Pestronk et al., 2012. In a larger cohort of 155 patients with iSFN, 37% had TS-HDS AAbs and were significantly more frequent in females, along with a non-length dependent pattern of pain that was acute onset (Levine et al. 2020). In a cohort of 322 idiopathic SFN patients, 28% of patients had TS-HDS-Abs and this seropositivity was associated with autonomic dysfunction (Trevino and Novak, 2021)

Preclinical Studies

There are no *in-vitro* or *in-vivo* studies that have tested the pathogenicity of anti-TS-HDS AAbs. However, it must be noted that AAbs against TS-HDS are of the IgM class and thus, are less associated with pathogenicity and are very strong complement activators making cell-based assays very difficult due to the death of HEK293T cells (van de Mortel et al., 2024; Peter Isaac Lobo, 2016). However, there was a recent study on the pathogenicity of FGFR3, wherein a local transfer model was administered with patient anti-FGFR3 AAbs injected into peripheral nerve terminals in the hindpaw skin of rats (Salih et al., 2025). Paw withdrawal thresholds from von Frey filament tests measured tactile (mechanical) hypersensitivity, which was significantly heightened in this model. This was mechanistically studied to find that anti-FGFR3 AAbs can detect their antigen within the DRG, also confirming the presence of FGFR3 in nociceptive sensory neurons which was validated using RNAscope (Salih et al., 2025). Moreover, whole-cell patch-clamp recordings on DRG neurons showed a direct effect between sensory neuron exposure to anti-FGFR3 AAbs and increased action potential firing of those sensory neurons, supported by a marked reduction in rheobase (Salih et al., 2025). However, there are limitations in this paper including the fact that patient sera was used instead of purified IgG, making causal inferences impossible it is unknown its FGFR3-IgG specifically that is causing the painful phenotype or some other serum component. Additionally, this paper found that while previous evidence has shown that these patients have IgG against the intracellular epitope of FGFR3, there are also patients with IgG against the extracellular epitope of FGFR3; however, the clinical difference between patients with IgG against the intra- and extra-cellular components of FGFR3 remains unexplored (Salih et al., 2025). Patients with IgG against the intracellular component of FGFR3 target the tyrosine kinase domains (TKD) of the protein that are essential in FGFR3 function (Tholance et al., 2021). Additionally, a preprint paper failed to demonstrate FGFR3

mRNA expression in human DRG neurons upon in situ hybridisation but did demonstrate expression in human spinal cord making the pathogenicity of IgG against FGFR3 unclear with a possibility of indirect mechanisms involved (Chamessian et al., 2025). But it must be noted that even if these IgG are not pathogenic, they have been suggested to serve as biomarkers for dysimmunity in SFN (Moritz et al., 2020).

Plexin D1

Prevalence

Similarly, Plexin D1 is another protein autoantigen in SFN patients and is a transmembrane protein with an extracellular domain, with its main substrate being semaphorin 3E; this SEMA-Plexin complex mediates immune and nervous system development among other functions, which includes synapse formation and axonal growth (Murin et al., 2024). The overall prevalence of anti-Plexin D1 AAbs is 12.7 – 20.8% in SFN patients (Zeidman et al., 2024. 2022, 2021; Fujii et al., 2021). Plexin D1 AAbs have also been associated with other conditions including multiple sclerosis (MS), atopic myelitis, erythromelalgia, neurosarcoidosis, and Neuromyelitis Optics Spectrum Disorder (NMOSD), as well as a few healthy controls (Fujii et al., 2021).

Correlation to clinical phenotype

With regards to clinical characteristics of anti-Plexin D1 IgG positive patients, they are skewed to a higher frequency of female patients and younger onset neuropathic pain, similar to anti-FGFR3 IgG patients; however, clinical phenotype correlation studies for anti-Plexin D1 IgG positive SFN patients have only been done on small cohorts (Murin et al., 2024; Fujii et al.,

2018). These AAbs specifically bind to unmyelinated pain-responsive sensory DRG neurons (Fujii et al., 2018). A retrospective study analysing anti-Plexin D1 IgG in putative SFN patients found that 15% of the idiopathic SFN (iSFN) patients were positive for these AAbs and had a high prevalence of pricking pain 21.8% than seronegative patients (Fujii et al., 2021). However, this study found that seropositive patients had a longer disease duration as compared to other studies (Fujii et al., 2021; Fujii et al., 2018). Moreover, in a newer study, the prevalence of these AAbs in idiopathic SFN was lower at 9% (Zeidman et al., 2022). Additionally, seropositive patients are also more likely to have allergies that could increase autoantibody production (Fujii et al., 2019). However, these AAbs are not specific SFN as they have been found in atopic myelitis as well (Kira et al., 2025)

Preclinical Studies

An *in-vivo* study using purified anti-Plexin D1 IgG demonstrated specific binding to unmyelinated DRG neurons in mice and led to pathogenicity in the form of thermal and mechanical hypersensitivity as compared to IgG from healthy controls (Fujii et al., 2021). The authors believe the mechanism of pathogenicity to be cytoskeleton activation mediated cell death of DRG neurons, however, this mechanism has not been further explored (Fujii et al., 2018). IgG1 and IgG2 against Plexin D1 have shown pathogenic potential from their binding to DRG neurons that caused cell membrane permeabilization and cell swelling (Fujii et al., 2018). Thus, the authors proposed that this IgG is involved in cell death via the role of Plexin D1 in cytoskeleton activation, however, this hypothesis was never tested. Moreover, transfer of Plexin D1-IgG caused thermal and mechanical hypersensitivity in mice (Fujii et al., 2022).

MX1

Prevalence

MX1, or interferon-induced GTP-binding protein MX1, has been extensively studied as an antiviral protein with its involvement in the cell defence response during innate and adaptive immune function of any cell type involved in these immune branches (Chan et al., 2022). While MX1 has not been studied in the context of pain neuroscience before, it has been associated with TRPC6, a receptor-activated non-selective calcium ion channel (Lussier et al., 2005). This autoantigen target was identified using a protein array screening platform called *Sengenics* and anti-MX1 AAbs were found to be significantly higher in SFN patients compared to healthy controls, but particularly so in iSFN patients making this is a target of interest in diagnosing iSFN (Chan et al., 2022). Other targets, KRT8 and DBNL, were also identified by this platform but there was no significant difference between the secondary SFN (sSFN) patients and iSFN patients (Chan et al., 2022). With regards to the prevalence of AAbs against these targets, there are no robust studies, however, a recent paper found a seropositivity rate of 8 – 12% for anti-MX1 IgG out of 59 definite, skin-biopsy validated SFN patients (Chan et al., 2025).

Pathogenicity and correlation to clinical phenotype

In the same study mentioned earlier, pathogenicity of anti-MX1 IgG was assessed using several methods. Patient sera positive for anti-MX1 IgG did not cause any change to DRG physiology, but MX1 over-expression in murine DRG resulted in significant depolarisation that could lead to sensory neuron hyperexcitability (Chan et al., 2025). However, the mechanism by which the overexpression of MX1 causes hyperexcitability of DRG neurons was not elucidated. Thus, the pathogenic role of anti-MX1 IgG remains unclear.

c) Response of AAb seropositive patients to immunotherapy

Case reports have found that immunotherapy, such as IVIg and subcutaneous immunoglobulin, and immune-suppressing agents like corticosteroids have shown reductions in SFN-associated pain symptoms and halting treatment led to a relapse of these symptoms (Pindi Sala et al., 2020; Dabby et al., 2006). Case reports have progressed to larger clinical trials using IVIg that found 76% of sarcoidosis-associated SFN patients showed symptom improvement after treatment (Tavee et al., 2017). Moreover, a more targeted immunotherapy, like rituximab which is a monoclonal antibody that targets the gatekeeping CD20 receptor on B cells, resulted in improved pain scores in autoantibody-associated SFN patients (Chan et al., 2025). In terms of AAb-specific SFN, a retrospective analysis with iSFN patients positive for FGFR3-IgG and/or TS-HDS-IgM showed an improvement in IENFD and reduction in pain symptoms with IVIg and plasma transfer (Olsen et al., 2022; Zeidman and Kubicki, 2021). Similar results were observed for a case series of patients with FGFR3-IgG and TS-HDS-IgM where one patient was given IVIg and showed subsequent improvement in pain severity (Bayraktutar et al., 2022). Another retrospective study that included Plexin D1-IgG positive patients along with FGFR3-IgG and TS-HDS-IgM positive patients given corticosteroids or Fremanezumab showed improvement in pain and IENFD, but was not significant due to small sample size (Zeidman et al., 2022). Moreover, a randomized, placebo-controlled, double-blind study investigating the effects of IVIg on iSFN patients showed no significant effect (Gibbons et al., 2023). Thus, whether autoantibody seropositivity in SFN correlates to positive immunotherapy response in relation to pain scores remains unclear.

Target of Autoantibodies	Subcellular Location	Pathogenicity	Supporting Evidence
FGFR3	Transmembrane	Passive transfer model Response to immunotherapy (IVIg, corticosteroids, monoclonal antibodies, plasma transfer	Salih et al., 2025 Chan et al., 2025 Gibbons et al., 2023 Zeidman et al., 2022 Bayraktutar et al., 2022 Olsen et al., 2022 Zeidman and Kubicki et al., 2021
TS-HDS	Extracellular	No passive transfer model done Response to immunotherapy (IVIg, corticosteroids, monoclonal antibodies, plasma transfer	Gibbons et al., 2023 Zeidman et al., 2022 Bayraktutar et al., 2022 Olsen et al., 2022 Zeidman and Kubicki et al., 2021
Plexin D1	Transmembrane	Passive transfer model Response to immunotherapy (IVIg, corticosteroids, monoclonal antibodies, plasma transfer	Gibbons et al., 2023 Zeidman et al., 2022 Fujii et al., 2021
MX1	Intracellular	Passive transfer model Functional tests	Chan et al., 2025
KRT8	Intracellular	Not done	-
DBNL	Intracellular	Not done	-

Table 1*:* Identified targets of autoantibodies in Small Fiber Neuropathy with their location, studies on their pathogenicity, and the references for the pathogenicity studies.

1.3 Fibromyalgia Syndrome

a) Clinical Overview

Fibromyalgia Syndrome (FMS) is a chronic pain disorder, characterised by widespread pain. It is a complex disorder with conflicting pathophysiology that is also associated with central nervous system (CNS) dysfunction like sleep disturbances and fatigue (Wolfe and Rasker, 2021). It is a nociplastic pain disorder, but has features associated with neuropathic pain, including the association with small fiber pathology (Falco et al., 2024). It has a prevalence of ~2% globally, with probable underdiagnosis due to heterogeneity in symptoms and poorly understood pathology (Siracusa et al., 2021). Currently, diagnosis is made solely based on clinical evaluation using the American College of Rheumatology criteria such that there is: widespread pain, at least three consecutive months with pain, and *"pain points"* with digital palpation; no biomarker assays exist for FMS due to a lack of significant evidence of such (Siracusa et al., 2021). Overall, it is widely agreed that there is widespread pain amplification in FMS involving components of the CNS, but also the PNS e.g., A-delta and C fibers, and there are suggestions that neuroinflammation plays a role (Grayston et al., 2019; Uceyler et al., 2015).

b) Secondary Small Fiber Neuropathy in FMS Patients

Over the last decade, research has shown that a large proportion of FMS patients also present with SFN or small fiber pathology (Martínez-Lavín, 2018). More specifically, 20% of FMS patients were found to have reduced sensory nerve fiber density and neuropathic pain and a meta-analytical study found that 49% of FMS patients have some sort of small fiber pathology (Dumolard et al., 2023; Grayston et al., 2019).

c) Autoantibody Targets in Fibromyalgia Syndrome and their relevance

The pathophysiology of FMS remains under debate, but one side of this debate is that some FMS cases are of autoimmune etiologies (Clauw et al., 2024). The most comprehensive sources of evidence of this claim are the induction of mechanical and thermal hypersensitivity upon injecting mice with IgG from FMS patients and the identification of specific autoantibodies in FMS patients (Israel et al., 2025; Seefried et al., 2025; Krock et al., 2023; Goebel et al., 2021).

Passive Transfer Model

It has been found that passive transfer of IgG from FMS patients causes mechanical and thermal hyperalgesia via the sensitisation of Aβ fibers in mice both *in vivo* and *ex vivo* (Israel et al., 2025). Another passive transfer model, with a number of tests like the Randall-Selitto paw-pressure test for mechanical hypersensitivity and noxious cold stimuli tests for thermal hypersensitivity were administered (Goebel et al., 2021). The heightened thermal and mechanical hypersensitivity was not dose-dependent on serial volumes of purified IgG, instead the effect saturated at the first dose of 8mg itself; it may have been worth to try lower dosages of IgG to check for a dose-dependent relationship between IgG levels and this clinical hypersensitivity phenotype (Goebel et al., 2021). Apart from pain, other FMS characteristics were mimicked by these mice like locomotor disturbances, lower intraepidermal fiber density, and reduced grip strength. Moreover, IgG from these patients bound to multiple cell types, with particularly high colocalisation with satellite glia cells, in mouse DRG as well as in human DRG (Goebel et al., 2021).

Specific Autoantibody Targets in FMS

Considering the cell-type with the highest colocalisation with purified IgG from FMS patients were satellite glia cells (SGCs), this correlation was further explored to find SGC-specific autoantibodies using a murine cell culture assay (Krock et al., 2023). Anti-SGC AAbs in specific

were found to be pronociceptive, putting SGCs as targets of interest for potentially autoimmune mediated FMS (Berwick et al., 2025). Additionally, there was a recent study that not only replicated the passive transfer model but also found specific autoantibody targets in FMS patients, which were anti-citrullinated peptide AAbs, anti-SOX1 AAbs, anti- 5HT1AR AAbs, and most interestingly anti-FGFR3 AAbs (Seefried et al., 2025). Moreover, tissue specific autoantibodies (TSAs) associated with early-stage Sjögren's syndrome were also found in FMS patients (Applbaum and Lichtbroun, 2019). Overall, the case for the existence of specific autoantibodies in FMS patients is well supported with reason to further investigate this.

1.4 Rationale and Aims

Rationale

Enzyme-Linked Immunosorbent Assays (ELISAs) have been developed to detect AAbs against FGFR3, TS-HDS, and Plexin D1 (Malik et al., 2019; Fujii et al., 2019; Antoine et al., 2015). More recently, an ELISA and a Cell-Based Assay (CBA) were developed to detect AAbs against MX1 as well (Chan et al., 2025). Thus, tools to detect such AAbs are important in understanding their role in SFN and FMS as well as to find patient eligibility for immunotherapy. These assays, however, have not been used on large idiopathic SFN patient cohorts that have been well clinically phenotyped. Therefore, this project will determine whether these assays can be further optimized and replicated with in-house materials to develop AAb detection assays that are also cost effective. Additionally, the growing evidence that SFN occurs in some FMS patients provides rationale for the investigation of these AAbs in FMS as well (Dumolard et al., 2023; Grayston et al., 2019; Martinez-Lavin et al., 2018). For this project, only IgG specific antigens that are significant in iSFN were investigated, so FGFR3, Plexin D1, and MX1. TS-HDS-IgM

was not explored due to its widespread prevalence in other non-SFN related conditions, its lack of pathogenicity, and its potent activation of the complement signaling cascade as discussed earlier in the chapter.

Aims

a) To develop and improve detection assays against specific targets in SFN
b) To correlate specific autoantibody presence with clinical phenotypes in SFN and FMS patients

Chapter 2: Assay Development

2.1 Introduction

a) Current assays for autoantibody detection in peripheral neuropathies

Considering the importance of autoantibodies in SFN, it's crucial to understand how these specific targets of AAbs were identified. There are multiple techniques to detect antibodies but all of them make use of the core concept of protein-protein interactions between the antibody and antigen, it's the way that this is visualized and/or quantified that differs between techniques. Thus, this section will provide an overview of some general techniques to detect AAbs as well as will demonstrate which assays were developed for this project and why.

Enzyme-Linked Immunosorbent Assays (ELISAs)

ELISAs can be used to quantify peptides and protein molecules, like the antibodies against a specific antigen (Hayrapetyan et al., 2023). This is measured in the form of the optical density (OD) of colour change intensity by a horseradish peroxidase (HRP) enzyme-catalyzed reaction between antibody-antigen complexes and an HRP substrate, usually 3,3'-5,5' Tetramethylbenzidine (TMB) or o-Phenylenediamine (OPD) (Hayrapetyan et al., 2023). This OD value is related to the antibody titers in an S-shaped curve wherein OD values stop increasing upon antigen saturation by antibody binding against the antigen of interest coated on the plate, which is made of polystyrene and is usually comprised of 96-wells if not more allowing for a greater number of samples to be tested in one go. Thus, ELISAs provide a convenient and quantitative approach to identifying autoantibodies in peripheral neuropathy patient samples (Aydin et al., 2025).

The plates are either purchased with the antigen of interest purified and coated on the plate or this can be done by incubating the plates overnight with the purified antigen in phosphate buffered saline (PBS) to make a solution that keeps the antigen in a stable conformation (Waters et al., 2016). Following this, the plates are blocked with a buffer to reduce non-specific binding and incubated with patient sera or purified immunoglobulin from one hour up to several days. These antibodies are either conjugated directly with an enzyme or a secondary antibody that is enzyme-conjugated is required (Aydin et al., 2025). The substrate contains a chromogen that yields a colour change upon reacting with the enzyme conjugated with the antibody-antigen complex, thus a yellow, blue, or green colour is produced (Aydin et al., 2025). This reaction is stopped using an acid or base and a reading is made using a spectrophotometer at a wavelength depending on the colour change produced by the specific substrate (Aydin et al., 2025).

1) Direct ELISA

In a direct ELISA, the principle used to detect antibodies is exactly as mentioned earlier and between each step at least on wash is conducted to wash away unbound antibodies. The antibody added is already conjugated to an enzyme, like HRP, giving it the name direct ELISA (Aydin et al., 2025).

2) Indirect ELISA

This ELISA method is what was developed to detect IgG against FGFR3 and Plexin D1 (Fujii et al., 2019; Antoine et al., 2015). An indirect ELISA uses a secondary antibody that is conjugated with an enzyme rather than the primary antibody itself being part of the chemical reaction (Aydin et al., 2025). This method works well for patient samples where the presence of antibodies is unknown and a titer can be calculated.

3) Sandwich ELISA

In a sandwich ELISA, the plate is coated with a capture antibody to which the antigen binds followed by a detection tool, like a biotinylated antibody, to detect the bound antigen upon adding S-HRP enzyme (Aydin et al., 2023). It's crucial the respective antibodies bind to separate epitopes of the antigen. Alternative to the biotinylated antibody, an antibody bound to an enzyme, like HRP, itself can be used. This technique is mostly used to capture and detect antigen and not for antibody detection itself (Aydin et al., 2025).

4) Competitive ELISA

The competitive ELISA uses a similar concept as radioimmunoassays wherein there are: a known quantity of antigen coated on the plate that is labelled with an enzyme marker; a known quantity of patient antibodies; and an unknown quantity of patient antigen (Aydin et al., 2025). When all these components are in a well of a plate together, the labelled antigen competes for binding with the patient antibody with the patient antigen and this eventual binding of both antigens can be calculated using the enzyme label on the coated antigen (Hayrapetyan et al., 2023). This process can be inversed wherein the analyte is the antibody instead. Moreover, there are several types of competitive ELISAs based on whether the analyte is the antibody or the antigen, which are based on the existing types of ELISAs – direct, indirect, and sandwich (Hayrapetyan et al., 2023).

Cell-Based Assays

In cell-based assays (CBAs), mammalian cell lines are used to overexpress a protein of interest via transfection methods, like transient or chemical transfection, so the cells can take up and integrate the plasmid DNA after which the cells are incubated with patient antibodies to

determine antigen-antibody binding (Woodhall et al., 2022). This method has been observed to work well for proteins on the cell surface so that the assay is done on live cells, keeping their cell membrane and native conformation of the protein of interest intact. Moreover, avoiding fixing of these cells reduces background noise from antibodies binding to dead cells due to the paraformaldehyde, however, without fixing cells intracellular epitopes of antigens cannot be examined (Woodhall et al., 2022). This assay can be used not only to detect the presence of antibodies from patient samples, like sera and cerebrospinal fluid (CSF), but also to quantify the titers of antibodies within these samples (Woodhall et al., 2022). This detection of antibodies is done using a fluorescent secondary antibody or via flow cytometry. For the first two techniques, a confocal or Epifluorescent microscope is needed to visualize the fluorescence.

These cell lines need to be meticulously maintained in a specialized lab and the most commonly used mammalian cell line for this purpose as a diagnostic assay is the human embryonic kidney (HEK293) T cells that has the SV40 allele of the T antigen, thus a plasmid with a SV40 origin of replication is able to be expressed in high levels upon transfection into these cells (Waters et al., 2016). For flow cytometry on the other hand, the cells are trypsinised before incubation with patient sample to bring the mixture into a solution followed by quantification with a fluorescent secondary antibody (Waters et al., 2016). As control for both assays, untransfected cells can be used to determine if the antibody binding is specific to the antigen or if it is background binding to the membrane of these cells or to dead cells. Furthermore, healthy controls can be used to further validate the specificity of the assay, wherein seropositivity in healthy controls could either mean the patient sera is too concentrated or that assay yields false positives. Such assays are actively used to detect antibodies in peripheral nervous system autoimmunity such as those against LGI1 and CASPR2 (Yeo et al., 2017).

Immunohistochemistry

Indirect immunohistochemistry (IHC) is a very common method used to detect antibodies in patient sera or CSF via their binding to neural tissue sections (Waters et al., 2016). The section of neural tissue taken and used, usually fixed with formalin or frozen, depends on the target of the neurological disorder; for peripheral neuropathies, sections of the DRG are commonly used and antibodies from passive transfer of patient sera are detected using fluorescent secondary antibodies or enzyme-linked antibodies (Waters et al., 2016). Considering the vast number of components within such tissues, identifying the exact location of antibody binding is crucial, thus, counterstaining the nuclei with 4',6-diamidino-2-phenylindole (DAPI) or Hoechst allows for the visualisation of nuclei and pinpoints the antibody binding relative to this (Waters et al., 2016). This technique is particularly useful for the discovery of novel autoantibody targets since it is not specific to a singular antigen (Waters et al., 2016).

Radioactive or Fluorescence-Based Immunoprecipitation Assays

Radioactive immunoprecipitation assays (RIPAs) use an antigen that is either already directly radiolabeled or uses a radiolabeled ligand, usually with iodine-125, is added that binds to the antigen (Waters et al., 2016). Patient sample and secondary antibodies are added, allowing the complexes to be precipitated by centrifugation separating from any unbound antigen and antibodies. The radioactivity within the precipitate is quantified using a gamma counter and the exact quantification of antibodies can be done using serial dilutions to make a standard curve (Waters et al., 2016).

Immuno-dot

An immuno-dot is similar to a western and line blot, but skips the gel electrophoresis step thereby making a convenient assay (Jentzer et al., 2024). This is a relatively new technique and has been used as a diagnostic assay for autoimmune nodopathy, showing promise for other neurological autoimmune conditions with known autoantibody targets (Jentzer et al., 2024).

Induced Pluripotent Stem Cells (iPSCs) and Organoids

iPSCs are less of a diagnostic tool and more of a way of modelling diseases, including peripheral neuropathies, using stem cells that can differentiate into neural cell types (Lampert et al., 2020). Also, iPSCs can be used to test different treatment options *in vitro* (Lampert et al., 2020). A more novel approach is the use of organoids, which allows for a more systemic model to understand antibody-antigen interactions and their effect on nervous system function (Ganassi and Zammit, 2022).

Assay	Strengths	Limitations
ELISA	• Highly sensitive • Quick results • Low patient sera volume	• Lower specificity, possibility of false positives • Uses recombinant protein
CBA	• Representative of cell physiology + protein native conformation • Good specificity	• Need to permeabilize cell if target is intracellular
IHC	• High diagnostic specificity and sensitivity	• Needs lots of optimizing

	• Allows the use of ex-vivo models	• Low specificity due to cross-reactivity of antibodies • Epitope ambiguity
RIPA	• High sensitivity • No denaturing of protein needed	• Regulatory issues • Low accessibility
Immuno-dot	• Convenience • Good sensitivity	• Subjective scoring • Under-researched
iPSCs and Organoids	• Patient-specific disease modelling • Treatment response modelling	• Lack full immune system and interactions • No standards for neural damage set yet

Table 2: Comparative analysis of assays for autoantibody detection in peripheral neuropathies

2.2 Methods

a) Developing cell-based assays (CBAs)

Given that CBAs can express proteins in their native conformation supports that it can more accurately represent antibody-antigen interactions; this paired with the ability to visualize such interactions were reasons this assay was used. Additionally, overexpressing the protein of interest in a mammalian cell line allows antibody binding in a physiological environment rather than the standalone purified protein.

Bacterial Transformation

Preparation

Plasmids with cDNA encoding FGFR3, Plexin D1, MX1, KRT8, or DBNL with a SV40 origin of replication, a Myc-tag, and Kanamycin antibiotic resistance were purchased (in respective order RC215533, RC216518, RC227878, RC209570, RC203435; Origene). Before starting the

bacterial transformation, LB broth and LB agar plates were prepared; 20g of LB broth powder (L3022, Sigma Aldrich) in 1L of distilled water and 16g of agar powder (15885368, Thermo Scientific) in 500mL of distilled water. These bottles were autoclaved for 15 minutes at 121 degrees Celsius and were retrieved the next day, The LB agar bottle was heated under hot runner water for 2 to 3 minutes until melted. Under an open flame, Kanamycin sulfate (M02038, Fluorochem) was added in 1:1000. To do this, first a stock solution of 50mg/mL in distilled water was made to go onto make a final concentration of 50ug/mL, while keeping the antibiotic solution on ice. Then the LB agar was poured into plates about halfway under the open flame and was done quickly to prevent midway solidification as well as carefully to avoid the creation of bubbles. The plates were left to dry under the open flame with their lids slightly open for 1 minute. The plates for future use were parafilmed, labelled, and placed in 4 degrees Celsius. The block heater was prepared by setting it to 42 degrees Celsius for later. 5-α competent E. coli (C2987, New England Biolabs) were thawed on ice and 15uL was transferred into 5 separate 0.5mL Eppendorf tube.

Procedure

For each of 5 plasmids, 2uL was taken and put into the separate tubes and labelled with plasmid name. This mixture of E. coli and each plasmid was incubated on ice for 30 minutes. The mixture was then heat shocked on the block heater at 42 degrees Celsius for exactly 30 seconds and put back on ice for 5 minutes. This heat shock allows the bacterial wall to become temporarily permeable and take up the plasmid DNA and the subsequent cooling allows the bacterial wall to return to its normal state. This essentially transforms the bacterial DNA so that the E. coli now reproduces with all later generations including the plasmid DNA. Thus, the bacteria was allowed to grow and reproduce using 250uL of SOC outgrowth incubator for 1 hour

at 37 degrees Celsius at 250 rpm. After 1 hour, under an open flame, 50uL of the E. coli and plasmid mixture was dripped onto the agar plate using an L stick. The mixture was allowed to dry on the plate for 3 minutes with the lid slightly off and was incubated upside down overnight at 37 degrees Celsius to generate colonies. As a negative control, a tube having undergone the same procedure but without any plasmid was also dripped onto one of the agar plates. The next day, the sample plate should have a multitude of colonies and the negative controls should have no growth due to kanamycin in the plate and no kanamycin resistance gene in untransformed E. coli.

Midi-Prep for DNA Amplification

The most isolated bacterial colony from each plate was selected under an open flame and picked using a tip from a newly opened tip box and inserted into 5 separate 15mL Falcon tube containing 5mL of LB broth (with pre-added kanamycin antibiotic). As a negative control, a tip with no bacteria was ejected into a 6^{th} tube with LB broth. The tubes were incubated in a shaking incubator for 4 hours at 37 degrees Celsius at 250 rpm. At the end of 4 hours, 5mL of broth from each tube was added into separate 1L Durans with 100mL of broth each. The bottles were left securely in the shaking incubator overnight at 37 degrees Celsius at 250 rpm. The next day, there should be a change in colour of broth from pale brown to cloudy yellow paired with a pungent odour as compared to the negative control with no colour change or odour. A midi-prep kit was purchased (12143, Qiagen) and for this the bottles were divided into 2x 50mL Falcon tubes. All tubes were centrifuged at 4600 rpm for 15 minutes, supernatant discarded, and the block heater set at 65 degrees Celsius for a later step. The precipitate was resuspended in 10mL of resuspension buffer and the 2 tubes of each plasmid DNA was combined. 10mL of lysis buffer

was added and mixed by inverting the tubes 6 times followed by incubation at room temperature for 3 minutes; the lysis was complete when there was colour change to dark purple. Then 10mL of precipitation buffer was added and mixed by inverting 6 times till the colour turns yellow when the neutralization was complete. Lysate is loaded into a syringe filter, new tubes were placed under and the plunge slowly pushed out the filtered lysate. 10mL of binding buffer was added and mixed by inverting 10 times. 10mL of the lysate was added to the column and spun at 500g for 2 minutes, discarding the flow through. This was done till all the lysate is passed through the column. The bottom of the column was disconnected and added to a 1.5mL Eppendorf tube. 700uL of wash buffer 1 was added and spun at 17kg for 1 minute, discarding the flow through and repeated with wash buffer 2 twice. The tube was spun twice at 17kg for 1 minute to remove any wash buffers. The collection tube was added into a new 1.5mL tube for final collection. The elution buffer was placed on the heat block at 65 degrees Celsius for 5 minutes and 100uL of it is added to the collection tube and let to elute for 10 minutes. The tube was spun at 17kg for 1 minute, keeping the flow through which is then measured using NanoDrop where a concentration above 2000ng/uL is desirable with a A260/280 ratio between 1.8 and 2.0 indicating negligible protein contamination and a A260/230 ratio between 2.0 and 2.2 indicating negligible organic compound contamination. The purified plasmid sequences were validated using Oxford Nanopore Technologies Ltd.

Cell-Based Assay

Human embryonic kidney cells with an SV40 T-antigen (HEK293T) were used for the CBA and a growth medium comprised of Dulbecco's Modified Eagle's Medium with high glucose (DMEM, D6429, Sigma Aldrich) as a base solvent with fetal bovine serum (FBS, F7524, Sigma-

Aldrich) and Antibiotic-Antimycotic (Anti-Anti, 15240-062, Thermo Fisher Scientific). For maintenance of cells, the cells were kept in a T-75 culture flask with 10mL of growth media in a sterile CO_2 incubator at 37 degrees Celsius, 80%+ humidity, and 5% O_2 until 95% confluency was reached and so was routinely passaged twice a week. Before the start of a CBA, glass cover slips (631-0149, VWR) were coated with 0.01% Poly-L-lysine (PLL, P1399, Sigma-Aldrich) in phosphate buffer saline (PBS). The cover slips were coated with PLL overnight at room temperature in 6-well polystyrene plates with 4 cover slips per well; the solution was aspirated the next day and plates were allowed to dry in a laminar flow hood within the culture lab before being parafilmed and stored for future use.

1. Cell Seeding

When cells reached 95% confluency in flasks, the cells were either passaged or seeded out for CBA. For seeding, the growth media was aspirated from the flask, leaving behind the cells adhered to the bottom surface of the T-75 flask. 2mL of 0.25% trypsin-EDTA (25200056, Thermo Fisher Scientific) was added and the flask was tapped for 2-3 minutes to dissociate the cells from the flask. 8mL of growth medium was added to this mixture and was added to 50mL Falcon tube after mixing thoroughly. In a 1.5mL tube, 25uL of 0.04% trypan blue in PBS solution (15250061, Thermo Fisher Scientific) and 25uL of HEK293T cells were added and 10uL of this solution was added to each side of hemocytometer slide for cell counting under an Epifluorescent microscope (DM2500, Leica) with a simple white light setting. t\The Falcon tube with the cells was centrifuged at 1100rpm for 15 minutes. The supernatant was aspirated leaving behind a pellet that is resuspended in 10mL of growth media. The total number of cells needed is determined using the formula:

(n + 1) plates x 6 wells x 0.935 x 10^6 cells/well (pre-determined optimal number of cells per well without overcrowding of well) = B x 10^6 cells/mL

The volume of cell suspension needed:

Total number of cells needed (B) / cell concentration (A) = C

Total volume of cells and growth media needed to coat cover slips:

(n + 1) plates x 6 wells x 2mL/well = D

Growth media needed:

Total volume of cells and growth media needed (D) – Total volume of cell suspension needed = E (rounded up)

The new working solution of cells was made and 2mL is added to each well, leaving the plate in the incubator to 4-6 hours followed by gently tapping the cover slips that have floated up with a pipette tip.

2. Transfection

As preparation, the transfection buffers were made with polyethyleneimine (PEI) with a PEI to DNA ratio of 1:2. 3ug of DNA was used per well and the volume used was calculated based on the concentration of plasmid DNA obtained from midi-prep. The PEI-DNA mixture was added to DMEM as a solvent and diluting agent, where 50uL of DMEM is needed per well. The PEI-DNA complexes for each protein target were let to form over 10 minutes at room temperature. Followed by this, the media in the wells with cover slips was aspirated and fresh media was added along with transfection mix and left in the incubator for 8 hours after which the media with the transfection mix was aspirated and fresh media was added.

3. Immunocytochemistry

24 hours after the transfection mix was added, the binding assay was started. The cover slips were transferred to a 24-well plate, fixed, and permeabilised using 2mL of 4% paraformaldehyde (PFA) for 5 minutes, followed by 0.2% Trition-100 for another 5 minutes. This was done since all the protein targets have a Myc-tag on their C-terminals that are in their cytoplasmic domains, thus, permeabilization is needed to visualise them and for anti-Myc antibodies to bind to this tag. Anti-Myc tag antibody (ab9106, Abcam) grown in rabbit was prepared at 1:1000 diluted in a block buffer comprised of DMEM, 0.6% bovine serum albumin (BSA, A8806, Sigma-Aldrich), and 0.6% 4-(2-hydroxyethyl)-1-piperazineethanesulfonic acid (HEPES, H3375, Sigma-Aldrich). The same block buffer was used to prepare all antibodies and a wash buffer was prepared with same components but without BSA. Upon fixation and permeabilization, the cells were incubated with anti-Myc tag antibody for 1 hour, followed by staining with goat anti-rabbit IgG (H+L) secondary antibody Alexa Fluor 568 (A-11011, Thermo Fisher Scientific) at 1:750 to visualise the Myc-tag on the protein if successfully transfected and 4',6-diamidino-2-phenylindole (DAPI, D1306, Thermo Fisher Scientific) counterstaining at 1:1000 to visualise the nuclei. Between each step, the cells were washed 3 times with wash buffer and after the last step the cells were washed twice with wash buffer and twice with PBS. The cover slips were then mounted on frosted slides with antifade mounting buffer for storage in 4 degrees Celsius or immediate imaging on the confocal microscope (LSM700, Zeiss) using a 20x objective lens. Images were analysed using Fiji ImageJ2 Version 2.16.0.

b) Developing Indirect ELISAs

ELISAs were also used due to their high convenience with a large cohort able to be tested at once as well as to reproduce the existing assays for FGFR3 and Plexin D1. ELISAs were

developed for the cytoplasmic domain of FGFR3 and the extracellular domain of Plexin-D1 as more focused binding assays to better understand the SFN-focused epitopes of these proteins and since recent literature has used these assays to help identify seropositive SFN patients. Thus, these assays were attempted to be replicated and optimised for in-house diagnostics.

1. Detecting Intracellular FGFR3 Antibodies

Clear flat-bottom immuno 96-well plates (442404, Thermo Fisher Scientific) were coated with 50 uL/well of 5ug/mL recombinant human intracellular FGFR3 (PV3145, Thermo Fisher Scientific) diluted in PBS pH7.4 (10010023, Thermo Fisher Scientific) overnight at 4 degrees Celsius. This concentration was later reduced to 1 ug/mL for conservation of protein and cost effectiveness. Following this, the wells were blocked with 50uL/well of 2% skimmed milk (in-house protocol block buffer). The wells with protein were blocked for 2 hours at room temperature and rabbit anti-human anti-intracellular FGFR3 commercial antibody (GTX31549, Genetex) at serial dilutions, a patient seropositive for FGFR3 (tested by Service de Neurologie at 1:30, CHU de Saint-Etienne, France), or healthy control sera at 1:30 in 2% skimmed milk were added for 1 hour at room temperature. All samples were run in duplicates and with blanks (uncoated wells) for intra-plate validity and to subtract non-specific background binding. An anti-rabbit HRP-conjugated secondary IgG (H+L) antibody (ab6721, Abcam) at 1:3000 was used to add the enzyme, followed by 50uL/well of o-phenylenediamine (OPD) chromogenic substrate (SigmaFast OPD, P9187, Sigma-Aldrich). The reaction was stopped after 30 minutes using 30uL/well of 4M sulfuric acid. Between each step, the wells were washed with 0.1% Tween-20 in PBS 4 times and before OPD substrate was added the wells were washed (last wash) 7 times. The optical density was then measured with a plate reader spectrophotometer (FLUOstar Omega, BMG Labtech) at 450nm wavelength. Under optimisation, the other block buffers used included

the buffer used by the original developers of this assay at Saint-Etienne, which was 0.06% Tween-20, 0.1% fish gelatin, 3% BSA in PBS, and the final block buffer used for all later ELISAs was 2% BSA in PBS. Data was analysed using Microsoft Excel where raw data of duplicates was averaged, blanks were subtracted from sample OD values, and a threshold was set at 3 standard deviations above the mean of healthy controls (Antoine et al., 2015). Bar graphs were made on Microsoft Excel and merged dot plots were made on GraphPad Prism Version 10.6.1.

2. Detecting Anti-Extracellular Plexin-D1 Antibodies (Credited to Omar Alzharany, DPhil Candidate)

The same immuno 96-well plates were used and in each well 50uL of 0.1ug/mL of recombinant extracellular Plexin D1 protein was added (4160-PD, R&D Systems) overnight at 4 degrees Celsius. The wells were blocked with 5% skimmed milk in PBS for 1 hour at room temperature. This was followed by incubation with anti-Plexin D1 commercial antibody (AP22374PU-N, Origene) in serial dilutions, anti-His tag antibody, patients seropositive for anti-Plexin D1 autoantibodies (tested and delivered by From the Department of Neurology, Neurological Institute, Graduate School of Medical Sciences, Kyushu University, Fukuoka, Japan)
SFN patient sera or healthy controls at 1:100 in 2% skimmed milk for 1 hour at room temperature then and HRP-conjugated secondary IgG (H+L) antibody was added at 1:3000 also for 1 hour at room temperature. The OPD substrate was made fresh and wells incubated with it for 20 minutes at room temperature. The reaction was stopped with 4M of sulfuric acid and optical density was measured at 492nm using the same spectrophotometer and analytical tools as for the FGFR3 ELISA. However, the positivity threshold was set at 5 standard deviations above the mean of the healthy controls (Fujii et al., 2021).

c) Developing protein carry-on systems in CBAs

1. Truncated cytoplasmic domain FGFR3 carry-on CBA

As mentioned in part *a)*, HEK293T cells need to be permeabilised in order to determine the presence of antibodies against the intracellular component of FGFR3 protein and as mentioned in the Introduction, this is the epitope of FGFR3 against which there are autoantibody seropositive patients. While autoantibodies against the extracellular domain of FGFR3 have been found to be pathogenic, this has not yet been explored for AAbs against the intracellular epitope of FGFR3 despite more patients testing positive for this epitope (Tholance et al., 2021). Thus, using the same protocol as earlier but without a permeabilization step and antibody binding done on live cells, this "carry-on" CBA was developed wherein the intracellular epitope of FGFR3 was expressed outside the cell. The plasmid cDNA design was developed in-house and put into production by Twist Biosciences and included the FGFR3 secretory signal sequence, FGFR3 cytoplasmic domain, interleukin 22 (IL22) signal sequence, a Myc tag, a Kanamycin resistance sequence, amino acid linkers, and a CASPR2 transmembrane tail); this design was meant to express the intracellular component of FGFR3 outside the cell held in place by a CASPR2 tail held within the membrane. The Myc tag allows the use anti-Myc antibody to detect the protein rather than anti-FGFR3 antibody, proving more cost effective.

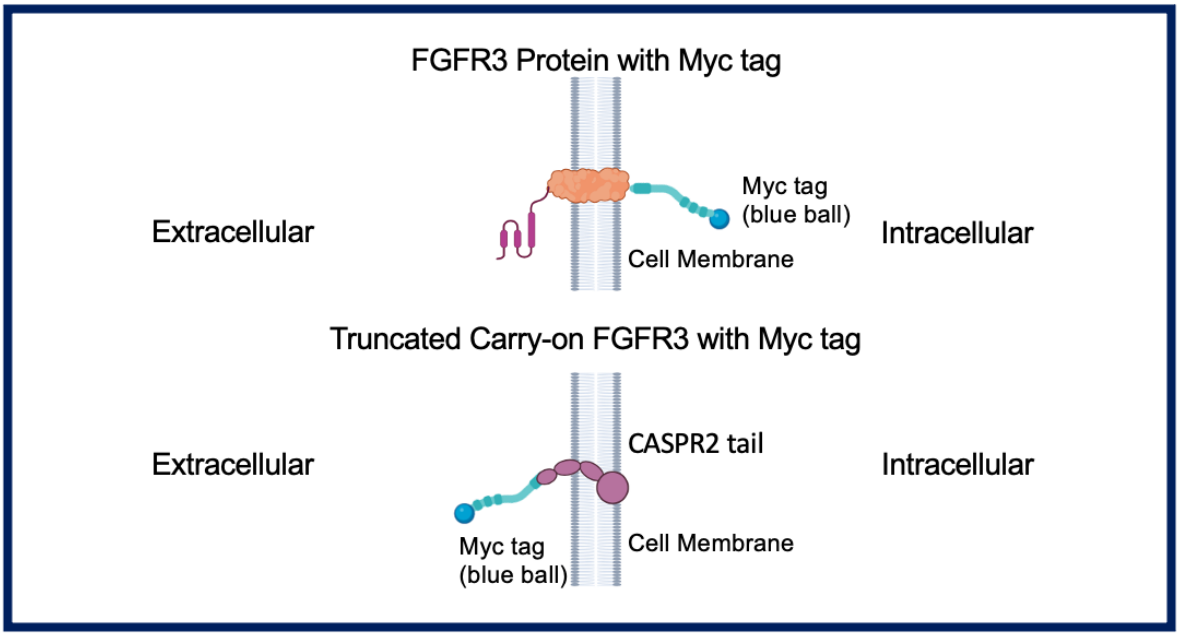

Figure 1: Schematic representation of the carry-on system with truncated intracellular FGFR3 expressed outside the cell with the help of its native signal sequence, a CASPR2 tail for positioning, and a myc-tag for detection.

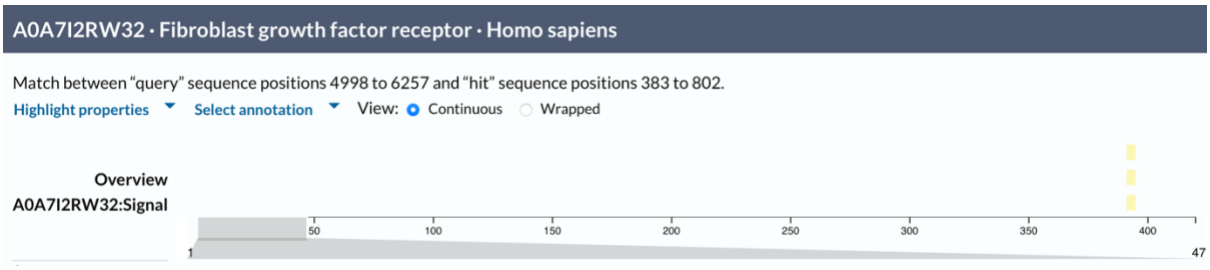

Figure 2: UniProt BLAST software used to find protein hits for the "query" sequence, which is the whole plasmid construct nucleotide sequence. The protein hit most closely found was the cytoplasmic domain of FGFR3 (amino acid sequences 383 to 802), confirming the desired FGFR3 epitope cDNA.

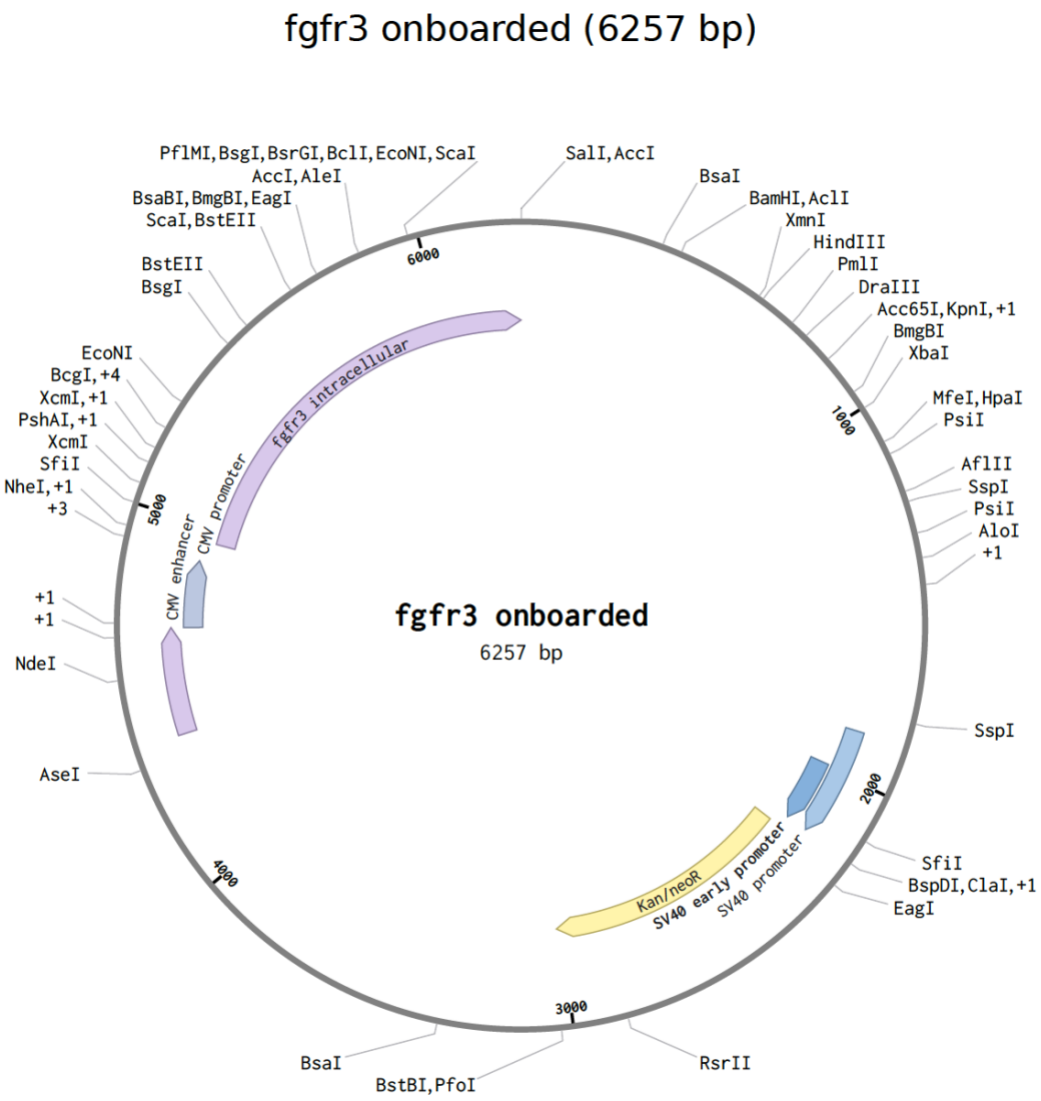

Figure 3: Benchling was used to make a basic plasmid map of the nucleotide sequence sent to Twist Biosciences. The map includes features like the intracellular component of FGFR3, CMV promotor, SV40 promotor, and kanamycin resistance. Not shown in the map are the myc tag, IL22 signal sequence, and CASPR2 tail, which are encoded after FGFR3.

2. MX1 carry-on CBA

The same concept was used with the Twist Biosciences platform for the completely intracellular protein, MX1. MX1 was found to be significantly higher in idiopathic SFN patients, as mentioned in the Introduction, and no assay to detect autoantibodies against MX1 have been well-established. The design for this plasmid was the same as for FGFR3, except here the whole

protein's cDNA was used and MX1 does not have its own signal sequence, making the IL22 signal sequence crucial.

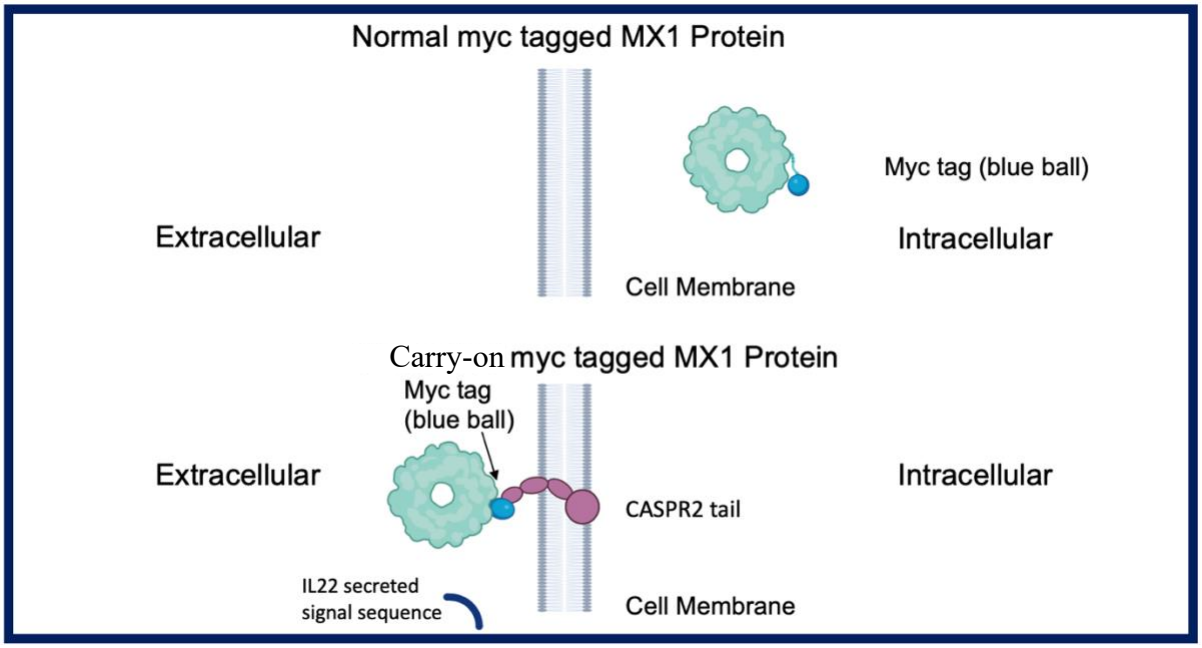

Figure 5: Schematic representation of the carry-on system with intracellular MX1 expressed outside the cell with the help of an IL22 signal sequence, CASPR2 tail for positioning, and a myc-tag for detection.

2.3 Results

2.3.1 HEK293T cells can successfully overexpress FGFR3, Plexin-D1, MX1, KRT8, and DBNL upon transient transfection

The CBA with HEK293T cells was done to determine whether these cells can overexpress FGFR3, Plexin-D1, MX1, KRT8, and DBNL and whether this expression can be detected using an anti-myc antibody that binds to the Myc tag on these proteins (Figure 4). The detection of fluorescence using an Alexa Fluor secondary antibody determines this as a starting point for a potential model to detect autoantibodies against these targets from patient sera.

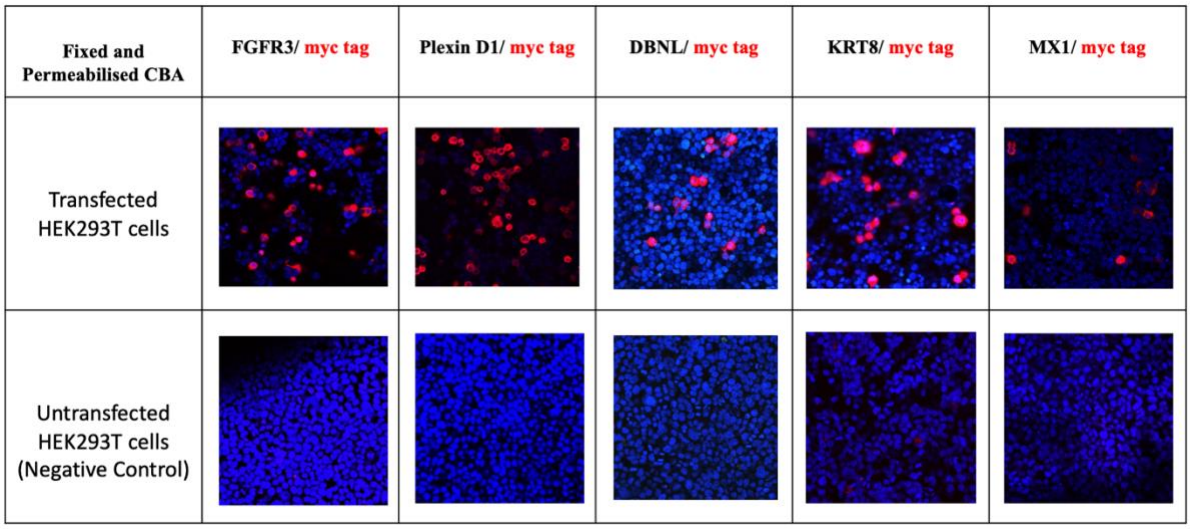

Figure 4: HEK293T cells pictured at 20X zoom using confocal microscopy with myc-tag on proteins of interest fluorescing red (AlexaFluor 586) and the nuclei of cells in blue (DAPI). The untransfected HEK293T cells do not show red fluorescence, signifying the absence of protein of interest.

2.3.2 ELISA with commercial antibody against intracellular FGFR3 at serial dilutions showed proportional optical density (OD) reductions with negligible healthy control and standard OD values

An ELISA protocol developed by Antoine et al. at Saint-Etienne, France was replicated but with 2% skimmed milk in PBS as a block buffer (in-house protocol) rather than their block buffer of 0.06% Tween-20, 0.1% fish gelatin, and 3% BSA in PBS. A commercial anti-FGFR3 antibody at serial dilutions was tested to check for its binding to intracellular FGFR3 protein. This was done successfully showing a saturation in binding at around 1:1000 of commercial antibody (Figure 5). There is also negligible non-specific binding to the polystyrene in the plates as seen in the blanks highlighting the high specificity of the commercial antibody for intracellular FGFR3. The healthy control obtained from a clinical study on sciatica at the John Radcliffe Hospital, Oxford, United Kingdom showed negligible seropositivity at 1:30 as did the standard, which followed the same protocol but without any primary antibody, thereby validating the background noise from HRP-conjugated secondary antibodies.

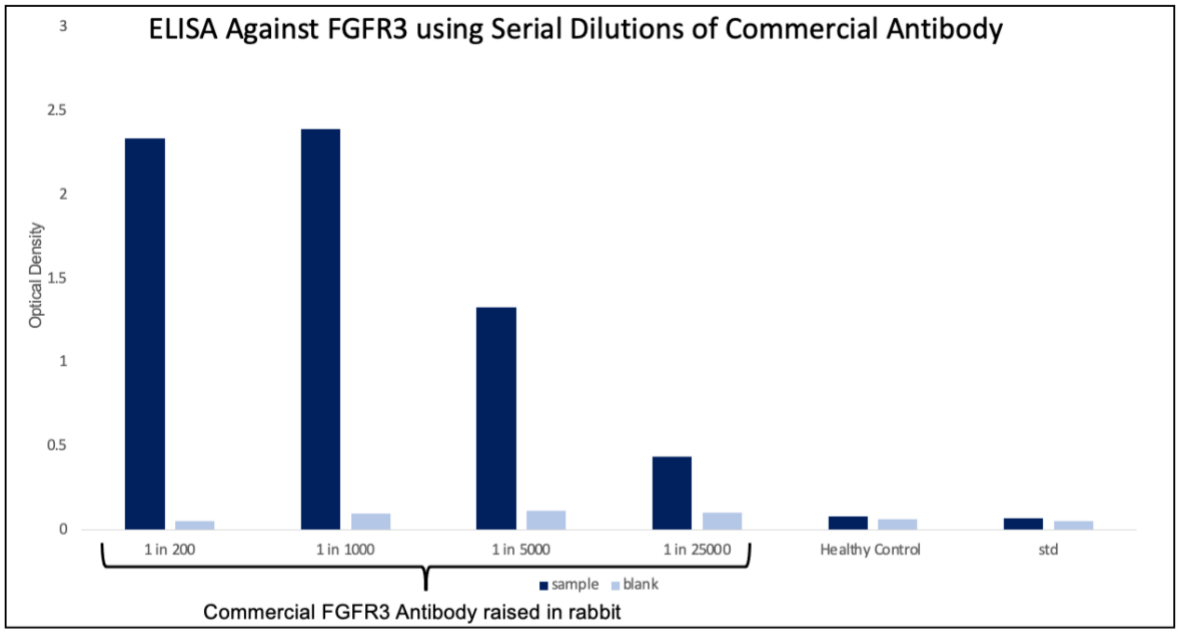

Figure 5: ELISA bar graph with 5ug/ml of intracellular FGFR3 coated wells in dark blue (sample) and no protein coating in light blue (blank). Optical Density (OD) values are on the y-axis and the different samples (commercial antibody in serial dilutions of 1:200, 1:1000, 1:5000, 1:2500, healthy control, and standard (no primary antibody)) are on the x-axis.

2.3.3 Commercial anti-FGFR3 antibody shows a positive OD signal with 1ug/mL of intracellular FGFR3 and 2% skimmed milk, but the pre-tested patient positive is negative for anti-intracellular FGFR3 autoantibodies

Due to the high cost of intracellular FGFR3, 1ug/mL concentration was attempted instead of 5ug/mL. This yielded similar results for the commercial antibody but failed to replicate seropositivity of the patients pre-tested as positive from the same lab in Saint-Etienne, France (Figure 6). Thus, proving that the assay does not work on patient sera as the patient positive resulted in similar OD values as the healthy controls.

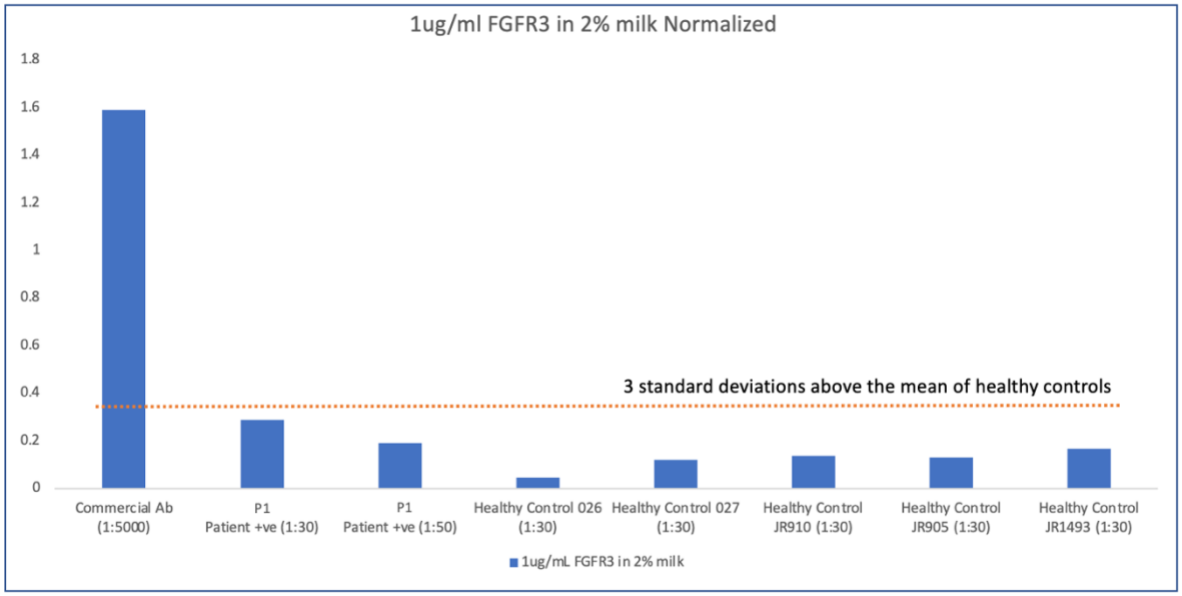

Figure 6: ELISA bar graph with commercial anti-FGFR3 antibody at 1:5000, a patient seropositive for FGFR3 at 1:30 and 1:50, 5 healthy controls at 1:30 on the x-axis and optical density (OD) on the y-axis. The orange line is the positivity threshold set at 3 standard deviations above the mean of the healthy controls. Values are normalized by subtracting blank OD values and averaging duplicates, intracellular FGFR3 is coated at 1ug/mL and 2% skimmed milk in PBS is used as the block buffer.

2.3.4 For ELISAs, 1ug/mL of intracellular FGFR3 and 2% BSA in PBS as a block buffer gave the most cost-effective results with the patient positive for autoantibodies against intracellular FGFR3 resulting in a true positive in this assay and healthy controls as negative

The ELISA was re-attempted with 3 different protocols, using the same protocol as previous attempts but with 5ug/mL of intracellular FGFR3 rather than 1ug/mL resulted in a positive for the patient positive control, but significantly increased the OD values of healthy controls thereby making the positivity threshold much higher (orange line at 3 standard deviations above the mean of the healthy controls). Trying the exact same protocol as the lab in France with their block buffer of 0.06% Tween-20, 0.1% fish gelatin, 3% BSA in PBS and 5ug/mL of intracellular FGFR3 did not yield a positive result for the patient positive (tested using the same protocol in

France) (Figure 7 C). Lastly, 1ug/mL of intracellular FGFR3 and 2% BSA in PBS was used as a block buffer following the same steps and yielded the best results in terms of the patient positive coming out positive on this assay, 5X less protein used, and lower healthy control OD values as compared to the first protocol (Figure 7 B).

A

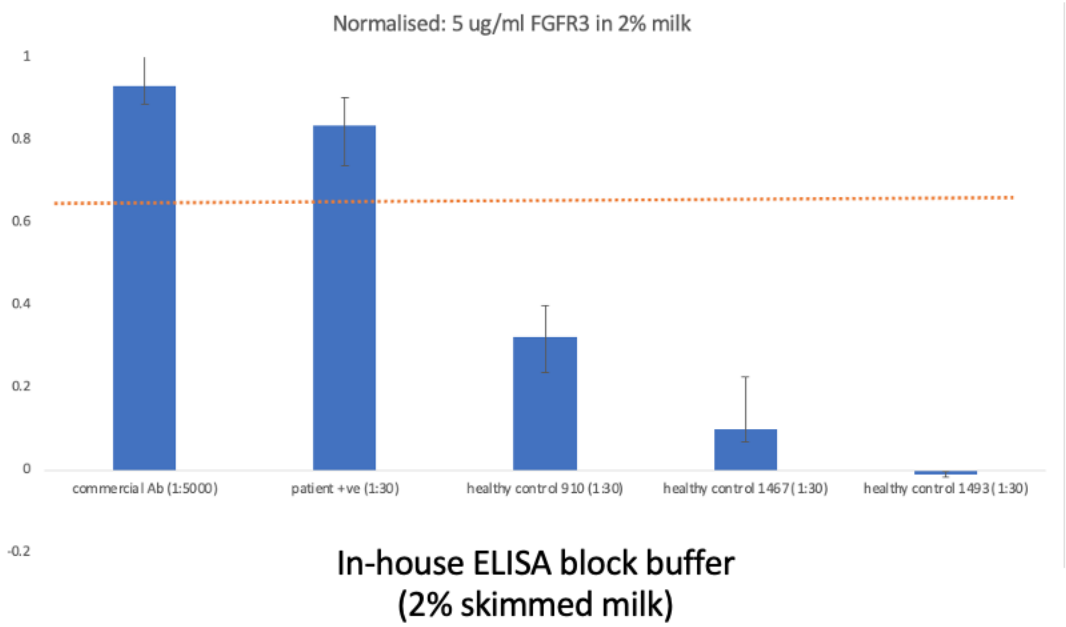

B

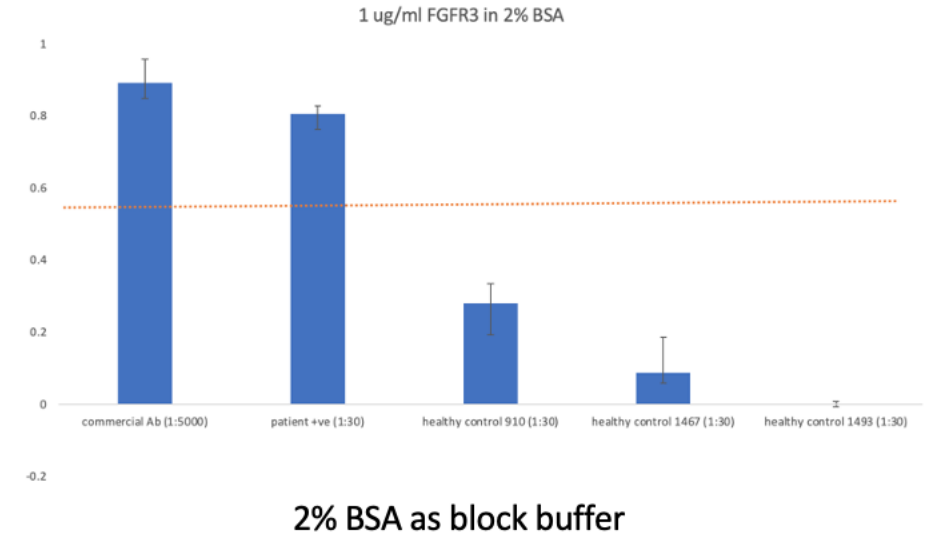

2% BSA as block buffer

C

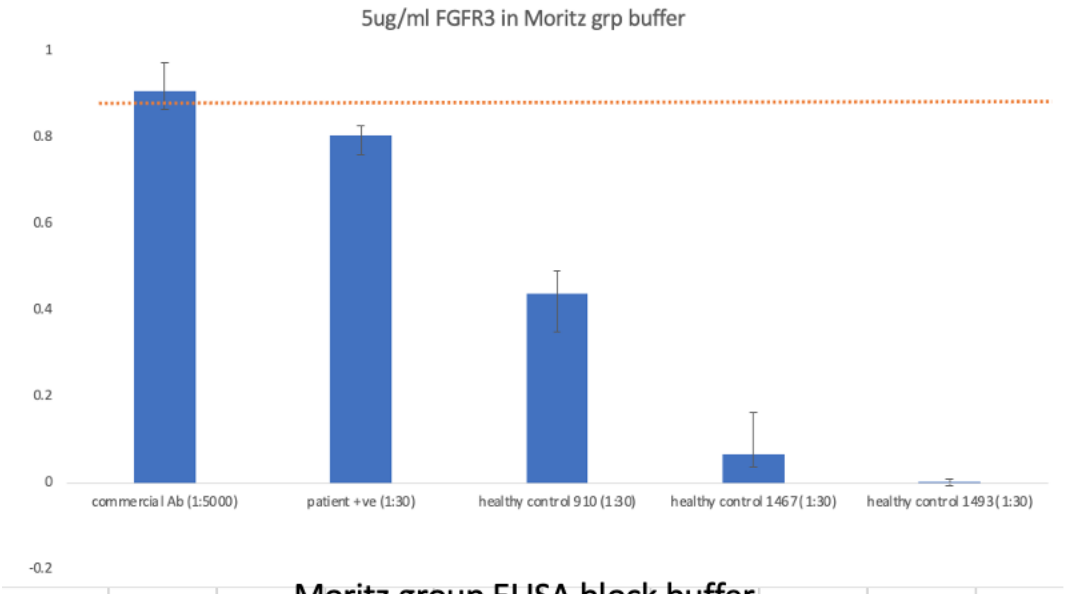

Moritz group ELISA block buffer

(0.06% Tween-20, 0.1% fish gelatin,
3% Bovine Serum Albumin (BSA))

Figure 7: A) ELISA bar graphs with 5ug/mL intracellular FGFR3 in 2% skimmed milk B) 1ug/mL intracellular FGFR3 in 2% BSA. C) 5ug/mL intracellular FGFR3 in 0.06% Tween-20, 0.1% fish gelatin, 3% BSA in PBS. The bars signify commercial antibody at 1:5000, patient positive at 1:30, 3 healthy controls at 1:30 (from left to right on each graph). The orange line signifies the positivity threshold set at 3 standard deviations above the mean of the healthy controls. Error bars are based on the technical duplicates.

2.3.5 The ELISA using 1ug/mL intracellular FGFR3 and 2% BSA as a block buffer was validated as an effective assay by testing 20 healthy controls, all of which were seronegative

Using the protocol with 1ug/mL of intracellular FGFR3 and 2% BSA in PBS as a block buffer, an ELISA was carried out with the same commercial antibody, patient positive (P1), and 20 healthy controls to validate that the positive samples stay positive and that healthy controls are correctly identified as seronegative according the assay and the threshold, which is the same threshold used by the lab in Saint-Etienne, France (Figure 8). The reuse of the commercial antibody and patient positive for each assay is crucial due to inter-plate assay result differences.

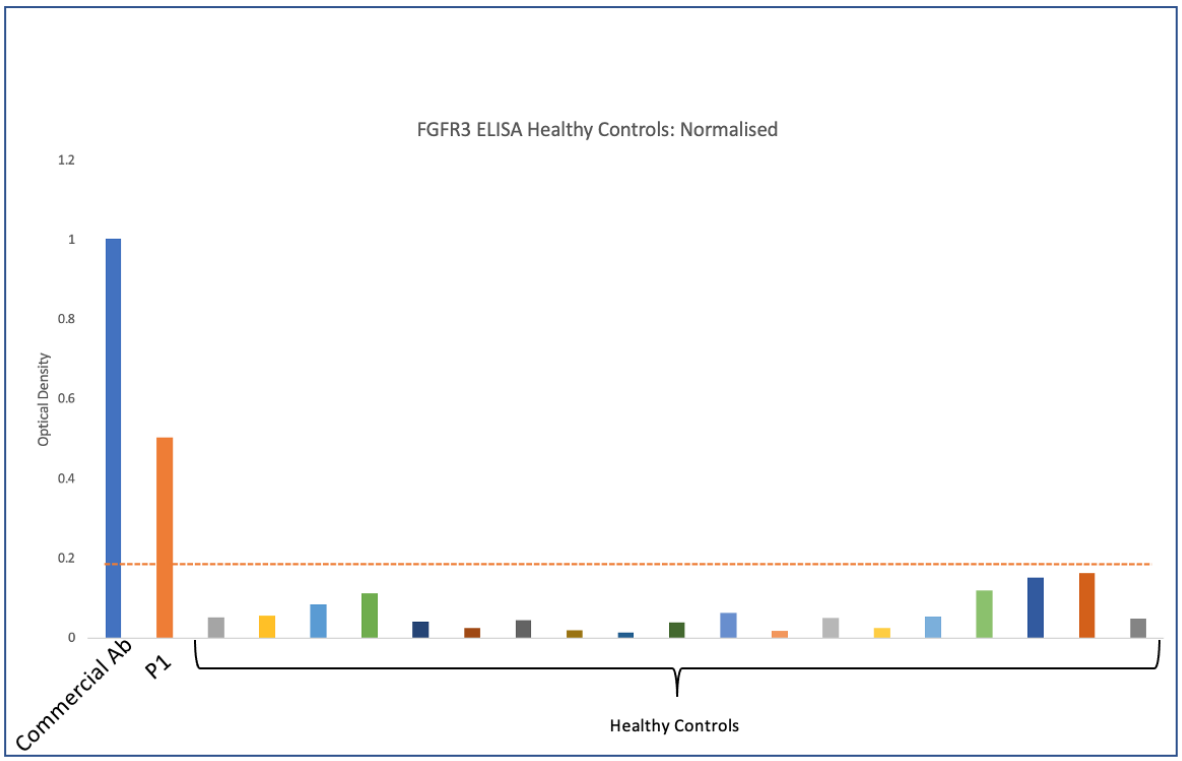

Figure 8: ELISA bar graph testing 20 healthy controls at 1:30 with an anti-FGFR3 antibody at 1:5000 and patient positive (P1) at 1:30 for anti-intracellular FGFR autoantibodies using 1ug/mL intracellular FGFR3 and 2% BSA in PBS as a block buffer. Optical density is on the y-axis and samples are o the x-axis. The orange line is the positivity threshold set at 3 standard deviations above the mean of the healthy controls.

2.3.6 The ELISA against extracellular Plexin-D1 autoantibodies picks up positivity from commercial antibodies that specifically target the extracellular domain of Plexin-D1, but all patients were seronegative including patient samples tested seropositive by developers of this assay, Fujii et al., in Japan (by Omar Alzharany, DPhil Candidate)

This ELISA was developed by Omar Alzharany (DPhil Candidate) and was validated using an anti-His antibody to detect the His-tag on the extracellular Plexin-D1 coated on the wells of the plate as well as an anti-extracellular Plexin-D1 commercial antibody, both at serial dilutions (Figure 9). 12 healthy controls and 10 disease controls were seronegative as were iSFN and DPN patients. However, the patient positives received from the developers of the assay (Fujii et al., Japan) were seronegative upon multiple attempts even at higher antigen concentration of 1ug/mL and with 2% BSA in PBS as a block buffer (not shown). The data was normalised by averaging technical replicates and subtracting the respective blank OD values.

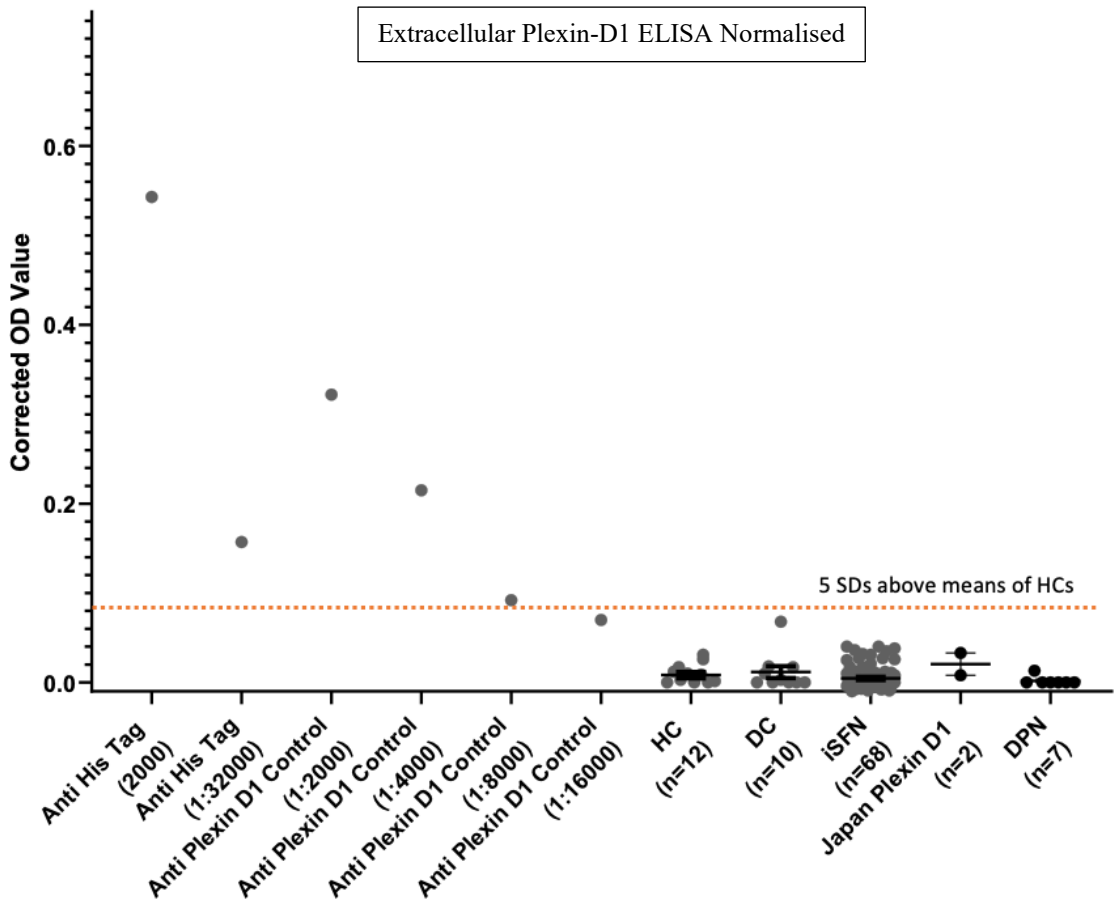

Figure 9: ELISA dot blot graph for anti-extracellular Plexin-D1 autoantibody detection using 0.1ug/mL of extracellular Plexin-D1 and 5% skimmed milk as the block buffer. The y-axis corresponds to optical density values and the x-axis corresponds to anti-His tag antibody (1:2000, 1:32000), anti-Plexin D1 antibody (1:2000, 1:4000, 1:8000), 12 healthy controls, 10 disease controls, 68 idiopathic SFN patients, and 2 patient positives (Fujii et al., 2021), and diabetic peripheral neuropathy (DPN) patients all at 1:100 (from left to right).

2.3.7 HEK293T cells were successfully transfected with the engineered truncated FGFR3 protein with only its cytoplasmic domain upon transient transfection

The CBA with engineered cytoplasmic domain of FGFR3 protein attached to the membrane via a CASPR2 tail was successful and limits the use of permeabilization that disrupts the HEK293T cell physiology and conformation of the protein of interest. There was lower detection of this engineered FGFR3 protein with commercial antibody, or direct binding to the protein, compared to indirect FGFR3 detection using an anti-myc antibody for detection of the myc tag on the

protein. There was a significantly higher detection of the protein when the cells are permeabilised rather than not (Figure 10). This could be due to most cells continuing to express the intracellular domain of FGFR3 within the cytoplasm, thus, negating the "carry-on" effect wherein the subcellular location of the FGFR3 component is flipped outside the cell.

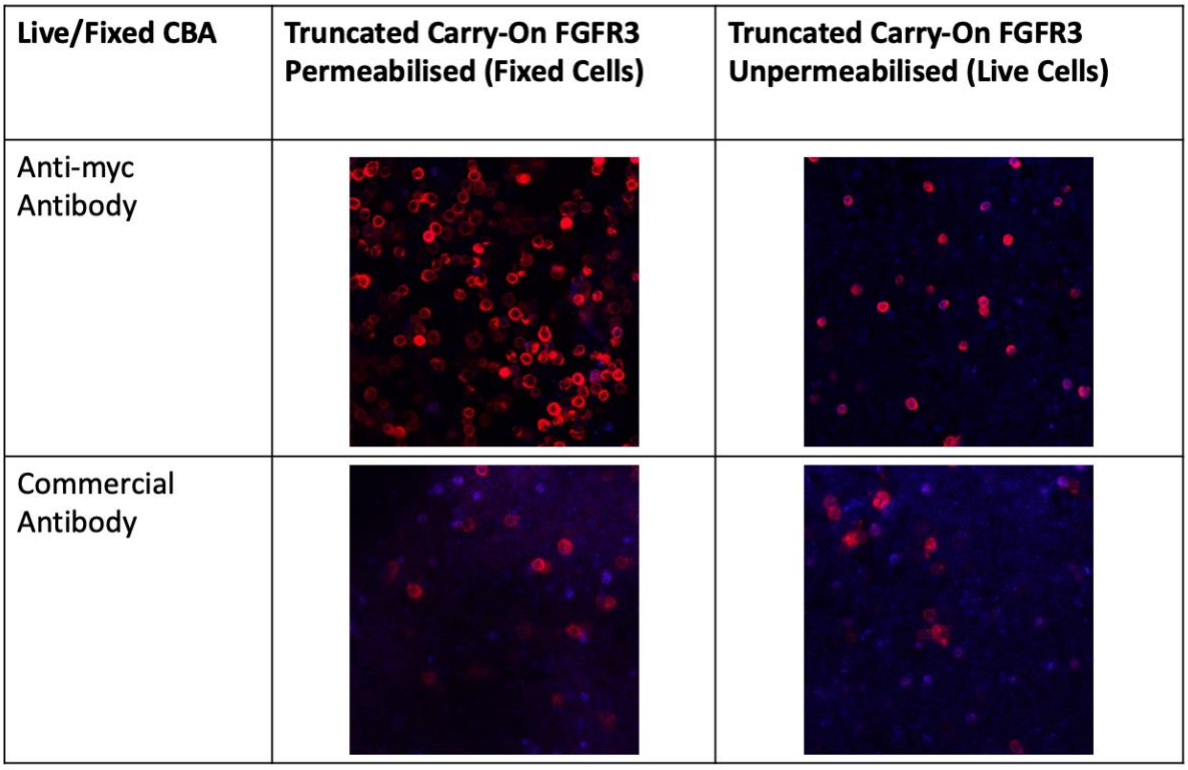

Figure 10: HEK293T cells transfected with the engineered plasmid containing the cytoplasmic domain of FGFR3 anchored to the membrane with a CASPR2 tail. The Myc tag on the protein detected in the top panel (red) and the cytoplasmic domain of FGFR3 itself detected in the bottom panel (red). The HEK293T cells show unclear nuclei counterstaining with DAPI (blue).

2.3.8 HEK293T cells are successfully transfected with the engineered full-length MX1 protein expressed extracellularly, unlike its native intracellular subcellular location, upon transient transfection

The CBA with HEK293T cells transiently transfected with engineered full-length MX1 on a CASPR2 tail was detected with anti-Myc antibody to detect the myc-tag on the MX1 protein.

This CBA was done unpermeabilised and thus, with MX1 in a somewhat native conformation. The permeabilised counterpart image is not shown due to high cell death.

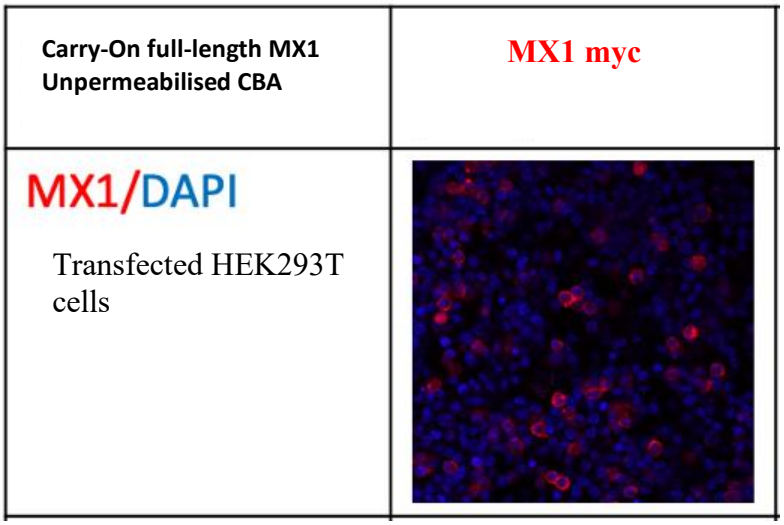

Figure 11: CBA with HEK293T cells transfected with engineered full-length intracellular MX1 overexpressed extracellularly anchored to the membrane by a CASPR2 tail with a Myc-tag fluorescing in red (Alexa Fluor 586) and the nuclei of cells in blue (DAPI).

2.4 Discussion

Based on the results, for the detection of anti-intracellular FGFR3 IgG, both the ELISA and carry-on CBA were developed. The final protocol for the ELISA included a 5x less amount of protein used with 2% BSA, it is possible that the other block buffers resulted in the positive control as negative due to masking of the antibodies (Bloch et al., 2025). The innovative carry-on system was first developed in a DPhil project by Pao-Sheng Chang and supervised by Patrick Waters at The Nuffield Department of Clinical Neuroscience, University of Oxford using interleukins. This concept was tested using a truncated version of FGFR3, a transmembrane protein, to express only its cytoplasmic epitope extracellularly with a Myc-tag for transfection confirmation and the tail of the CASPR2 protein to hold it in place within the membrane. The

same concept was tested on the full-length MX1 protein, which is entirely intracellular. However, when testing this carry-on CBA to confirm expression of intracellular FGFR3, the permeabilised HEK293T cells showed a greater transfection rate (Figure 10). This could be because some cells are still expressing the intracellular epitope of FGFR3 in the cytoplasm of the cell, however, given that some cells do express it outside the cell this CBA was still tested with patient sera in the next chapter. With regards to Plexin D1, the CBA successfully showed expression of the Myc-tag on the protein signifying that the assay can be used to detect patient IgG. The same was observed for MX1, DBNL, and KRT8 but only MX1 was put forward due to its significance in iSFN while other targets showed no difference in prevalence in iSFN compared to secondary SFN. But, for MX1 only the carry-on CBA was used in further testing due to the permeabilization step in a standard CBA.

Chapter 3: Testing Patient Sera on Developed Assays

3.1 Introduction

3.1.1 The Developed Autoantibody Detection Assays Chosen for Patient Testing

From the assays to detect autoantibodies developed as proof of concepts in the previous section, the CBA for anti-Plexin D1 IgG, the ELISA for anti-FGFR3 IgG, and the "carry-on" CBAs for anti-FGFR3 IgG and anti-MX1 IgG were chosen. Considering the ELISA for Plexin-D1 could not be replicated and given the benefits of a CBA, like modelling the native conformation of the protein target, the CBA tested against the myc-tag on Plexin-D1 was used for patient testing. Moreover, given that patients bind to the extracellular domain of Plexin-D1, testing for patient IgG binding can be done on live HEK293T cells signifying a better assay by reducing non-specific background binding (Fujii et al., 2021). For FGFR3, the revised ELISA protocol using 5X less protein and a different block buffer compared to the original developers of the assay had yet to be used in patient testing and given the convenience and fast pace of this assay, this was also used on SFN and FMS patient samples (Antoine et al., 2015). Lastly, the concept a "carry-on" CBA has never been used in the context of SFN and poses as an innovative technique to express the cytoplasmic domain of proteins extracellularly. Thus, the carry-on CBA was tested on intracellular components of FGFR3 and the full-length intracellular MX1 using FMS and SFN patient samples.

The identification of patient positives from any of these assays would be beneficial in understanding if their phenotypic disease characteristics can be stratified based on AAbs against specific targets. However, testing negative on these assays also supplements the existing literature on prevalence of these AAbs as well as their relevance in iSFN.

3.1.2 CBAs to Detect Anti-LGI1 and Anti-CASPR2 AAbs for Benchmarking Seropositivity in Patients

LGI1 and CASPR2 are two protein antigen targets that were described in the Introduction, AAbs against these targets have been explored in the context of inflammatory conditions (Graus et al., 2016). CBAs to detect anti-LGI1 and anti-CASPR2 AAbs have been set up and are routinely administered to diagnose autoimmune disorders, like Morvan's syndrome, limbic encephalitis, faciobrachial dystonic seizures, and neuromyotonia, wherein these voltage-gated potassium channel complexes are targeted and, in some cases, small fiber pathology is seen (Lang et al., 2017). These assays have been well-developed since their generation and considering these AAbs target the extracellular region of these proteins, patient IgG binding is done on live HEK293T cells (Lang et al., 2017). Thus, images from these assays act as a strong benchmark for what patient seropositivity and seronegativity for anti-extracellular antigen epitope AAbs should look like, with minimal background noise. Moreover, the protocols for these assays are constantly being optimized by diagnostics labs that routinely test for the autoimmune inflammatory disorders, producing high transient transfection rates with healthy and confluent HEK293T cells.

Thus, CBAs to detect anti-LGI1 and anti-CASPR2 IgG in FMS patient cohorts and pre-tested patient positives were carried out to benchmark scoring of seropositivity in patients. SFN patient samples were not tested due to their limited serum volumes. Upon completion of these CBAs and developing an understanding of what clear seropositivity and seronegativity for AAbs looks like in CBAs, the assays to detect AAbs against SFN-specific antigen targets were carried out.

3.2 Methods

3.2.1 Samples

SFN Samples

The SFN patient sera were obtained from the DOLORisk study by our collaborators, which was a multi-centre observational study that put together detailed symptom phenotype data on neuropathic pain cohorts (Pascal et al., 2019). Data was obtained cross-sectionally and from these cohorts only idiopathic SFN patients were used in our AAb detection assays wherein all patients with SFN resulting from secondary causes were excluded, like diabetes, vitamin B12 deficiency, alcoholism, infection, and autoimmune conditions. Sera from 72 patients who were labelled as "Probable SFN" and "Definite SFN" from these cohorts were tested, based on the Devigili et al., 2008 definition of SFN wherein at least two of the following criteria must be met:

- Clinical symptoms of pinprick, thermal loss, allodynia, or hyperalgesia in a length dependent distribution starting at the feet
- Abnormal foot thermal thresholds or thermal QST
- Reduced IENFD at distal leg

The average age of the patients was 51 years and there was an even split of females to males. Further demographic and clinical details of this cohort will be discussed in depth in the next chapter.

FMS Samples

Sera from a total of 53 FMS patients were tested on our assays and these samples were obtained from our collaborators in Mayo Clinic, Florida. These patients were also well phenotyped with regards symptoms including those related to neuropathic pain, demographics, and relevant comorbidities. The average age of the patients was 48 years and there was a ratio of 52:1 of

females to males, thus there was only 1 male tested. Further demographic and clinical details of this cohort will be discussed in depth in the next chapter.

Healthy Controls

Healthy controls were obtained from the John Radcliffe (JR) Hospital, Oxford repository of control sample sera collected from 2017 to 2022. The average age of 74 healthy control patients used for sera was 50 years and the sex ratio was an even split.

Patient Cohort	Average Age	Sex Ratio (F:M)	Pain Phenotypes Available
SFN (n=72) (DOLORisk study)	51 years	Even Ratio	Yes
FMS (n=53) (Mayo Clinic)	48 years	52:1	Yes
Healthy Controls (n=20 for CBA, n=74 for ELISA) (JR Hospital)	50 years	Even Ratio	No

Table 3: SFN patient cohort, FMS patient cohort, and healthy controls sampled in the AAb detection assays.

3.2.2 ELISA

The protocol used for the ELISA to detect anti-intracellular FGFR3 AAbs was the same as that developed in the previous chapter. However, this assay was not only done in technical duplicates but also twice to account for inter-assay differences. After testing all patient samples, the positives were repeated with 54 more healthy controls for a statistical power of over 80%. Patient

positives and the additional healthy controls were tested in a scattered distribution on the plate rather than in one area due to intra-plate differences wherein OD values can be higher for wells around the perimeter of plates due to evaporation and temperature gradients, also known as "edge effect", that can create false positives (van Gorkom et al., 2021). The plots were created using GraphPad Prism Version 10.6.1.

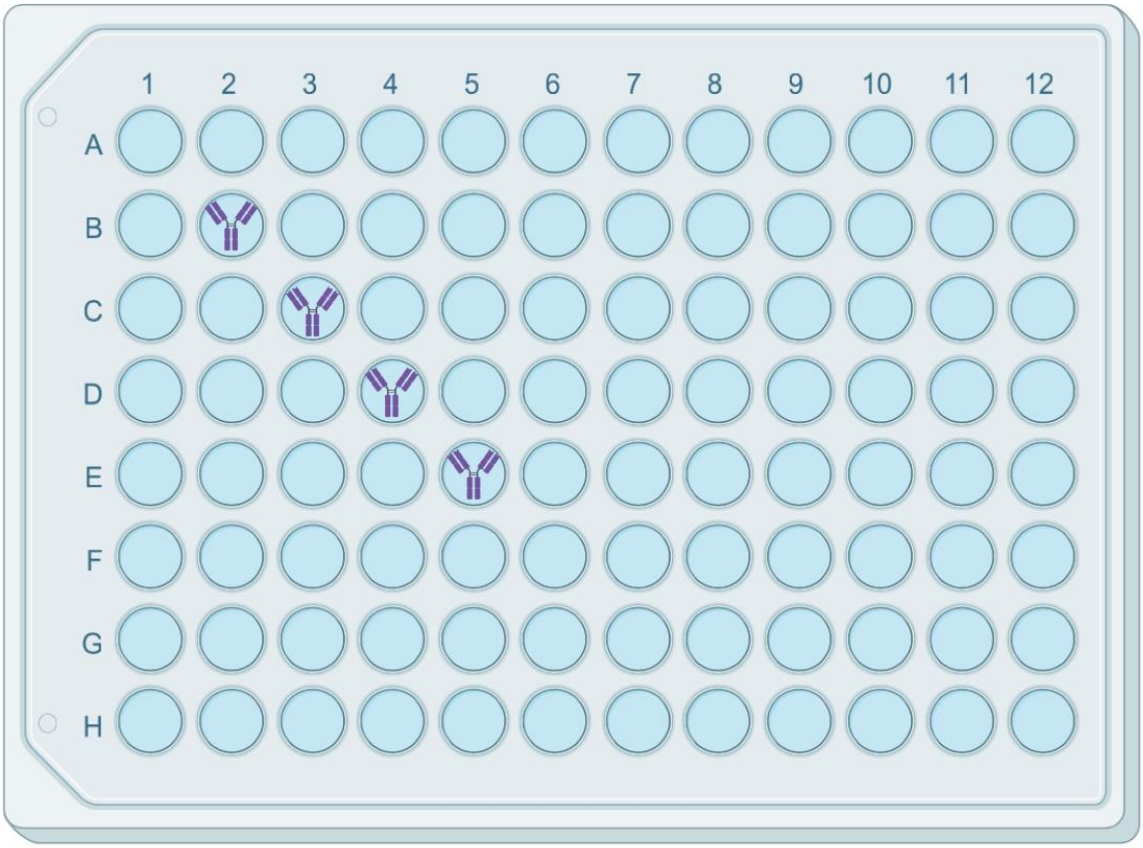

Figure 12: Schematic representation of the distribution of a patient positive sample tested in the repeat ELISA in duplicate with blanks (no protein coating). This distribution limits the edge effect by not using the wells on the perimeter of the plate and by averaging the OD values of wells that are not equidistant from the centre of the plate. In this case, B2 and D4 are test samples and C3 and E5 are the blanks.

3.2.3 96-Well Plate Optimized CBA

Due to overlapping projects using the same SFN samples, the volume of remaining sera had reduced significantly. This provoked a need for an optimized CBA wherein less serum volume

would be needed. Thus, the protocol shifted from the use of cover slips and a 24-well plate to a 96-well plate (CLS353376, Corning) without cover slips. 200uL of 0.01% PLL in PBS solution was added to the wells of the plate for an hour after which the wells were aspirated and left to dry in the laminar flow hood for 4 hours.

1. Cell seeding

The same cell seeding preparation protocol was used as in the previous chapter to count the HEK293T cells. The cell concentration per well was adjusted to 40,000 per well or 0.267 x 10^6 cells/mL. The total volume of cell suspension required was calculated using the adjusted formula:

Total volume (of cells and media) = (n + 1) plates x number of wells x 150 uL/well

Additionally, instead of using all the wells on the plate only 60 wells were used each time to avoid the edges. This reduced the edge effect and also allowed better images to be taken using the confocal microscope since the wells around the perimeter of plates cannot be properly centered under the microscope lens due to mechanical limitations. Lastly, the plates were centrifuged at 1200 rpm for 3 minutes to bring the cells to the bottom of the plate for better surface adherence. The cells were left for 24 hours in the CO_2 incubator at 37 degrees Celsius and 5% O_2.

2. Transient Transfection

The transfection mixture per plate was 25.2ug of DNA + 420uL growth media + 12.6uL PEI that was incubated at room temperature for 10 minutes followed by an additional 15.2 mL of growth media. This kept the DNA:PEI ratio at 2:1, the same as the previous protocol. All supernatant was removed from the wells and 150uL of transfection mix was gently added to the side of each well.

3. Immunocytochemistry

The patient samples were prepared in a 1:20 dilution in the same block buffer used as the last protocol. Final volumes of 50uL were prepared, thus only 2.5uL of sera was used per patient as compared to 12.5uL of sera that would be required for a 24-well plate CBA, an 80% reduction in volume. The cells were incubated with patient sera for 1 hour at room temperature on a plate shaker on low setting. Remaining steps were the same as in the previous chapter, except for all solutions a final volume of 50uL was used and no mounting of cover slips was needed, so the cells were kept in 100uL of PBS for imaging on the confocal microscope using the 20X lens. Between each step, the cells were washed 3 times with the same wash buffer as in the previous chapter. Images were analyzed using Fiji ImageJ2 Version 2.16.0.

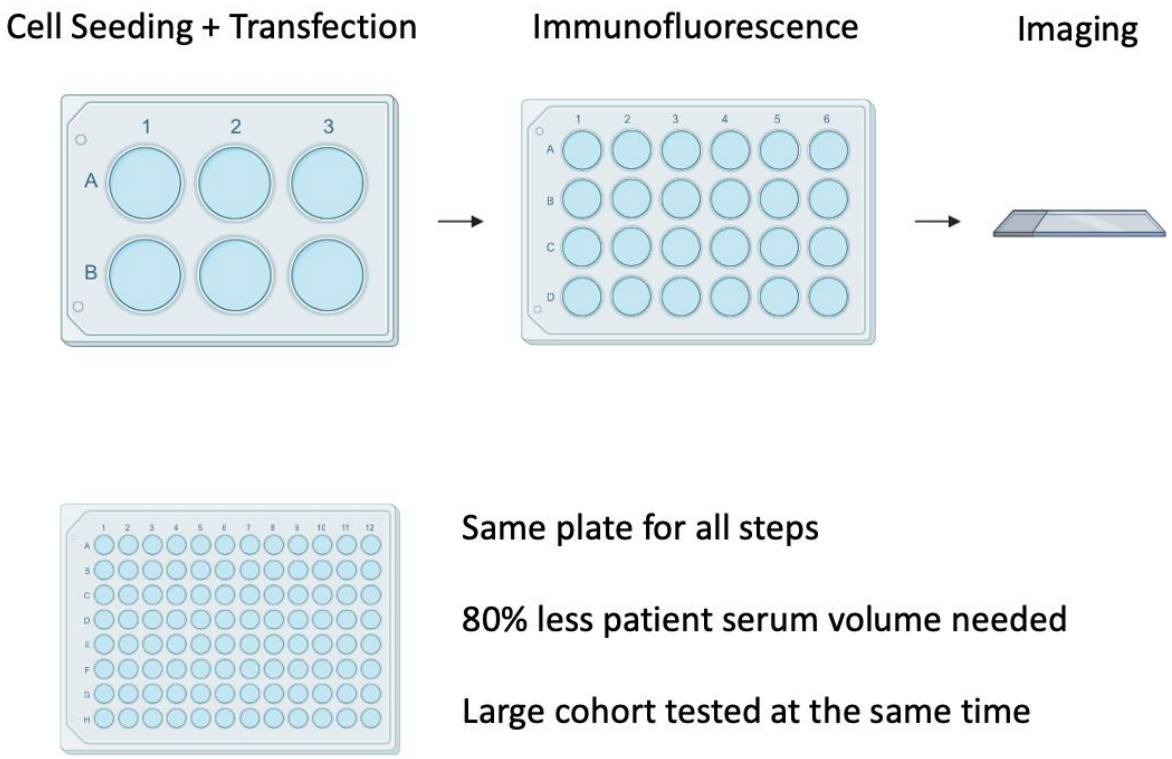

Figure 13: Schematic representation of a standard CBA with glass cover slips versus the 96-well plate optimized CBA.

3.2.4 Cell-Based Assay

1. LGI1 and CASPR2 CBAs

For the anti-LGI1 AAbs and anti-CASPR2 AAbs detection CBAs the same protocol was used as the previous chapter with a 24-well plate and with an LGI1 plasmid (NM_005097) for the former assay and a CASPR2 plasmid (NM_014141) for the latter assay. The pretested patient positive sera samples received from the autoimmune neurology diagnostic lab at John Radcliffe Hospital were tested. Serum from the anti-LGI1 AAb positive patient was tested at serial dilutions of 1:20, 1:50, and 1:100 in block buffer with 1:20 being the standard dilution used and sera from the anti-CASPR2 AAb positive patient was tested at 1:100, 1:500, 1:1000 with 1:100 being the standard dilution used. The cells were incubated with patient sera for 1 hour at room temperature. The remaining steps were the same as in the previous chapter except cells were fixed after the incubation with patient sera step and not permeabilised. The plasmids were tagged with enhanced green fluorescent protein (eGFP), thereby removing the anti-Myc tag antibody step and the subsequent anti-rabbit secondary IgG staining. Instead, the cells were stained for patient IgG binding with goat anti-human IgG, Alexa Fluor 568 (A-21090, Thermo Fisher Scientific) at 1:750 with DAPI at 1:1000 in block buffer for 30 minutes. The mounting of cover slips and imaging steps were the same as the previous chapter. The FMS patient cohort and healthy control cohort were then tested for anti-LGI1 and anti-CASPR2 AAbs using this protocol at 1:20 and 1:100 respectively.

2. Plexin D1 CBA

The 96-well plate CBA protocol was used to detect anti-Plexin D1 AAbs. Patient sera were added to live cells followed by fixation and permeabilization of cells, using the same reagents as earlier but at a volume of 100uL. The cells were permeabilised due to the Myc tag on Plexin-D1

being located on its cytoplasmic domain. The following steps carried out were the same as in the previous chapter, except the addition of a secondary goat anti-human IgG (H + L), Alex Fluor 488 (A-11013, Thermo Fisher Scientific) to detect the patient IgG with a green fluorescence. Thus, the staining mixture comprised of goat anti-human IgG (Alexa Fluor 488) at 1:750, goat anti-rabbit IgG (Alexa Fluor 568) at 1:750, and DAPI at 1:1000 in block buffer. The cells were imaged whilst in a PBS solution. This CBA to detect anti-Plexin D1 AAbs was validated using 20 healthy controls and the patient positives were re-tested on a 24-well plate CBA at serial dilutions of 1:20, 1:50, and 1:100 as well as on untransfected cells.

3.2.5 Carry-on CBA

The optimized 96-well plate CBA protocol used for the normal CBA protocol matched the carry-on CBA protocol for patient testing, except the permeabilization step. This was due the Myc-tag being expressed extracellularly for both "carried-on" antigen targets, cytoplasmic FGFR3 and full-length MX1. Thus, both patient sera and anti-myc tag antibodies were added in a singular step with 1:10 patient sera in 25uL block buffer and 1:500 anti-Myc tag antibody in 25 uL block buffer that added up to 50uL of 1:20 patient sera and 1:1000 anti-Myc tag antibody. These were prepared separately due to the extremely low volume of anti-Myc tag antibody required for a total volume of 25uL at 1:500 as each patient sera sample was prepared individually. Thus, a 10mL stock solution of 1:500 anti-Myc tag antibody was first prepared and added to each well with patient sera. The remaining steps were the same as the normal CBA. The carry-on CBAs to detect anti-cytoplasmic FGFR3 AAbs and anti-MX1 AAbs were validated using 20 healthy controls and the patient positives were retested on a 24-well plate CBA at serial dilutions of 1:20, 1:50, and 1:100 as well as on untransfected cells. As a comparison to the carry-on CBAs, a fixed

and permeabilised CBA was also performed using the standard MX1 and FGFR3 plasmids used in the previous chapter. For MX1, the whole FMS patient cohort was tested at 1:20 due to lack of a pre-tested patient positive, and for FGFR3, the patient positive from Saint Etienne, France was tested at 1:20.

3.3 Results

Testing the SFN and FMS patient cohorts on the anti-intracellular FGFR3 AAb detection ELISA resulted in 11.1% seropositivity in SFN patients and 5.7% seropositivity in FMS patients, but reduced to 6.4% and 3.8% respectively in repeat testing

Each 96-well plate tested ~20 patients ~4 healthy controls to allow each plate to have its own positivity threshold set at 3 standard deviations above the mean of the healthy controls. Initial testing with the 20 healthy controls used to develop the ELISA with the additional healthy controls tested on each plate resulted in a positivity threshold of 0.28 OD units calculated as 3 standard deviations above the mean of the healthy controls (Figure 13, A). However, it can be seen that there is a gap on the plot at about 0.4 OD units, which could signify a true positivity threshold. This resulted 8/72 SFN patients testing as seropositive for anti-intracellular FGFR3 AAbs (11.1%) and 3/53 FMS patients testing as seropositive for anti-intracellular FGFR3 AAbs (5.7%). The same positive patient samples were retested using the same protocol but with an additional 50 healthy controls to increase the statistical power of the assay to >80%. Figure 3.1 B shows the reduction in patient positive samples to 6.4% in SFN patients and 3.8% in FMS patients. It must be noted that 1 patient positive sample from the SFN patient cohort could not be retested due to insufficient patient serum volume (SFN371). The reduction in patient positives is

due to an increased positivity threshold set by the higher than before OD values of the healthy controls. It can be observed that the positive samples that tested negative upon retesting had lower antibody titres that were close to the positivity threshold, signified by lower OD values, than those that remained positive (Figure 13, A and B). Thus, the ELISA's ability to detect low-positive samples is critically dependent on the positivity threshold set.

A

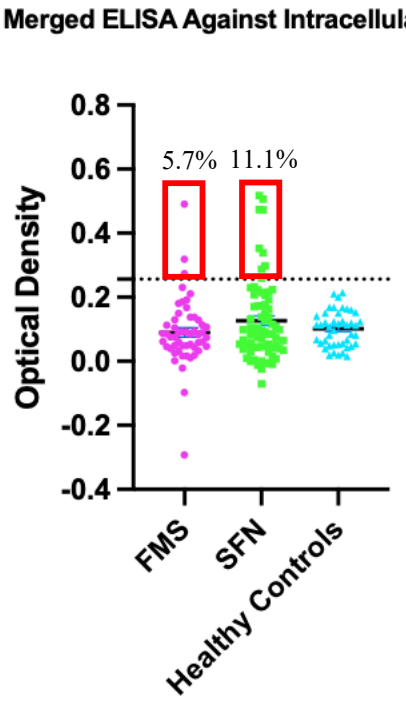

B

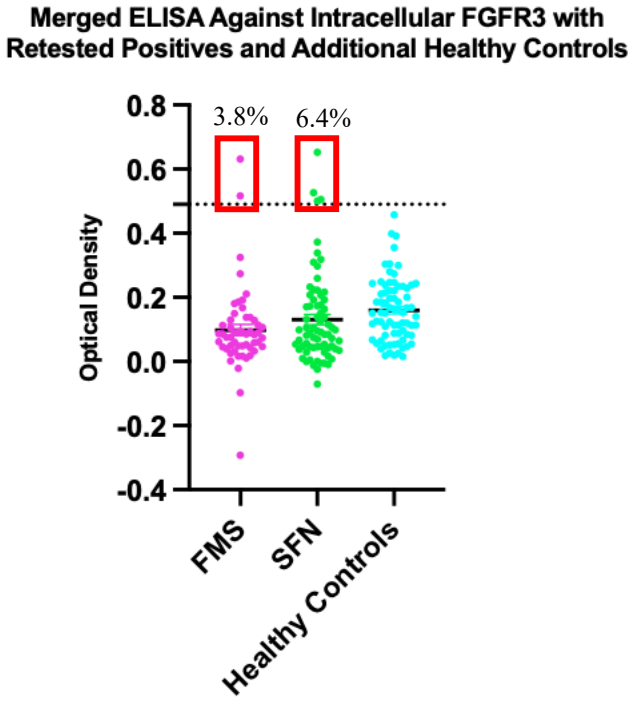

Figure 13: A) The dot blot shows merged and normalized data from the multiple plates tested using the anti-intracellular FGFR3 AAb detection ELISA on SFN and FMS patients with healthy controls. B) This merged plot retesting the patient positives resulted in a new positivity threshold as it combines more healthy control OD values. The red boxes highlight the patients with normalized OD values above the positivity threshold and the percentages correspond to the proportion of anti-intracellular FGFR3 AAb positive patients in each total cohort.

Testing the anti-LGI1 patient positive sera on the CBA at serial dilutions produced gradually less intense binding to LGI1 and testing the FMS patient cohort on the CBA resulted in 0% seropositivity for anti-LGI1 AAbs

For benchmarking what a patient seropositivity for AAbs against surface antigens looks like under the confocal microscope, the LGI1 CBA was used with a pre-tested patient positive sample received by our collaborator in the autoimmune neurology diagnostic lab at the JR Hospital, Oxford. The patient positive sample was tested at serial dilutions of 1:20, 1:50, and 1:100 with 1:20 being the standard dilution (Figure 14 A). This allowed the visualization of

strong to weak seropositivity. The FMS patient cohort was tested for anti-LGI1 AAbs and resulted in 0% seropositivity (Figure 14 B).

A

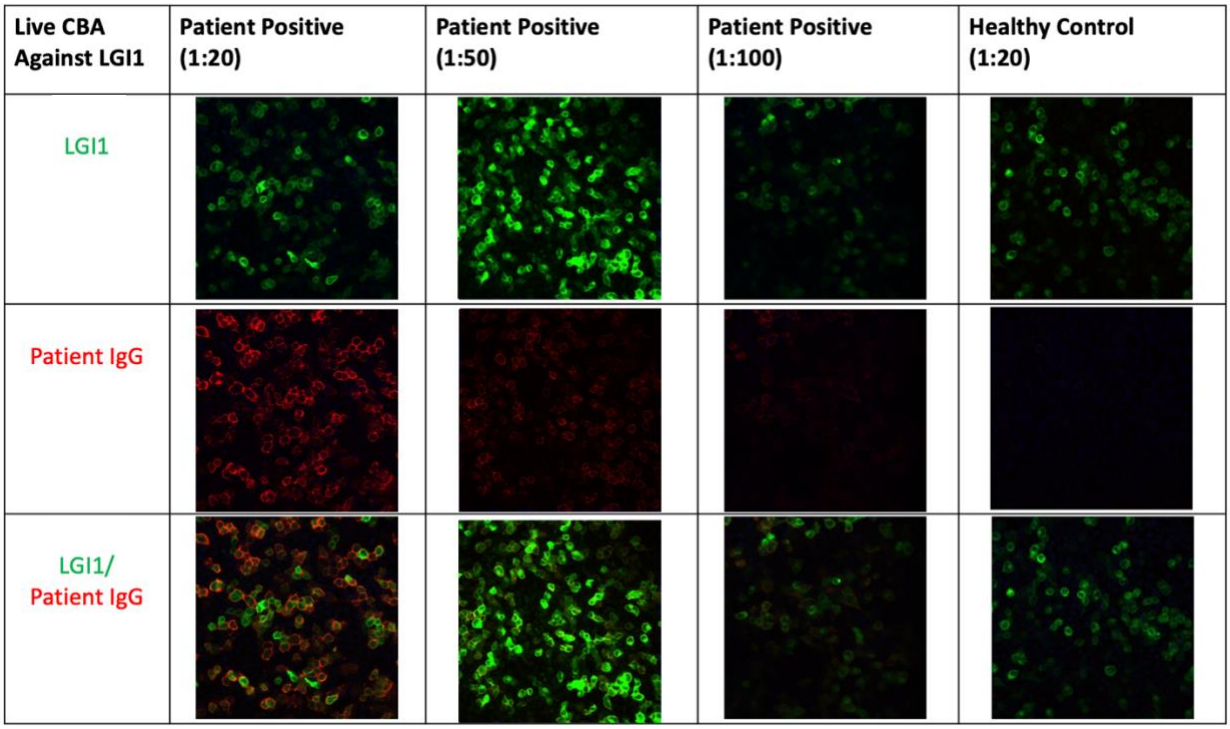

B

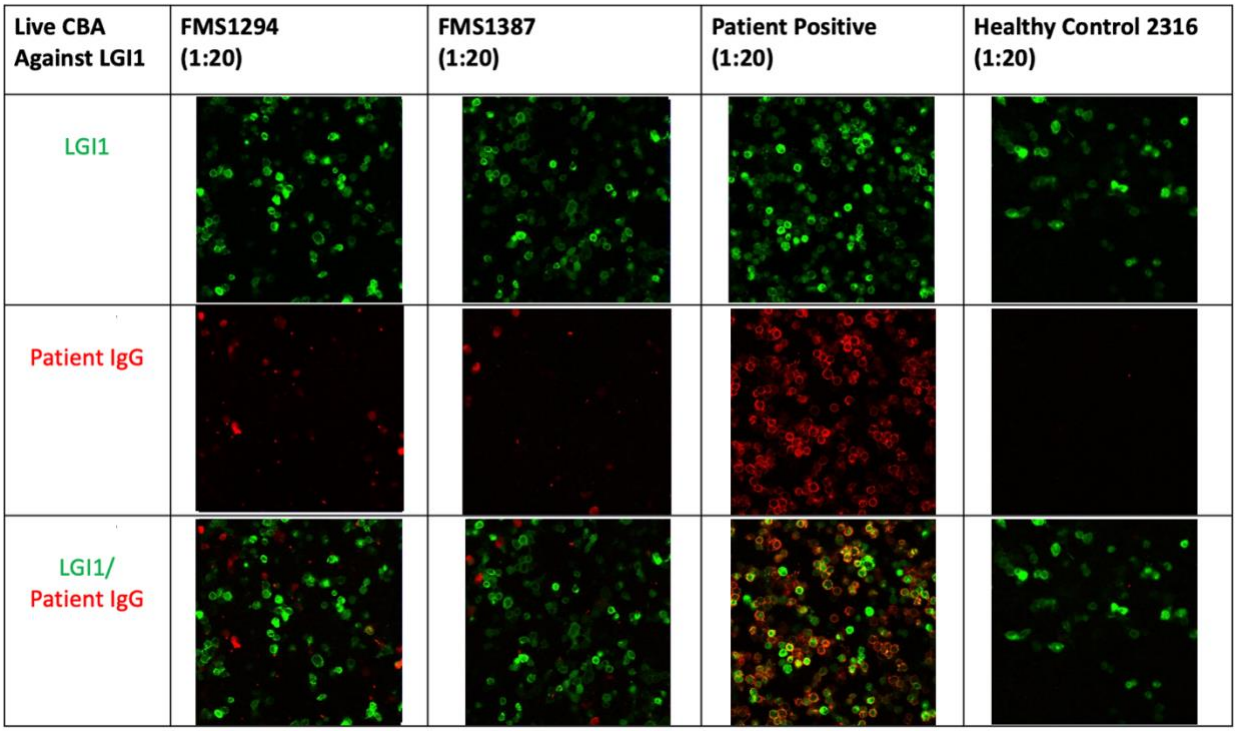

Figure 14: A) Anti-LGI1 AAb detection CBA using a pre-tested patient positive sample at serial dilutions of 1:20, 1:50, and 1:100. Seropositivity is measured in the composite images with patient IgG binding (red) overlapping with eGFP-LGI1 (green). B) Anti-LGI1 AAb detection CBA using a pre-tested patient positive sample, two representative FMS patient samples, and a healthy control at 1:20. Seropositivity in FMS patients = 0%.

Testing the anti-CASPR2 patient positive sera on the CBA at serial dilutions produced gradually less intense binding to CASPR2 and testing the FMS patient cohort on the CBA resulted in 0% seropositivity for anti-CASPR2 AAbs

For benchmarking what a patient seropositivity for AAbs against surface antigens looks like under the confocal microscope, the CASPR2 CBA was used with a pre-tested patient positive sample received by our collaborator in the autoimmune neurology diagnostic lab at the JR Hospital, Oxford. The patient positive sample was tested at serial dilutions of 1:100, 1:500, and 1:1000 with 1:100 being the standard dilution (Figure 15 A). This allowed the visualization of

strong to weak seropositivity. The FMS patient cohort was tested for anti-CASPR2 AAbs and resulted in 0% seropositivity (Figure 15 B).

A

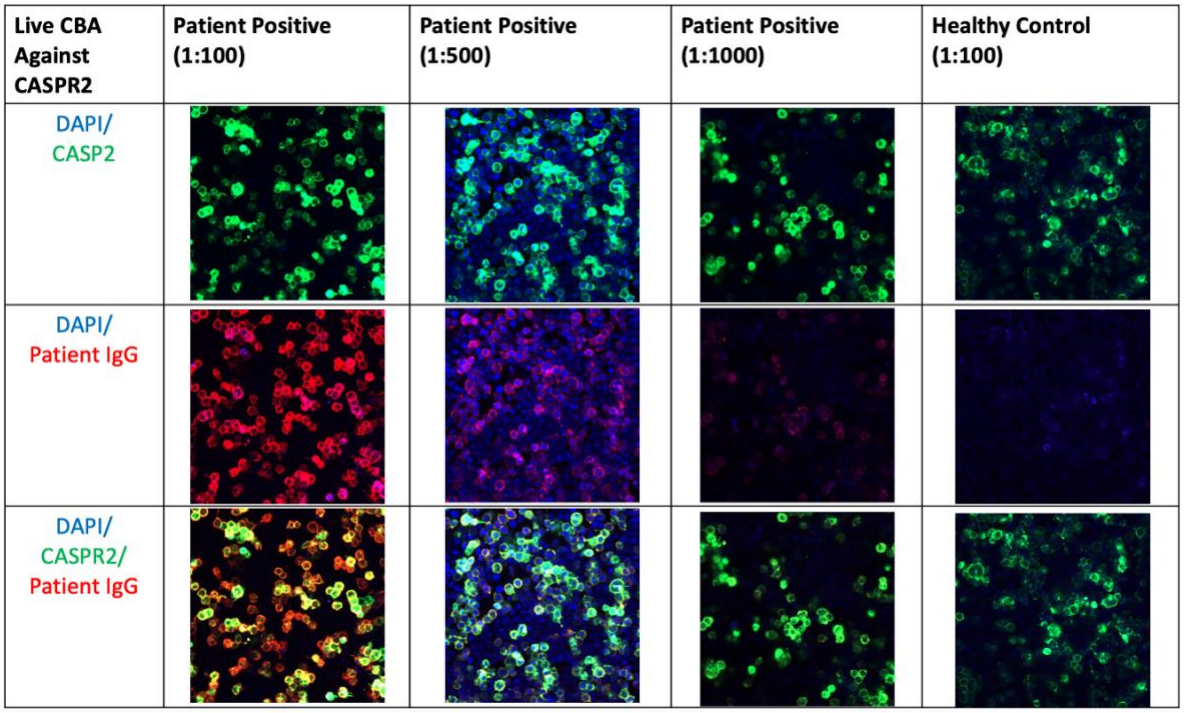

B

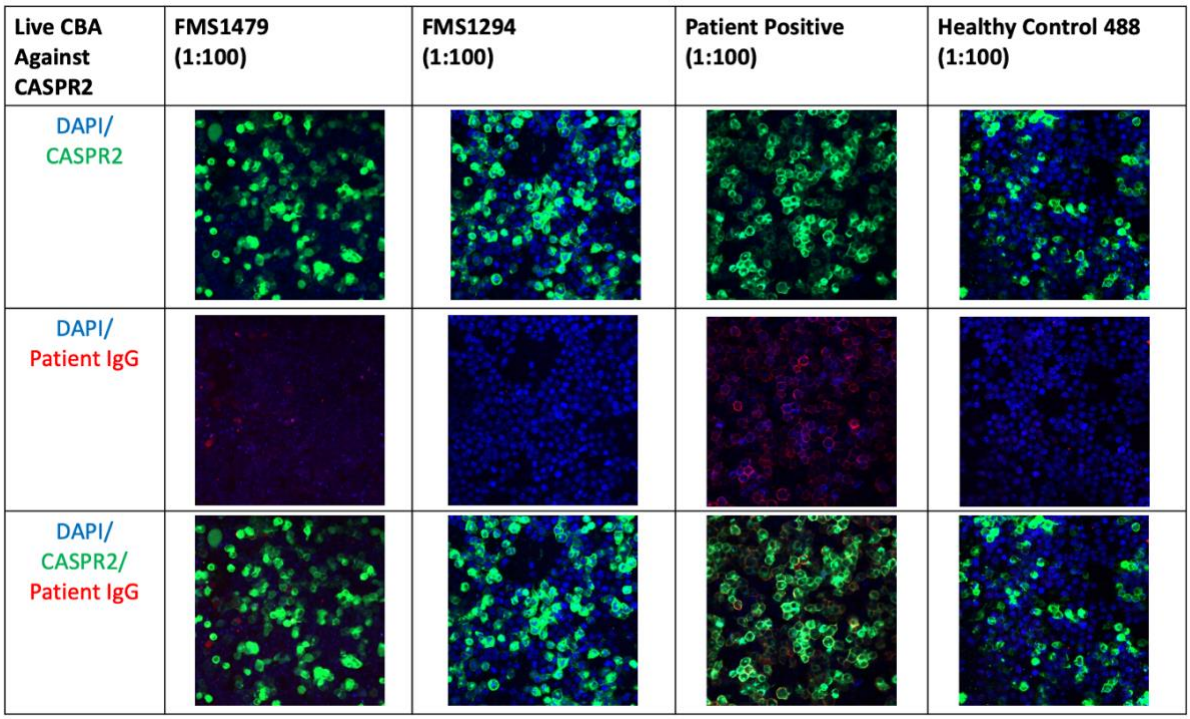

Figure 15: A) Anti-CASPR2 AAb detection CBA using a pre-tested patient positive sample at serial dilutions of 1:100, 1:500, and 1:1000. Seropositivity is measured in the composite images with patient IgG binding (red) overlapping with eGFP-CASPR2 (green) and the nuclei of the HEK293T cells. B) Anti-CASPR2 AAb detection CBA using a pre-tested patient positive sample, two representative FMS patient samples, and a healthy control at 1:100. Seropositivity in FMS patients = 0%.

Testing the SFN patient cohort on the Plexin D1 CBA resulted in 2.8% seropositivity for anti-Plexin D1 AAbs and 1.9% in the FMS patient cohort

The standard live CBA protocol to detect anti-extracellular Plexin D1 AAbs was tested using 20 healthy control samples at 1:20 followed by the testing of patient samples. This resulted in 2/72 SFN patients testing as seropositive for these AAbs (Figure 16 A). and 1/53 FMS patients testing as seropositive for these AAbs (Figure 16 B). The cells were counterstained with DAPI and showed significant cell size reduction and cell death (Figure 16, A and B). Apart from the myc-tag used to identify successful transfection of Plexin-D1 in the HEK cells, a commercial antibody against the extracellular domain of Plexin-D1was also used on unpermeabilized HEK

cells to confirm that the extracellular domain was oriented in its proper conformation, thus acting as a positive control. However, this positive control was only used during the development of the assay and not on the cells tested with patient samples due to potential competitive binding between the commercial antibodies and the patient antibodies.

A

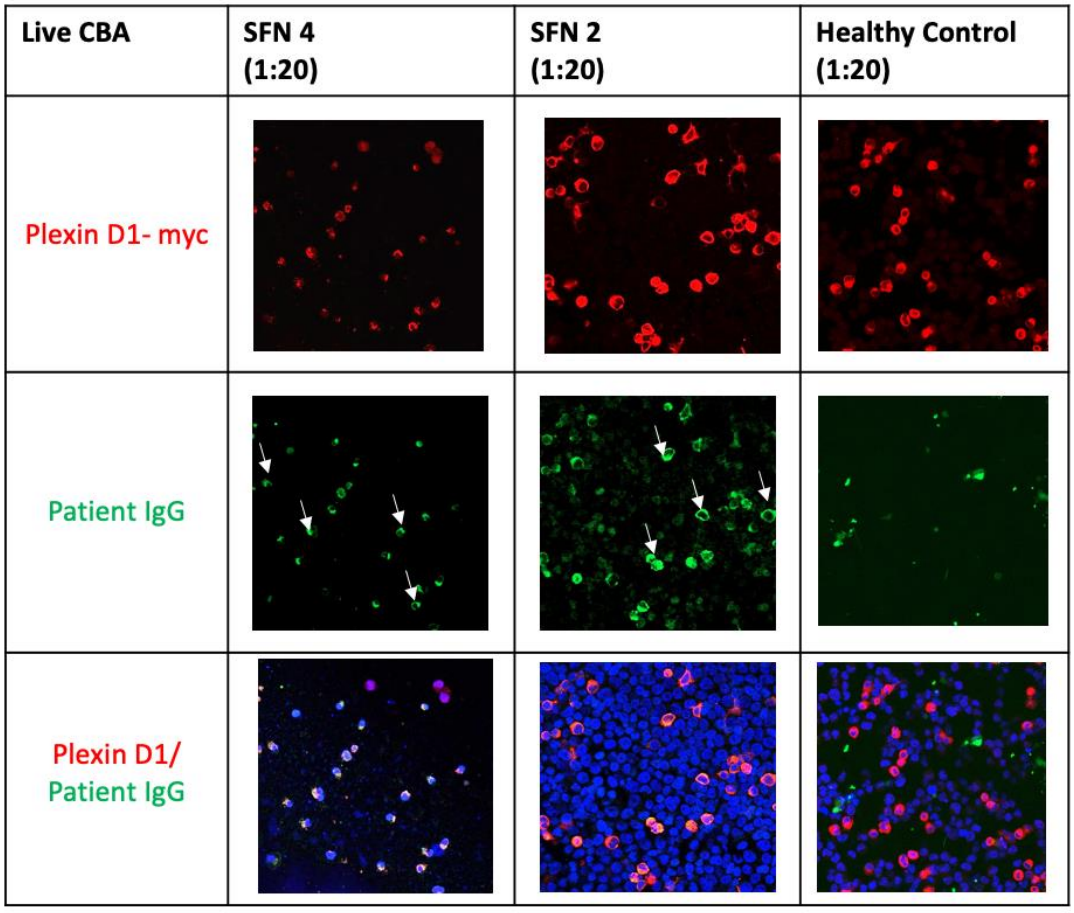

B

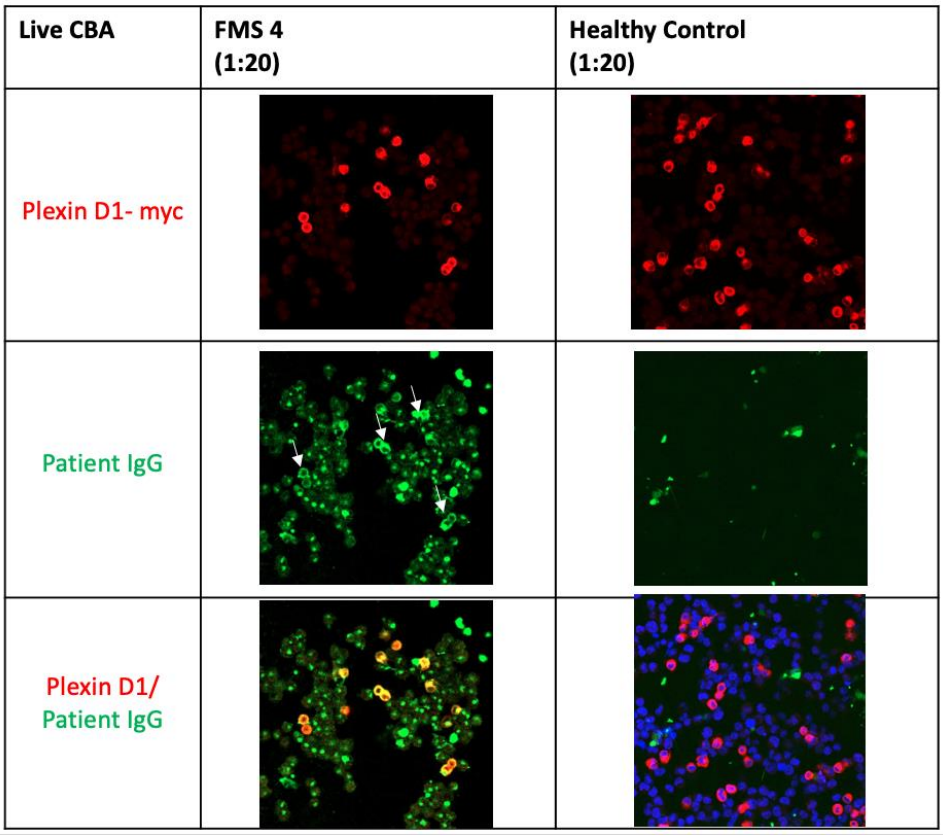

Figure 16: A) Anti-extracellular Plexin D1 AAb detection CBA used to test SFN patient cohort with the 2 seropositive patients shown. Seropositivity in SFN patients = 2.8%. Seropositivity is measured by observing colocalisation of patient IgG binding (green) with Plexin D1-myc (red) and nuclei of HEK293T cells were counterstained with DAPI. B) Anti-extracellular Plexin D1 AAb detection CBA used to test FMS patient cohort with the 1 seropositive patient shown. Seropositivity in FMS patients = 1.9%.

Testing the anti-intracellular FGFR3 AAb positive patient serum on a standard CBA with full-length FGFR3 in its native conformation resulted in high background binding of patient IgG and the same result was seen for the anti-MX1 AAb standard CBA

The standard fixed and permeabilised CBA protocol to detect anti-FGFR3 AAbs from Chapter 2, both intracellular and extracellular, was tested using the patient positive sample tested by Saint-Etienne, France at 1:20 but showed high background binding (Figure 17 A). The standard fixed and permeabilised CBA protocol to detect anti-MX1 AAbs from Chapter 2, with full-length

intracellular MX1, was used to test the entire FMS patient cohort at 1:20 resulting in 0% seropositivity (Figure 17 B). However, scoring could not be done with clarity due to high background patient IgG binding in all patent samples, similar to the fixed and permeabilised anti-FGFR3 CBA.

A

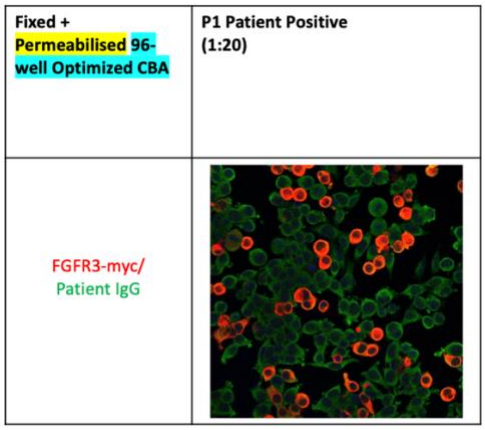

B

Fixed + Permeabilised CBA Against MX1	FMS 4 (1:20)	FMS 3 (1:20)
DAPI/ Myc	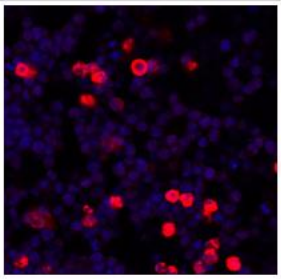	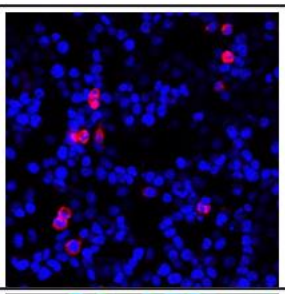
DAPI/ Patient IgG	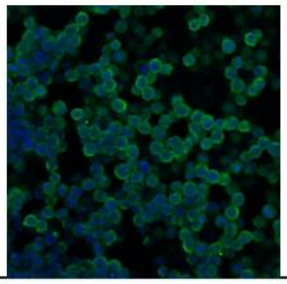	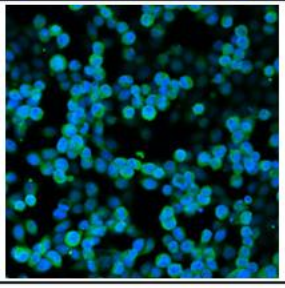
DAPI/ Myc/ Patient IgG	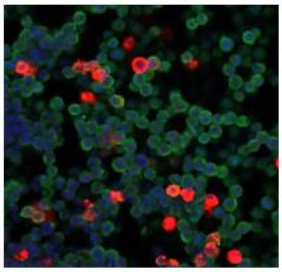	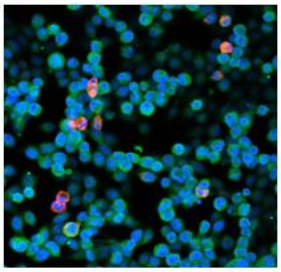

Figure 17: A) Anti-FGFR3 AAb detection CBA with fixed and permeabilised HEK293T cells used to test the pre-tested patient positive sample at 1:20. Seropositivity is measured by observing colocalisation of patient IgG binding (green) with FGFR3-myc (red). B) Anti-MX1 AAb detection CBA with fixed and permeabilised HEK293T cells used the FMS patient cohort at 1:20. Seropositivity is measured by observing colocalisation of patient IgG binding (green) with MX1-myc (red) and the nuclei of the HEK293T cells were counterstained with DAPI.

Testing the SFN patient cohort on the carry-on CBA with truncated cytoplasmic FGFR3 resulted in 12.5% seropositivity for anti-intracellular FGFR3 AAbs and 13.2% in the FMS patient cohort

The carry-on CBA to detect anti-intracellular FGFR3 AAbs on live HEK293T cells was tested using 20 healthy control samples at 1:20 followed by the testing of patient samples. This resulted in 8/72 SFN patients testing as seropositive for these AAbs (Figure 18 A) and 7/53 FMS patients testing as seropositive for these AAbs (Figure 18 B). The cells were counterstained with DAPI. The stronger the colocalisation of patient IgG binding (green) and carried-on cytoplasmic FGFR3, the more intense the yellow colour on the composite image is. Out of the 20 healthy controls tested, none showed positive binding at 1:20.

A

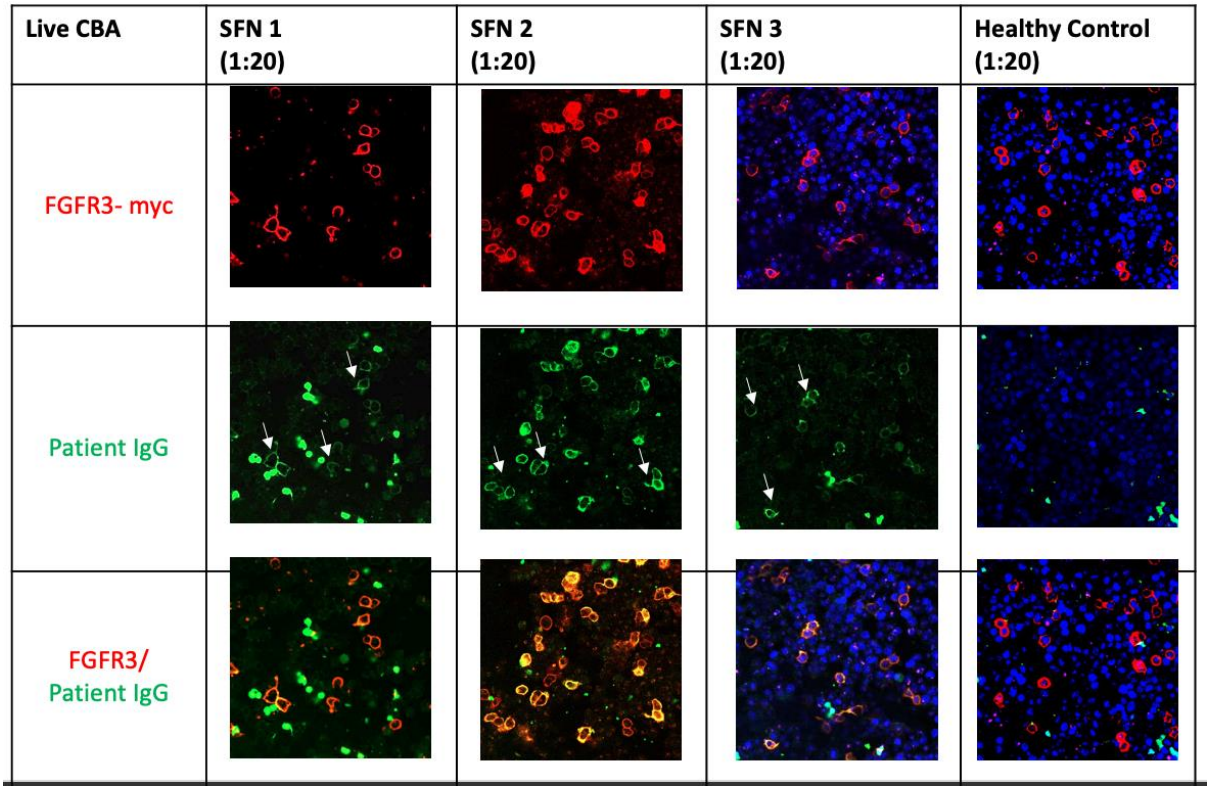

B

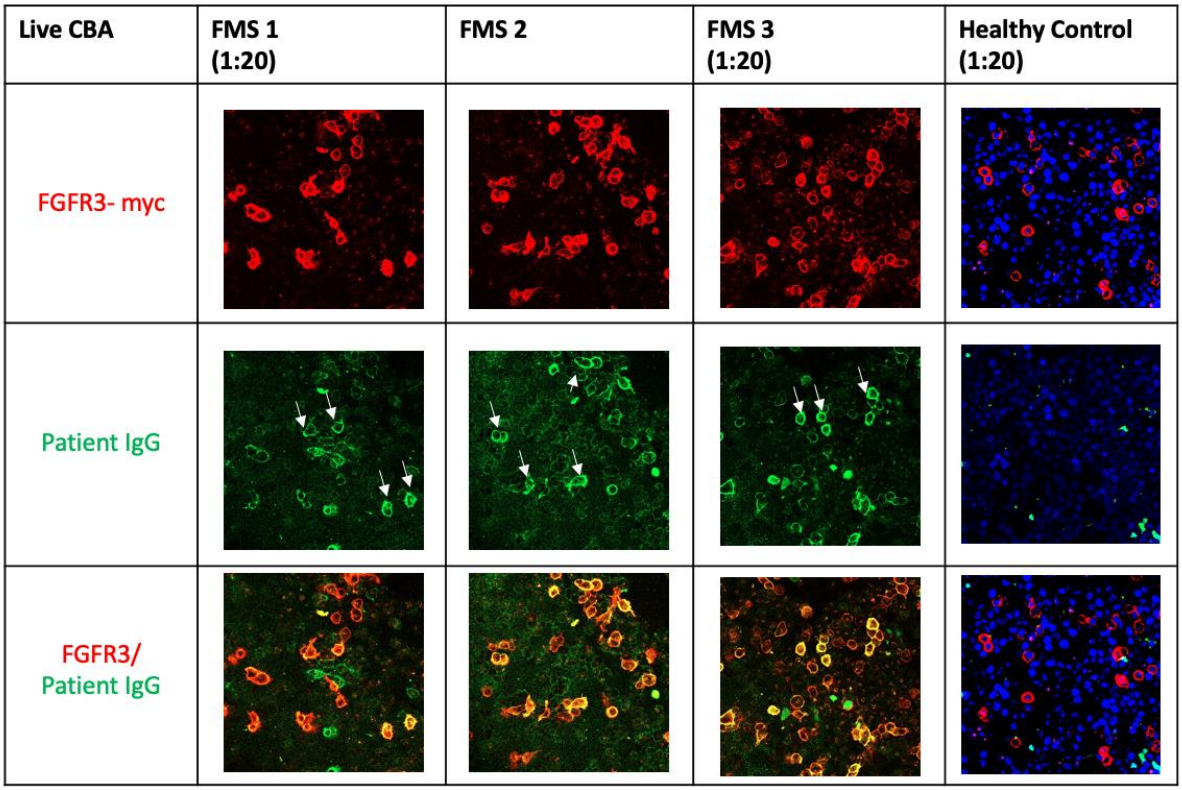

Figure 18: A) The carry-on CBA with truncated cytoplasmic FGFR3 was used to detect anti-intracellular FGFR3 AAbs in the SFN patient cohort. Seropositivity is measured by observing colocalisation of patient IgG binding (green) with carried-on cytoplasmic FGFR3-myc (red) and nuclei of HEK293T cells were counterstained with DAPI. Seropositivity in SFN patients = 12.5%. B) The carry-on CBA with truncated cytoplasmic FGFR3 was used to detect anti-intracellular FGFR3 AAbs in the FMS patient cohort. Seropositivity in FMS patients = 13.2%.

Testing the SFN and FMS patient cohorts on the carry-on CBA full-length MX1 resulted in 0% seropositivity for anti-MX1 AAbs in both patient cohorts

The carry-on CBA to detect anti-MX1 AAbs on live HEK293T cells was tested using 20 healthy control samples at 1:20 followed by the testing of patient samples. This resulted in no patients testing as seropositive for these AAbs in both cohorts, only background patient IgG binding to supposed dead cells (Figure 19). The cells were counterstained with DAPI.

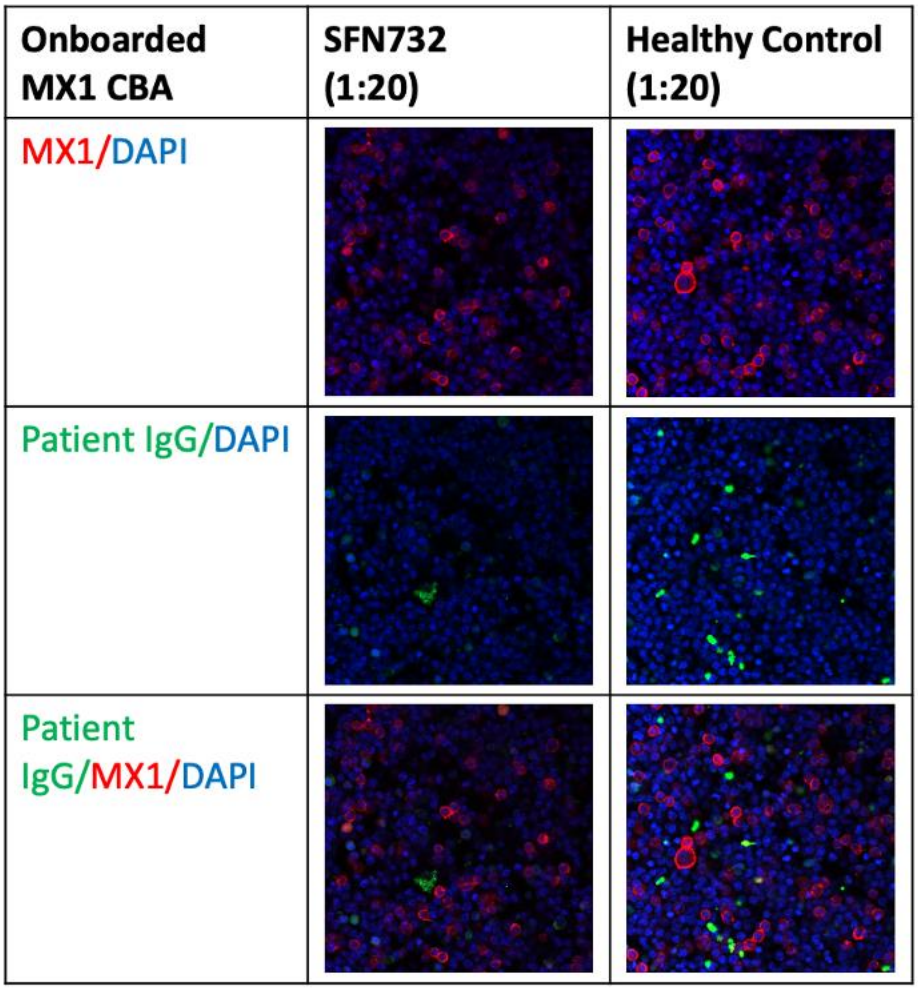

Figure 19: The carry-on CBA with full-length MX1 was used to detect anti-MX1 AAbs in the SFN and FMS patient cohorts at 1:20 with no patient positives found. Seropositivity is measured by observing colocalisation of patient IgG binding (green) with carried-on cytoplasmic MX1-myc (red) and nuclei of HEK293T cells were counterstained with DAPI. Seropositivity in SFN and FMS patients = 0%.

All anti-Plexin D1 AAb seropositive patients on the CBA were negative on the re-test

Re-testing the 3 total patient positives from both SFN and FMS patient cohorts on the anti-Plexin D1 CBA resulted in a loss of this seropositivity for anti-extracellular Plexin D1 AAbs (Figure 20). The cells looked healthier in this 24-well plate assay compared to the 96-well plate assay

(Figure 16 and Figure 20). There is some binding of patient IgG (green) but it looks more like background binding to the surface of HEK293T cells rather than localized to Plexin D1.

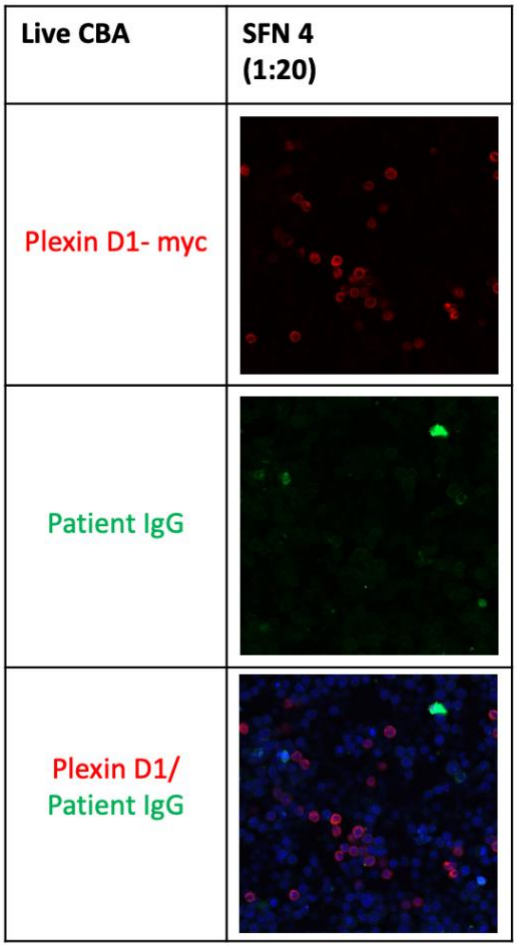

Figure 20: Anti-extracellular Plexin D1 AAb detection CBA used to re-test the patient positives from the SFN and FMS patient cohorts failed to replicate positivity. Seropositivity is measured by observing colocalisation of patient IgG binding (green) with Plexin D1-myc (red) and nuclei of HEK293T cells were counterstained with DAPI. Seropositivity in SFN and FMS patients = 0%.

All anti-intracellular FGFR3 AAb seropositive patients on the carry-on CBA remained positive on the re-test and showed a gradual reduction in binding at serial dilutions

Retesting the 8 SFN patient positive samples and the 7 FMS patient positive samples on the carry-on CBA with truncated cytoplasmic FGFR3 was 100% replicable in repeat seropositivity (Figure 21). Moreover, the patient positives were tested at serial dilutions of 1:20, 1:50, and

1:100 and on untransfected HEK293T cells as a negative control at 1:20. Anti-intracellular FGFR3 IgG from SFN 1 (SFN340) is shown to reduce with each serial dilution with the end point titer being between 1:50 and 1:100. The untransfected HEK293T cells show no patient IgG binding. All cells were counterstained with DAPI.

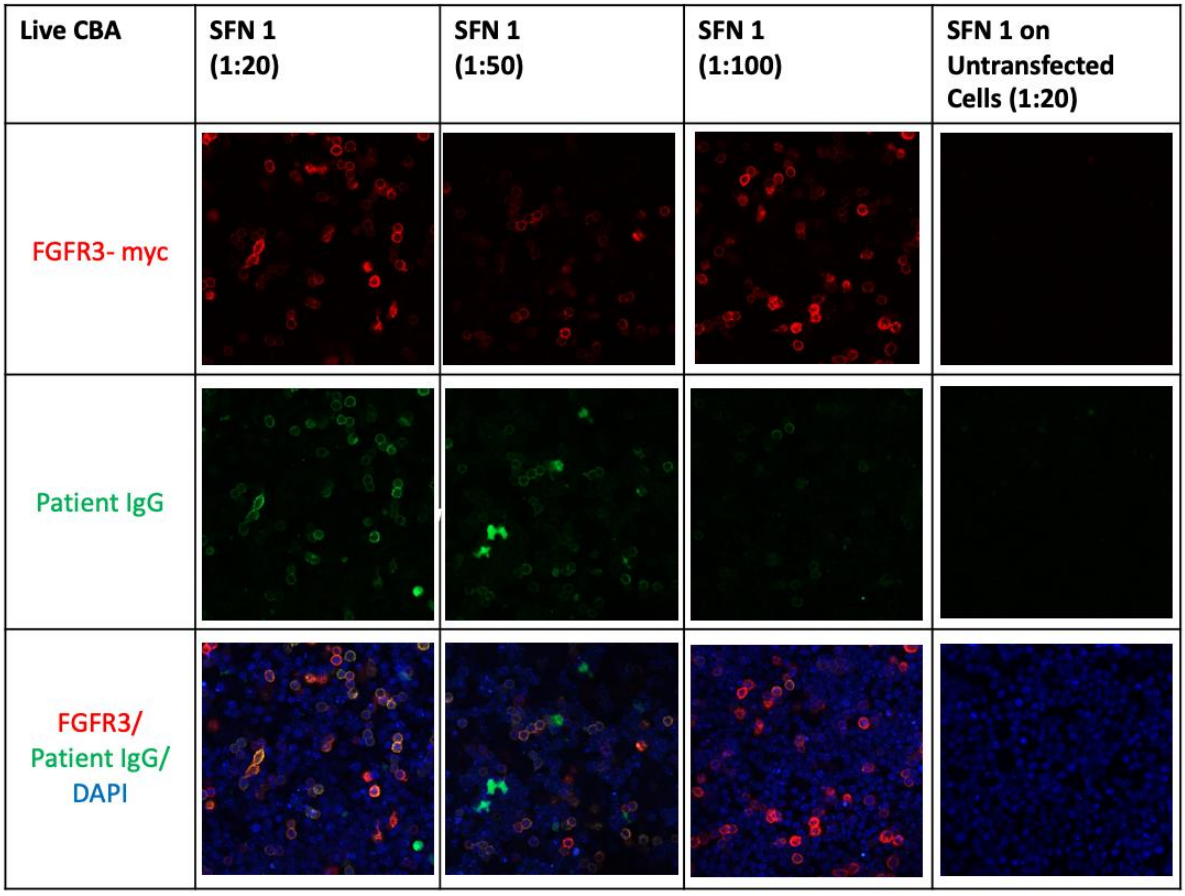

Figure 21: The carry-on CBA with truncated cytoplasmic FGFR3 re-testing patient positives for anti-intracellular FGFR3 in SFN and FMS patient cohorts showed replicability of all previous patient positives, with 1 representative sample shown (SFN 1). There was also a gradual reduction in patient IgG binding with serial dilutions from 1:20 to 1:100. Seropositivity is measured by observing colocalisation of patient IgG binding (green) with FGFR3-myc (red) and nuclei of HEK293T cells were counterstained with DAPI.

Antibody detection rates between the carry-on truncated cytoplasmic FGFR3 CBA and the cytoplasmic FGFR3 ELISA are associated rather than independent

Two assays were done to test for the presence of anti-intracellular FGFR3 AAbs: the ELISA and the carry-on CBA. The CBA found a total of 15 seropositive patients, 8/72 from the SFN patient cohort and 7/53 from the FMS patient cohort. While the ELISA found a total of 7 seropositive patients, 5/72 from the SFN patient cohort and 2/53 from the FMS patient cohort. There were 10 seropositive patients on the CBA that tested negative on the ELISA, 5/8 from the positive SFN patients and 5/7 from the positive FMS patients (Figure 3.9). In contrast, there were 2 seropositive patients on the ELISA that tested negative on the CBA, 2/5 from the positive SFN patients and 0/2 from the positive FMS patients. Thus, the carry-on CBA detected more seropositive patients, making it a more sensitive assay for detecting anti-intracellular FGFR3 AAbs. This association of antibody detection rates between the carry-on CBA and the ELISA was tested for significance using Fisher's exact test ($p = 0.0002$) (Table 3.2). This association means that positivity on this ELISA is more likely if the sample tested positive on the CBA as well.

Table 4

P value and statistical significance			
Test	Fisher's exact test		
P value	0.0002		
P value summary	***		
One- or two-sided	Two-sided		
Statistically significant (P < 0.05)?	Yes		
Data analyzed	**Positive on ELISA**	**Negative on ELISA**	**Total**
Positive on CBA	5	10	15
Negative on CBA	2	108	110
Total	7	118	125
Percentage of row total	**Positive on ELISA**	**Negative on ELISA**	
Positive on CBA	33.33%	66.67%	
Negative on CBA	1.82%	98.18%	
Percentage of column total	**Positive on ELISA**	**Negative on ELISA**	
Positive on CBA	71.43%	8.47%	
Negative on CBA	28.57%	91.53%	
Percentage of grand total	**Positive on ELISA**	**Negative on ELISA**	
Positive on CBA	4.00%	8.00%	
Negative on CBA	1.60%	86.40%	

Figure 22

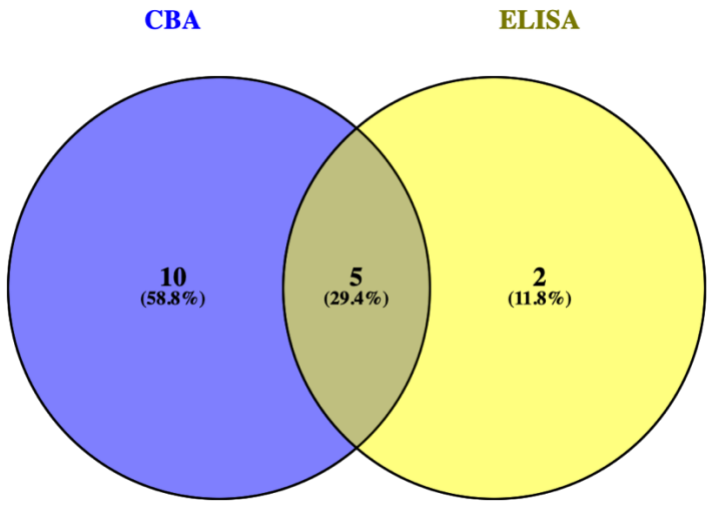

Table 4 and Figure 22: Table 4) A 2x2 contingency table with the results of the ELISA and CBA to detect anti-intracellular FGFR3 IgG. A Fisher's exact test found a significant association between seropositivity on the ELISA and seropositivity on the CBA ($p = 0.0002$). Figure 22) A Venn diagram measuring the number of seropositive patients for anti-intracellular FGFR3 IgG on the CBA (blue) and on the ELISA (yellow).

3.4 Discussion

The aim of this chapter was to use the assays developed in Chapter 2 on patient samples to test for AAb presence. Out of the antigen targets related to SFN, extracellular Plexin D1, intracellular FGFR3, and full length MX1 were chosen for patient AAb testing. For CBA seropositivity scoring, a benchmark was required to establish strong positive, weak positive, and seronegativity in patients. This was achieved using well-established LGI1 and CASPR2 CBAs on live HEK293T cells. The procurement of strong patient positives for each of these antigens helped mark this spectrum of positivity and acted as a positive control when testing the FMS patient cohort for anti-LGI and anti-CASPR2 AAbs.

The optimized 96-well plate CBA was used in place of a 24-well plate CBA with cover slips due to low SFN patient sera volumes and thus, all initial screening of patient samples was done on this optimized protocol, while repeat CBAs of patient positives were done on 24-well plate CBAs with cover slips. This was due to the 96-well plate CBA causing significant cell lift-off from the surface of the plate during washes, especially after fixation of cells. Moreover, the small surface area of the wells in the 96-well plate resulted in insufficient area for the cells to grow and thus, resulted in cell constriction and cell death.

The Plexin-D1 CBA developed in the previous chapter was used to test healthy controls, SFN, and FMS patient cohorts for anti-extracellular Plexin D1 AAbs using live HEK293T cells.

Not permeabilizing the cells allowed for the detection of only the AAbs against only the extracellular epitope of Plexin D1 since it is a transmembrane protein with its other components nested in the membrane and the cytoplasm of cells. Initial testing found 2/72 SFN patients positive for anti-extracellular Plexin D1 IgG and 1/53 FMS patients positive for this IgG. However, the cells were shrunken and there was high background patient IgG binding to cell fragments highlighting cell death, which could have been due to increased contact with 4% PFA in smaller wells. These patient positives were retested in a standard 24-well CBA with cover slips to find no positivity with low-level background patient IgG binding. The prevalence for anti-Plexin D1 IgG in SFN patients has been shown to be 12.7% using the ELISA, but the results from this project strongly contradict this (Fujii et al., 2021). The background binding can be general or due to the high concentration of patient sera (1:20) or due to the high reactivity of the patients' IgG to the HEK293T cell surface from possible previous immunotherapy.

The ELISA to detect anti-intracellular FGFR3 IgG that was developed in the previous chapter and tested on healthy controls was used to test SFN and FMS patient cohorts as well as an additional 50 healthy controls. After initial screening of patient samples and retesting of the positives, 5/72 SFN patients were seropositive and 2/53 FMS patients were seropositive. The prevalence of anti-FGFR3 IgG in SFN patients is 15 – 17% and the ELISA picked up 6.4% seropositivity in this idiopathic SFN patient cohort (Levine et al., 2019). The reduction in patient positives in the repeated assay was due to the increase in the positivity threshold set by the OD values of the healthy controls and slightly lower OD values of some of the previous patient positives. The healthy controls had higher OD values, and this could be due to natural reasons while the reduced OD values of some of the previously positive patient samples could be due to

reduction in the edge-effect that was mitigated by avoiding the well on the edges by distributing each patient test sample in varying distances from the centre of the plate. Thus, the ELISA is highly dependent on this positivity threshold and may miss out of low positive samples.

The carry-on CBA with truncated cytoplasmic epitope of FGFR3 with a myc-tag and attached to a CASPR2 tail to hold it in the cell membrane was developed in the previous chapter. The system is labelled as "carry-on" due to the intracellular component of protein being carried on by the CASPR2 tail to express outside the cell. This CBA was validated by testing healthy controls as a negative control and the pre-tested patient positive sample as a positive control. 8/72 SFN patients tested positive for anti-intracellular FGFR3 IgG and 7/53 FMS patients tested positive for this IgG. Thus, this system is more sensitive than the ELISA at detecting anti-intracellular FGFR3 IgG from patient sera and allows for the visualization of binding as compared to a simple quantitative output in an ELISA. The same system was used for the entirely cytoplasmic protein, MX1, wherein the full-length protein was carried by a CASPR2 tail in the membrane and had a myc-tag as well as an IL-22 signal sequence for secretion out of the cell. This system was developed in the previous chapter. This assay found no patient positives in either patient cohort. There is no set prevalence of anti-MX1 IgG in SFN patients, but a recent study found 11.9% seropositivity in a SFN patient cohort as a pilot study detecting anti-MX1 IgG using an ELISA (Chan et al., 2025). However, as a system it yielded lesser background patient IgG binding to the surface of HEK293T cells as compared to the fixed and permeabilised CBA with MX1 in its native conformation. Thus, this potentially means that the assay does detect ant-MX1 IgG, but there were no patients with anti-MX1 IgG in the patient cohorts tested.

Chapter 4: Comparing autoantibody seropositivity with clinical phenotypes

4.1 Introduction

Clinical overview of anti-Plexin D1, anti-FGFR3 IgG, or anti-MX1 IgG Positive Patients

One of the central reasons why AAb detection assays were developed for SFN, and are continuing to be optimized, is due to the potential for antigen specific AAb positivity to allow for the stratification of SFN patients. This stratification would be possible if seropositive patients had a unique clinical phenotypic profile. For instance, anti-Plexin D1 IgG seropositive SFN patients were reported to have a distinct clinical symptom profile characterized by significantly lower levels of burning pain despite having similar levels of tingling and numbing pain as other SFN patients (Murin et al., 2024). Moreover, seropositivity for either anti-Plexin D1 IgG or anti-FGFR3 IgG in SFN patients is more closely associated with inflammation than seronegative SFN patients (Zeidman et al., 2024). For anti-intracellular FGFR3 IgG seropositivity specifically, frequent paresthesia has been more strongly associated as compared to seronegative sensory neuropathy patients (Tholance et al., 2019). Moreover, these anti-intracellular FGFR3 IgG seropositive patients had significantly more abnormal sensory nerve action potentials (SNAPs) than the seronegative group. However, it must be noted that these results have only been observed in sensory neuropathy patients in general rather than idiopathic SFN patients in particular. For anti-MX1 IgG seropositivity, the only clinical characteristics noted to be significant were that seropositivity is higher in the "definite" SFN group, as characterized in the previous chapter, and is higher in SFN patients with autoimmune etiologies (Chan et al., 20215).

However, testing of clinical phenotypes of these seropositive patients, for Plexin D1, FGFR3, and MX1, has never been done in comparison to a large cohort of well-phenotyped idiopathic SFN patients in specific.

Clinical Overview of Small Fiber Pathology in FMS patients

Misdiagnosis of SFN patients with FMS is not uncommon and recently it was found that up to 40% of FMS patients have SFN as well (Farhad Khosro, 2019). This is due to the heterogeneity of FMS symptoms with strong overlap of SFN signature symptoms like chronic pain. Thus, clinical stratification of FMS patients is also highly useful for diagnosis and its co-occurrence with SFN may be able to support this stratification. Furthermore, it was recently found that anti-FGFR3 IgG was present in 3 out of a cohort of 68 FMS patients, supporting the idea that some FMS patients have autoimmune SFN (Seefried et al., 2025). However, the clinical characteristics of these anti-FGFR3 IgG positive FMS patients have not been explored.

4.2 Methods

Association Between Anti-FGFR3 IgG Positivity and SFN Phenotypic Data

Out of the DOLORisk study iSFN patient data of 72 patients, the characteristics that looked at symptom profile were chosen along with basic demographics like age. A total of 15 characteristics that looked at neuropathic pain related symptoms that were measured in the study and so all of these were tested to find any significant differences between these in the anti-intracellular FGFR3 IgG seronegative iSFN patients and the seropositive iSFN patients:

1. Age
2. Chronic pain duration

3. Upper limb symptoms
4. Burning cold
5. Paresthesia
6. Itching
7. Tingling
8. Numbness
9. Skin biopsy (nerve fibers/mm)
10. Paroxysmal pain
11. Hyperesthesia upon touch
12. Pins and needles
13. Douleur Neuropathique 4 (DN4) total score
14. Toronto Clinical Scoring System (TCSS) total score
15. Neuropathic Pain Symptom Inventory (NPSI) total score

The questionnaires and exams chosen, DN4, TCSS, and NPSI, all measure the presence and extent of nerve fiber damage as well as the type of damage through the use of questionnaires and physical examinations. For binary data (score yes or no), a 2 x 2 contingency table was made to calculate the association between anti-FGFR3 IgG seropositivity and the characteristic. A Fisher's exact test was done with $\alpha = 0.05$. For visualization, grouped bar graphs were made. For discrete data, a Welch's t test was done to calculate the association between anti-FGFR3 IgG seropositivity and the characteristic with $\alpha = 0.05$. For visualization, a grouped dot blot with marked averages and standard error of the mean (SEM) were made. Raw data values and segregation of data into Group 1, anti-intracellular FGFR3 IgG positive, and Group 2, anti-intracellular FGFR3 IgG negative was done on Microsoft Excel. Data analysis, statistical tests,

and graph creation was done on GraphPad Prism 10.6.1. Benjamini-Hochberg corrections were made using Microsoft Excel due to repeat hypothesis testing on the same data set. This is a type of False Discovery Rate (FDR) correction to control Type 1 errors.

Association Between Anti-FGFR3 IgG Positivity and FMS Phenotypic Data

Out of the FMS patient data of 53 patients tested, the characteristics that looked at symptom profile were chosen along with basic demographics like age. A total of 15 characteristics were tested to find any significant differences between these in the anti-intracellular FGFR3 IgG seronegative FMS patients and the seropositive FMS patients:

1. Age
2. Years since diagnosis
3. Symptom duration
4. Anxiety
5. Depression
6. Chalder Fatigue Scale (CFS) total score
7. Pain interference
8. Sleep efficiency
9. Widespread pain index (WPI) score
10. FMS index
11. Pittsburgh Sleep Quality Index (PSQI) total score
12. Alcohol consumption
13. Symptom severity
14. Chronic Pain Acceptance Questionnaire (CPAQ) total score

15. SF-36 pain intensity score

The questionnaires and exams that were chosen measure a range of symptoms from pain to sleep. For binary data (score yes or no), a 2 x 2 contingency table was made to calculate the association between anti-FGFR3 IgG seropositivity and the characteristic. A Fisher's exact test was done with $\alpha = 0.05$. For visualization, grouped bar graphs were made. For discrete data, a Welch's t test was done to calculate the association between anti-FGFR3 IgG seropositivity and the characteristic with $\alpha = 0.05$. For visualization, a grouped dot blot with marked averages and standard error of the mean (SEM) were made. Raw data values and segregation of data into Group 1, anti-intracellular FGFR3 IgG positive, and Group 2, anti-intracellular FGFR3 IgG negative was done on Microsoft Excel. Data analysis, statistical tests, and graph creation was done on GraphPad Prism 10.6.1. Benjamini-Hochberg corrections were made using Microsoft Excel due to repeat hypothesis testing on the same data set. This is a type of False Discovery Rate (FDR) correction to control Type 1 errors.

<u>Differences Between the Phenotypes of SFN Patients that Tested Positive on ELISA Compared to CBA for Anti-FGFR3 IgG</u>

The same 15 parameters were tested as the previous SFN comparison and the same statistical tests were done to measure any significant difference between anti-FGFR3 IgG seropositivity on the ELISA versus the CBA for inter-assay comparability. Associations were not made for FMS positives due to the low n = 2 on the ELISA.

4.3 Results

Anti-intracellular FGFR3 IgG seropositive iSFN patients are more likely to have lower ataxia scores, lower tingling pain, and less than 5 years of chronic pain than seronegative iSFN patients

Conducting comparative analysis on the 15 parameters set out, 3 of them showed significant differences between anti-intracellular FGFR3 IgG seropositive iSFN patients and those that are seronegative. The only significant differences observed were the presence of tingling pain and the duration of chronic pain symptoms were significantly lower in anti-intracellular FGFR3 seropositive patients (Figures 4.1 A and B respectively). For duration of symptoms, the 77.8% of the seropositive patients had less than 5 years of pain ($p = 0.0238$). These p values were corrected for multiple hypothesis testing using the Benjamini-Hochberg correction. This marks that being seropositive for these AAbs is associated with less severe clinical symptoms in iSFN patients.

A

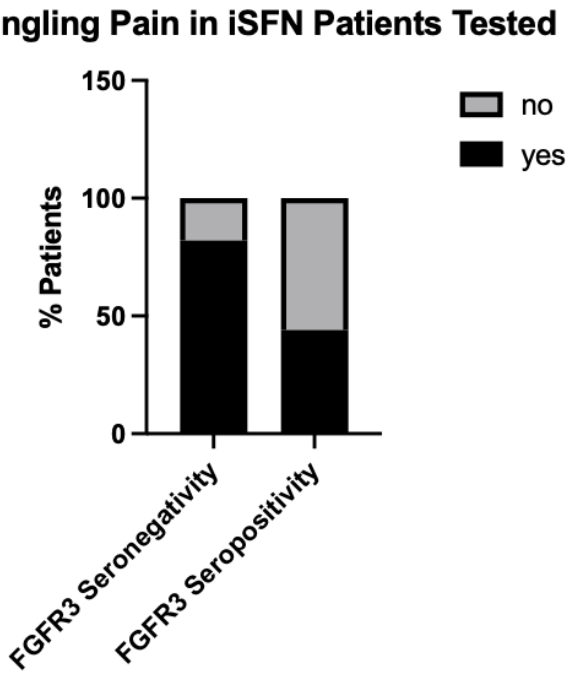
Tingling Pain in iSFN Patients Tested
150
100
50
0
% Patients
no
yes
FGFR3 Seronegativity
FGFR3 Seropositivity

B

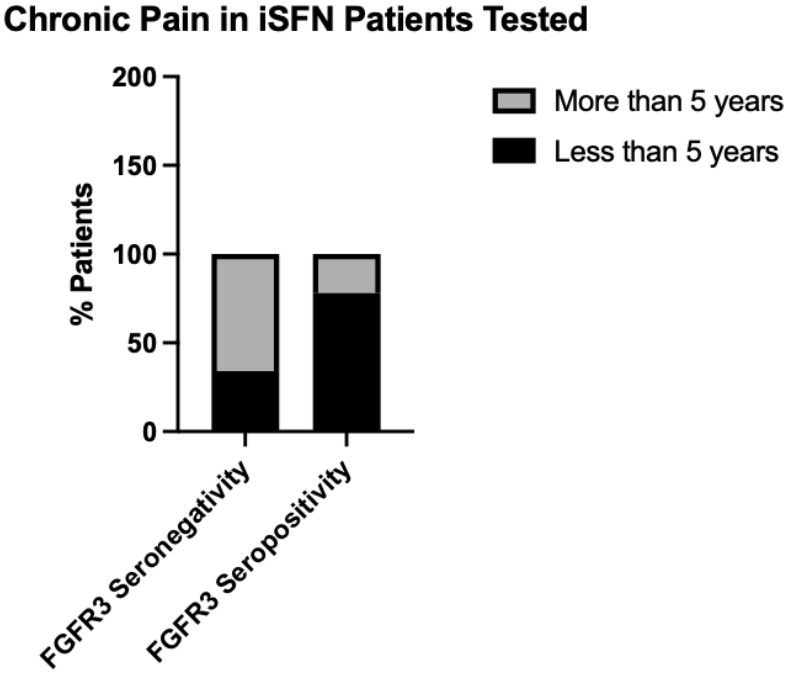
Chronic Pain in iSFN Patients Tested
200
150
100
50
0
% Patients
More than 5 years
Less than 5 years
FGFR3 Seronegativity
FGFR3 Seropositivity

C

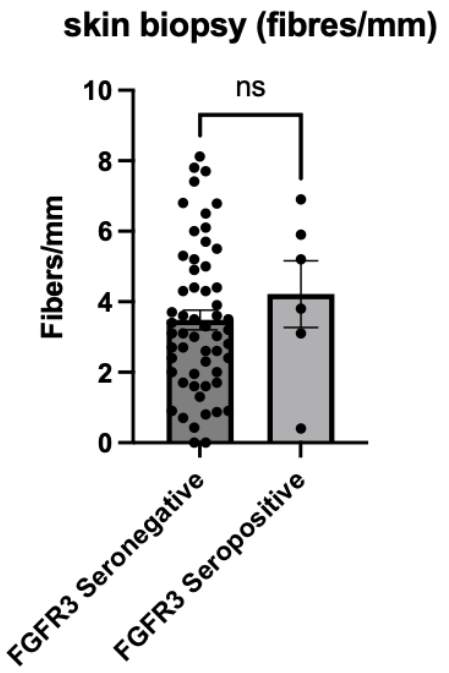
skin biopsy (fibres/mm)
ns
Fibers/mm
10
8
6
4
2
0
FGFR3 Seronegative
FGFR3 Seropositive

D

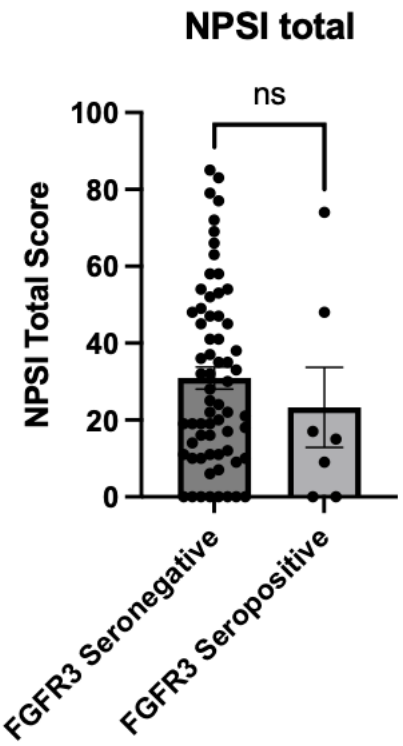
NPSI total
ns
NPSI Total Score
100
80
60
40
20
0
FGFR3 Seronegative
FGFR3 Seropositive

E

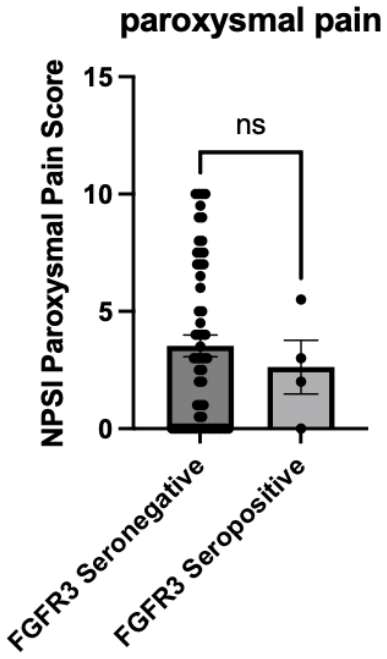
paroxysmal pain
NPSI Paroxysmal Pain Score
15
10
5
0
ns
FGFR3 Seronegative
FGFR3 Seropositive

F

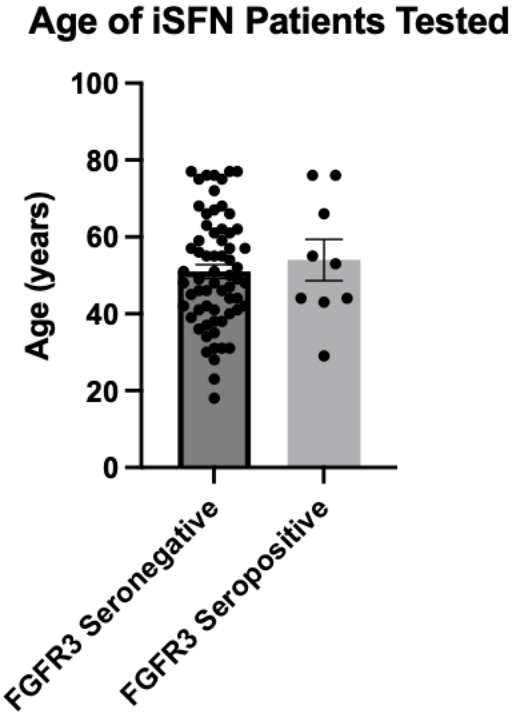
Age of iSFN Patients Tested
Age (years)
100
80
60
40
20
0
FGFR3 Seronegative
FGFR3 Seropositive

Figure 23: A) The 2x2 contingency analysis with the grouped bar graph shows that tingling pain scores are significantly higher in anti-intracellular FGFR3 IgG seronegative iSFN patients than seropositive patients with the y-axis representing the raw number of patients ($p = 0.0257$, Benjamini-Hochberg corrected). B) The contingency analysis with the grouped bar graph shows that there is a significantly higher number anti-intracellular FGFR3 IgG seronegative iSFN patients that have had chronic pain for over 5 years than seropositive patients ($p = 0.0238$, Benjamini-Hochberg corrected). C) A grouped dot plot with mean scores of nerve fiber density that were not significantly different between the anti-intracellular FGFR3 IgG seronegative iSFN patients and seropositive patients with the y-axis representing the fibers/mm ($p = 0.4872$). D) A grouped dot plot with mean scores of NPSI total scores that were not significantly different between the anti-intracellular FGFR3 IgG seronegative iSFN patients ($p = 0.5039$). E) A grouped dot plot with mean scores of paroxysmal scores that were not significantly different between the anti-intracellular FGFR3 IgG seronegative iSFN patients and seropositive patients ($p = 0.5009$). F) A grouped dot plot with mean age that were not significantly different between the anti-intracellular FGFR3 IgG seronegative iSFN patients and seropositive patients ($p = 0.6067$).

Anti-intracellular FGFR3 IgG seropositive FMS patients are more likely to have been diagnosed more recently than seronegative FMS patients

Conducting comparative analysis on the 15 parameters set out, 1 of them showed a significant difference between anti-intracellular FGFR3 IgG seropositive FMS patients and those that are seronegative. This was for the duration of FMS diagnosis, or the number of years since FMS diagnosis, and seropositivity for the AAbs was associated with a lower duration of FMS diagnosis ($p = 0.0033$, Figure 24). These p values were corrected for multiple hypothesis testing using the Benjamini-Hochberg correction. This marks that being seropositive for these AAbs is associated with less chronicity of diagnosis in FMS patients.

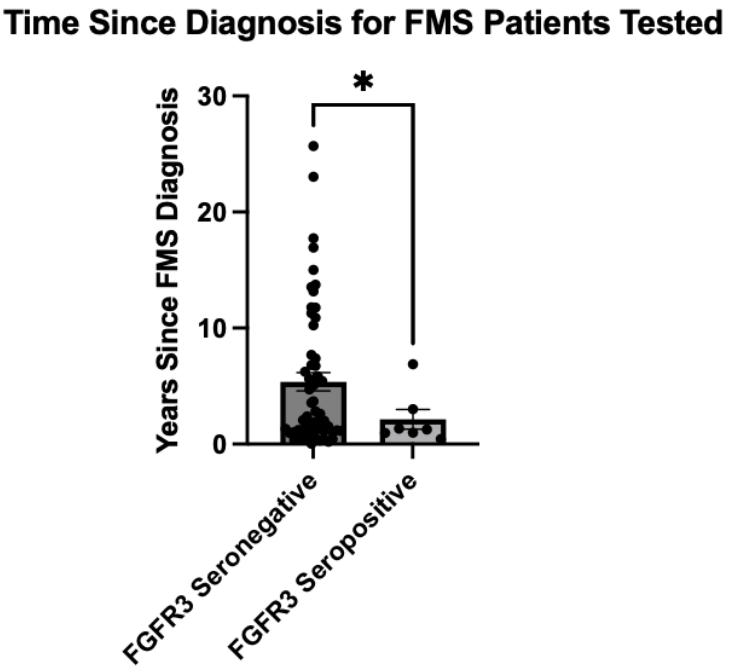

Figure 24: The grouped dot plot shows that anti-intracellular FGFR3 IgG seronegative FMS patients have been diagnosed for significantly longer than seropositive FMS patients with the y-axis representing years since FMS diagnosis ($p = 0.0113$, Benjamini-Hochberg corrected).

No phenotypic parameter was found to significantly differ between anti-intracellular FGFR3 IgG seropositive iSFN patients detected on the ELISA and those detected on the CBA

Out of the 15 parameters tested for a difference between anti-intracellular FGFR3 IgG seropositivity in iSFN patients detected on the ELISA versus the carry-on CBA, none were statistically significant. However, there was a marked difference in nerve fiber density values (nerve fibers/mm) wherein CBA positives had better skin biopsy results or a less clinically intense phenotype of iSFN than those detected on the ELISA ($p = 0.1814$, Figure 25). This could mean that in larger iSFN cohorts or with more patient positives, this association could become significant.

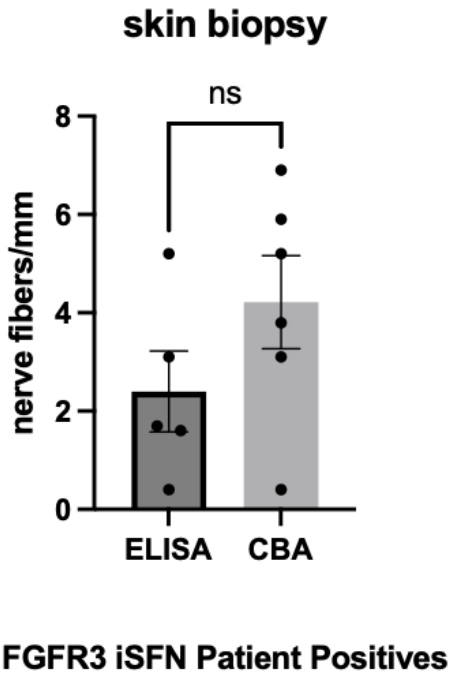

Figure 25: A grouped dot plot that shows no significant difference between nerve fiber density (nerve fibers/mm) in anti-intracellular FGFR3 IgG patient positives detected by ELISA and those detected by CBA (p = 0.1814, Benjamini-Hochberg corrected).

4.4 Discussion

One of the commonly seen clinical features of paresthesia that is associated with FGFR3 was not significantly different from the seronegative group (Nagaranjan et al., 2021; Tholance et al., 2020). Moreover, these results do not support a previous study where these AAbs were more common in females and patients with a more chronic disease course (Tholance et al., 2020). A limitation in this study of clinical phenotypes was a lack of skin biopsy tested for FMS patients and it was unknown if any of them had a small fiber pathology.

Chapter 5: Discussion

Efficiency and reliability of AAb detection assays are crucial, given that seropositivity can be important in determining diagnosis, prognosis, treatment approaches, and even provide insights into whether AAb presence plays a role in the pathogenesis of disease. As demonstrated, assays can be extremely sensitive to reagent changes and environmental factors making them difficult to universally reproduce. Moreover, existing antigen targets of AAbs found in SFN are promising but there are no studies detecting such AAbs in large cohorts of well-defined idiopathic SFN patients. Building on this novel concept of AAb mediated SFN, there is a growing interest in small fiber pathology in FMS patients as well as the presence of AAbs in these patients (Seefried et al., 2025). Thus, this thesis provides support to the ongoing work on AAbs in SFN, particularly those against FGFR3, as well as introduces the idea that these AAbs are present in FMS patients as well. This section highlights the key takeaways from this project and how they can help future endeavors in this field.

5.1 Summary of Key Findings and How They Fit with Current Literature

An effective ELISA and "carry-on" CBA system to detect anti-intracellular FGFR3 IgG in patient sera was developed

After optimization of a previously developed assay, a working ELISA to detect anti-intracellular FGFR3 IgG was developed. A possible reason for certain block buffers not working well to detect AAbs in patient sera is the masking of IgG by large proteins in the block buffer, like with casein in milk protein (Bloch et al., 2025). However, as compared to the literature, it only picked up 6.4% seropositivity in the SFN patient cohort as compared to the 15 – 17% prevalence reported (Nagaranjan et al., 2021; Tholance te al., 2020; Antoine et al., 2015), and compared to

the 12.5% from the carry-on CBA developed in this project. This is 48.8% less than the sensitivity of the carry-on CBA.

The carry-on system developed entails an engineered plasmid with the cytoplasmic component of the FGFR3 transmembrane protein stuck onto a CASPR2 tail with a Myc-tag in between. Some of these proteins managed to get expressed outside the cell, allowing for a dismissal of the permeabilization step of the CBA, significantly reducing background noise. This background makes interpretation of assays difficult and increases the chance of false positives. While this system does allow for targeting an intracellular epitope of a protein without cell permeabilization, it does not solve the issue of modelling the native conformation of this intracellular epitope. While the proposed conformation of the protein where the Myc-tag can be detected in unpermeabilised cells, the exact conformation of the expressed FGFR3 protein is unclear. Thus, while the Myc-tag does manage to get out of the cell, it is unknown if the cytoplasmic FGFR3 component folds into its functional sites, which are tyrosine kinase domains (TKD) (Tholance et al., 2021).

Additionally, a recent study has found that antibodies targeting the extracellular epitope of FGFR3 were pathogenic by inducing mechanical hypersensitivity in rat DRG neurons (Salih et al., 2025). This study only explored the extracellular epitope of FGFR3 despite the authors previously demonstrating that more patients are positive for IgG against the cytoplasmic epitope of FGFR3 (Tholance et al., 2021). Nevertheless, it adds a layer of complexity wherein patients with IgG against different epitopes of FGFR3 may be able to further stratify SFN patients if these patients have clinically distinct phenotypes.

A CBA to detect anti-Plexin D1 IgG was developed but is unclear regarding efficacy

The CBA to detect anti-extracellular Plexin D1 IgG was developed as an alternative to the ELISA developed by Fujii et al., 2021. While the CBA detected 3 seropositive patients from both SFN and FMS patient cohorts combined, these results were not replicable. This may be due to the decline in health of HEK293T cells in 96-well plates that caused background binding to the surface of these cells. Alternatively, the overexpression of Plexin-D1 may have contributed to the declining health of the cells. For example, it has been suggested that Plexin-D1 activates apoptosis pathways as seen with Semaphorin 3E suppressing tumor cell death triggered by the Plexin-D1 dependence receptor in metastatic breast cancers (Luchino et al., 2013). Another explanation is that antibodies binding to cells causes damage by activating complement pathways. It has been observed that certain AAbs can cause immune complement pathway activation and the incubation of patient sera with these complements, like C3 and C4, can cause significant HEK293T cell damage and death via membrane attack complexes (MAC) (Obaid et al., 2021). While not directly studied in anti-Plexin D1 specific IgG, this complement pathway activation could have acted synergistically with the constricted surface area of the wells to cause cell damage. A potential solution to limiting this would be to add heat-inactivated patient sera, however, this could denature the highly sensitive patient IgG proteins or cause them to aggregate (Hu et al., 2020). Moreover, the authors of the ELISA for Plexin D1 propose a cytoskeleton mediated cell death pathway, but this was not explored (Fujii et al., 2018).

The carry-on CBA to detect anti-intracellular FGFR3 IgG picked up the most seropositive patient samples at 12.5% for SFN patients and 13.2% for FMS patients

The carry-on CBA was far more sensitive than the ELISA as mentioned earlier and the results from it were 100% replicable. One particularly interesting finding was that 13.2% of the FMS patient cohort were found to be seropositive for these AAbs. My findings, now using our improved assay, suggest the number of FMS with FGFR3 might well be higher than previously thought and that FGFR3 might present a significant target in FMS (Seefried et al., 2025). Interestingly, these findings do support the idea of some overlap in idiopathic SFN and FMS, at least in terms of dysimmunity. Moreover, seropositive patients from both cohorts were comparatively early in their duration of disease which could mean that the presence of anti-FGFR3 IgG is associated with early onset SFN. This was met with a significantly lower frequency of seropositive SFN patients who answered yes to having ataxia and tingling pain compared to the rest of the cohort, which means the patients had lesser neuropathic damage. While ataxia is more commonly associated with dysfunction of large fibers and the cerebellum, it has been associated with SFN as well (Nolano et al., 2015).

The carry-on CBA to detect anti-MX1 IgG picked up no seropositive in both SFN and FMS patient cohorts, but reduced non-specific binding cell surface binding

The carry-on CBA developed for MX1 appears to work, however, without a positive control patient serum it is difficult to understand if it can detect seropositivity of patient anti-MX1 IgG. While it does detect the Myc tag on MX1 using an anti-Myc antibody, the detection of patient IgG itself was not seen. Thus, it is unclear if the system work or if the genuine prevalence of anti-MX1 IgG in both patient cohorts is 0%. So far, there is only one study examining the prevalence of MX1 and its pathogenicity in SFN patients (Chan et al., 2025). They do find seropositive patients using an ELISA and CBA, but the replicability of these results has not yet

been examined. Moreover, there is no overlap of seropositive patients detected on the ELISA and those detected on the CBA; a permeabilised CBA was utilized due to the intracellular subcellular location of MX1 and similar background binding of patient IgG to the cell surface was observed. However, in this case such background binding was considered seropositive despite the same level of patient IgG binding seen colocalized with MX1 as to cells that did not express MX1 (Chan et al., 2025). This widespread binding of patient IgG to the surface of HEK293T cells is considered background noise and would be considered seronegative for MX1 specific IgG because of a lack of conclusive colocalized binding (Woodhall et al., 2022).

5.2 Limitations

While this thesis provided insight, especially with regards to intracellular FGFR3 in SFN, there are limitations worth highlighting. In the ELISA to detect anti-intracellular FGFR3 IgG, the arbitrary seropositivity threshold set at 3 standard deviations above the mean of the healthy controls can often miss low positive samples. Moreover, this threshold is heavily dependent on the healthy controls' OD values, some of which may be high due to a number of reasons including background noise. This could be a reason for the lower number of seropositive samples resulting from the ELISA as compared to the "carry-on" CBA. As for the ELISA to detect the anti-extracellular Plexin-D1 IgG, it must be noted that a plausible explanation for the seropositive patient samples sent from Japan not coming up as positive on our ELISA is that the patient sera had denatured by the time they arrived in Oxford for testing.

For the CBA, using a 96-well plate caused significant HEK cell death and patient samples that tested negative were not repeated on the more favorable 24-well plate CBA,

potentially missing more patient positives for the "carry-on" CBA against intracellular FGFR3. Moreover, while serial dilutions of 1:20, 1:50, and 1:100 were done on the positive patient samples, the endpoint titres were not found. For the CBA against extracellular Plexin-D1, there was significant cell death potentially due to Plexin-D1's function in complement activation and overall toxicity to HEK cells. This signifies that a CBA may not be the best technique to test for anti-extracellular Plexin-D1 IgG seropositivity. For the MX1 CBA, other than the anti-myc antibody, there was no positive control to directly check for the presence and conformation of the MX1 protein; thus, a commercial antibody against MX1 would have been useful. Overall, for all CBAs there was variation in transfection rates that makes calculation of seropositivity scores less uniform. For the "carry-on" system specifically, the actual conformation of the intracellular FGFR3 protein and the full-length MX1 protein expressed extracellularly was not investigated. While for the FGFR3, a commercial antibody and an anti-myc antibody were used as positive controls, analyzing the actual conformations of these proteins with all their folding and active sites would have been useful. Overall, for the assays, having greater volumes of patient sera for the SFN cohort tested would have allowed for more robust testing on both the ELISA and the CBA. One of SFN patient positives could not be retested on the ELISA that was originally a high positive in terms of OD value.

Clinically, a few additional data measures would have been helpful for a better correlation of anti-intracellular FGFR3 IgG seropositivity with clinical phenotypes. One of the most important data points would have been nerve fiber density of the FMS patients tested and its relationship with anti-intracellular FGFR3 IgG seropositivity. This data would have provided a direct association of small fiber pathology in FMS patients to allow for correlation. Moreover,

for the clinical data tested, a few tests were not conducted on 1-2 seropositive patients. This would not have changed the significance of the difference between seropositive and seronegative patients but would still have been useful information. Additionally, while the Fisher's exact test statistically corrected for the small seropositive patient sample size being compared to the large seronegative patient sample size, the detection and addition of more seropositive patients to balance out the seronegative patients would have led to a more robust comparison.

5.3 Future Directions

This project completed its aims of developing and improving AAb detection assays against specific antigen targets associated with SFN as well as exploring the relationship between seropositivity of these AAbs and the clinical phenotypes of SFN and FMS patients. The use of an innovative approach to CBAs was also developed, labelled as the "carry-on" system to express cytoplasmic components of antigens outside the cells. Additionally, a clinically distinct phenotype was observed for anti-intracellular FGFR3 IgG seropositive SFN and FMS patients. This phenotype could demonstrate that IgG against FGFR3 signals autoimmune involvement in the early stages of SFN and increases the development of neuropathic pain, but is cleared out as the disease progresses. However, with the recent study on FGFR3 (Salih et al., 2025) on the pathogenicity of IgG against the extracellular component of FGFR3, there lies additional avenues of research that can be done. While this paper excludes anti-extracellular FGFR3 IgG seropositive patients, it adds a dimension wherein there may be a difference between the clinical phenotypes of patients seropositive for IgG against intracellular FGFR3 compared those seropositive for IgG against extracellular FGFR3. For FMS patients, this project provides the rationale for further exploration of the involvement of autoimmune SFN in FMS patients. The

findings of a robust number of patients positive for FGFR3 suggests a more prominent role of this antibody in FMS (Seefried et al., 2025). Next steps would be to screen for FGFR3 positivity in a much larger cohort of patients.

Lastly in terms of implications of seropositive patients in treatment, these patients may be eligible for immunotherapies such as IVIg as explored in the introduction. Alternatively, the development of monoclonal antibodies (mAbs) specifically targeting autoantigens, like FGFR3, to block the binding patient IgG could improve patient outcomes. Moreover, this thesis did not explore TS-HDS signifying that as both a limitation and a future avenue of study. Thus, this project has opened avenues of further exploration in the field of autoimmunity in idiopathic SFN.

References

Antoine, J.-C., Boutahar, N., Lassabliere, F., Reynaud, E., Ferraud, K., Rogemond, V., Paul, S., Honnorat, J., & Camdessanche, J.-P. (2015). Antifibroblast growth factor receptor 3 antibodies identify a subgroup of patients with sensory neuropathy. *Journal of Neurology, Neurosurgery & Psychiatry*, *86*(12), 1347–1355. https://doi.org/10.1136/jnnp-2014-309730

Baskozos, G., Hébert, H. L., Pascal, M. M. V., Themistocleous, A. C., Macfarlane, G. J., Wynick, D., Bennett, D. L. H., & Smith, B. H. (2023). Epidemiology of neuropathic pain: an analysis of prevalence and associated factors in UK Biobank. *PAIN Reports*, *8*(2), e1066. https://doi.org/10.1097/PR9.0000000000001066

Bloch, A., Zimmermann, J. F., Habermann, J., Ullrich, E., & Kolmar, H. (2025). A masking clamp for conditional activation of therapeutic antibodies. *Frontiers in Immunology*, *16*. https://doi.org/10.3389/fimmu.2025.1640427

Chamessian, A., Tavares-Ferriera, D., Payne, M., Govindarajan, R., Pestronk, A., Bertels, Z., Widman, A. J., Slivicki, R. A., del Rosario, J. S., Yi, J., Copits, B., Ornitz, D. M., Price, T. J., & Gereau, R. W. (2025). *Expression of Fibroblast Growth Factor Receptor 3 (FGFR3) in the Human Peripheral Nervous System: Implications for the Putative Pathogenic Role of FGFR3 Autoantibodies in Neuropathy*. https://doi.org/10.1101/2025.03.03.639509

Chan, A. C. Y., Huang, H., Shah, A., Zhang, B., Foo, N. W. J., Li, R., Mohammad Rizal, N. A. B., Wong, H. Y., Teoh, H. L., Mak, A., Soong, T. W., Sharma, V. K., & Schwarz, H. (2025). Interferon-induced GTP-binding protein MX1 drives hyperexcitability in peripheral nerves: a novel mechanism in small fiber neuropathy. *Journal of Neuroinflammation*, *22*(1), 219. https://doi.org/10.1186/s12974-025-03557-6

Chaudhary, U. J., & Rajabally, Y. A. (2021). Underdiagnosis and diagnostic delay in chronic inflammatory demyelinating polyneuropathy. *Journal of Neurology*, *268*(4), 1366–1373. https://doi.org/10.1007/s00415-020-10287-7

Cornacchini, S., Verza, M. U., Schiavolin, M., Spagni, G., Schiavo, E., Lotti, A., Farina, A., Leccese, D., Barilaro, A., Massacesi, L., & Damato, V. (2025). Neuropathic pain in CASPR2 antibody disease spectrum: A systematic review. *Journal of Neuroimmunology*, *408*, 578734. https://doi.org/10.1016/j.jneuroim.2025.578734

Daneshjou, K., Jafarieh, H., & Raaeskarami, S.-R. (2012). Congenital Insensitivity to Pain and Anhydrosis (CIPA) Syndrome; A Report of 4 Cases. *Iranian Journal of Pediatrics*, *22*(3), 412–416.

Danieli, M. G., Antonelli, E., Gammeri, L., Longhi, E., Cozzi, M. F., Palmeri, D., Gangemi, S., & Shoenfeld, Y. (2025). Intravenous immunoglobulin as a therapy for autoimmune conditions. *Autoimmunity Reviews*, *24*(1), 103710. https://doi.org/10.1016/j.autrev.2024.103710

Dawes, J. M., & Bennett, D. L. (2019). Autoantibodies and Neuropathic Pain. In *The Oxford Handbook of the Neurobiology of Pain* (pp. 833–850). Oxford University Press. https://doi.org/10.1093/oxfordhb/9780190860509.013.16

de Greef, B. T. A., Hoeijmakers, J. G. J., Gorissen-Brouwers, C. M. L., Geerts, M., Faber, C. G., & Merkies, I. S. J. (2018). Associated conditions in small fiber neuropathy – a large cohort study and review of the literature. *European Journal of Neurology*, *25*(2), 348–355. https://doi.org/10.1111/ene.13508

Devigili, G., Marchi, M., & Lauria, G. (2025). Small fiber neuropathy: expanding diagnosis with unsettled etiology. *Current Opinion in Neurology*, *38*(5), 485–495. https://doi.org/10.1097/WCO.0000000000001418

Devigili, G., Tugnoli, V., Penza, P., Camozzi, F., Lombardi, R., Melli, G., Broglio, L., Granieri, E., & Lauria, G. (2008). The diagnostic criteria for small fibre neuropathy: from symptoms to neuropathology. *Brain*, *131*(7), 1912–1925. https://doi.org/10.1093/brain/awn093

Do, L.-D., Moritz, C. P., Muñiz-Castrillo, S., Pinto, A.-L., Tholance, Y., Brugiere, S., Couté, Y., Stoevesandt, O., Taussig, M. J., Rogemond, V., Vogrig, A., Joubert, B., Ferraud, K., Camdessanché, J.-P., Antoine, J.-C., & Honnorat, J. (2021). Argonaute Autoantibodies as Biomarkers in Autoimmune Neurologic Diseases. *Neurology Neuroimmunology & Neuroinflammation*, *8*(5). https://doi.org/10.1212/NXI.0000000000001032

Esposito, M. F., Malayil, R., Hanes, M., & Deer, T. (2019). Unique Characteristics of the Dorsal Root Ganglion as a Target for Neuromodulation. *Pain Medicine*, *20*(Supplement_1), S23–S30. https://doi.org/10.1093/pm/pnz012

Farah, A., Patel, R., Poplawski, P., Wastie, B. J., Tseng, M., Barry, A. M., Daifallah, O., Dubb, A., Paul, I., Cheng, H. lao, Feroz, F., Su, Y., Chan, M., Zeilhofer, H. U., Price, T. J., Bennett, D. L., Bannister, K., & Dawes, J. M. (2025). A role for leucine-rich, glioma inactivated 1 in regulating pain sensitivity. *Brain*, *148*(3), 1001–1014. https://doi.org/10.1093/brain/awae302

Farhad, K. (2019). Current Diagnosis and Treatment of Painful Small Fiber Neuropathy. *Current Neurology and Neuroscience Reports*, *19*(12), 103. https://doi.org/10.1007/s11910-019-1020-1

Finnerup, N. B., Kuner, R., & Jensen, T. S. (2021). Neuropathic Pain: From Mechanisms to Treatment. *Physiological Reviews*, *101*(1), 259–301. https://doi.org/10.1152/physrev.00045.2019

Fiore, N. T., Debs, S. R., Hayes, J. P., Duffy, S. S., & Moalem-Taylor, G. (2023). Pain-resolving immune mechanisms in neuropathic pain. *Nature Reviews Neurology*. https://doi.org/10.1038/s41582-023-00777-3

Geerts, M., Hoeijmakers, J. G. J., Gorissen-Brouwers, C. M. L., Faber, C. G., & Merkies, I. S. J. (2023). Small Fiber Neuropathy: A Clinical and Practical Approach. *The Journal for Nurse Practitioners*, *19*(4), 104547. https://doi.org/10.1016/j.nurpra.2023.104547

Graus, F., Titulaer, M. J., Balu, R., Benseler, S., Bien, C. G., Cellucci, T., Cortese, I., Dale, R. C., Gelfand, J. M., Geschwind, M., Glaser, C. A., Honnorat, J., Höftberger, R., Iizuka, T., Irani, S. R., Lancaster, E., Leypoldt, F., Prüss, H., Rae-Grant, A., … Dalmau, J. (2016). A clinical approach to diagnosis of autoimmune encephalitis. *The Lancet Neurology*, *15*(4), 391–404. https://doi.org/10.1016/S1474-4422(15)00401-9

Hu, X., An, T., Situ, B., Hu, Y., Ou, Z., Li, Q., He, X., Zhang, Y., Tian, P., Sun, D., Rui, Y., Wang, Q., Ding, D., & Zheng, L. (2020). Heat inactivation of serum interferes with the immunoanalysis of antibodies to SARS-CoV-2. *Journal of Clinical Laboratory Analysis*, *34*(9). https://doi.org/10.1002/jcla.23411

Im, K., Mareninov, S., Diaz, M. F. P., & Yong, W. H. (2019). An Introduction to Performing Immunofluorescence Staining. *Methods in Molecular Biology (Clifton, N.J.)*, *1897*, 299–311. https://doi.org/10.1007/978-1-4939-8935-5_26

Irani, S. R., Alexander, S., Waters, P., Kleopa, K. A., Pettingill, P., Zuliani, L., Peles, E., Buckley, C., Lang, B., & Vincent, A. (2010). Antibodies to Kv1 potassium channel-complex proteins leucine-rich, glioma inactivated 1 protein and contactin-associated protein-2 in limbic encephalitis, Morvan's syndrome and acquired neuromyotonia. *Brain*, *133*(9), 2734–2748. https://doi.org/10.1093/brain/awq213

Jensen, T. S., Karlsson, P., Gylfadottir, S. S., Andersen, S. T., Bennett, D. L., Tankisi, H., Finnerup, N. B., Terkelsen, A. J., Khan, K., Themistocleous, A. C., Kristensen, A. G., Itani, M., Sindrup, S. H., Andersen, H., Charles, M., Feldman, E. L., & Callaghan, B. C. (2021). Painful and non-

painful diabetic neuropathy, diagnostic challenges and implications for future management. *Brain*, *144*(6), 1632–1645. https://doi.org/10.1093/brain/awab079

Ke, X., Cai, H., Chen, Y., & Chen, G. (2025). Exploring the therapeutic potential of TRPC channels in chronic pain: An investigation into their mechanisms, functions, and prospects. *European Journal of Pharmacology*, *987*, 177206. https://doi.org/10.1016/j.ejphar.2024.177206

Kira, J., Zhang, X., Fujii, T., Mitsuishi, M., Ushijima, M., Yoshidomi, S., Sakoda, A., Imamura, T., Kuwabara, S., Isobe, N., & Nakamura, Y. (2025). Nationwide Survey of Atopic Myelitis and Plexin <scp>D1</scp> -Immunoglobulin G-Related Pain. *Annals of Clinical and Translational Neurology*. https://doi.org/10.1002/acn3.70232

Lacagnina, M. J., Willcox, K. F., Boukelmoune, N., Bavencoffe, A., Sankaranarayanan, I., Barratt, D. T., Zuberi, Y. A., Dayani, D., Chavez, M. v., Lu, J. T., Farinotti, A. B., Shiers, S., Barry, A. M., Mwirigi, J. M., Tavares-Ferreira, D., Funk, G. A., Cervantes, A. M., Svensson, C. I., Walters, E. T., … Grace, P. M. (2024). B cells drive neuropathic pain–related behaviors in mice through IgG–Fc gamma receptor signaling. *Science Translational Medicine*, *16*(766). https://doi.org/10.1126/scitranslmed.adj1277

Lang, B., Makuch, M., Moloney, T., Dettmann, I., Mindorf, S., Probst, C., Stoecker, W., Buckley, C., Newton, C. R., Leite, M. I., Maddison, P., Komorowski, L., Adcock, J., Vincent, A., Waters, P., & Irani, S. R. (2017). Intracellular and non-neuronal targets of voltage-gated potassium channel complex antibodies. *Journal of Neurology, Neurosurgery & Psychiatry*, *88*(4), 353–361. https://doi.org/10.1136/jnnp-2016-314758

Lehmann, H. C., Wunderlich, G., Fink, G. R., & Sommer, C. (2020). Diagnosis of peripheral neuropathy. *Neurological Research and Practice*, *2*(1), 20. https://doi.org/10.1186/s42466-020-00064-2

Levine, T. D., Kafaie, J., Zeidman, L. A., Saperstein, D. S., Massaquoi, R., Bland, R. J., & Pestronk, A. (2020). Cryptogenic small-fiber neuropathies: Serum autoantibody binding to trisulfated heparan disaccharide and fibroblast growth factor receptor-3. *Muscle & Nerve*, *61*(4), 512–515. https://doi.org/10.1002/mus.26748

Lister, K. C., Bouchard, S. M., Markova, T., Aternali, A., Denecli, P., Pimentel, S. D., Majeed, M., Austin, J.-S., de C. Williams, A. C., & Mogil, J. S. (2020). Chronic pain produces hypervigilance to predator odor in mice. *Current Biology*, *30*(15), R866–R867. https://doi.org/10.1016/j.cub.2020.06.025

Lobo, P. I. (2016). Role of Natural Autoantibodies and Natural IgM Anti-Leucocyte Autoantibodies in Health and Disease. *Frontiers in Immunology*, *7*. https://doi.org/10.3389/fimmu.2016.00198

Luchino, J., Hocine, M., Amoureux, M.-C., Gibert, B., Bernet, A., Royet, A., Treilleux, I., Lécine, P., Borg, J.-P., Mehlen, P., Chauvet, S., & Mann, F. (2013). Semaphorin 3E Suppresses Tumor Cell Death Triggered by the Plexin D1 Dependence Receptor in Metastatic Breast Cancers. *Cancer Cell*, *24*(5), 673–685. https://doi.org/10.1016/j.ccr.2013.09.010

Malik, A., Lopate, G., Hayat, G., Jones, J., Atluri, R., Malo, B., & Pestronk, A. (2019). Prevalence of Axonal Sensory Neuropathy With IgM Binding to Trisulfated Heparin Disaccharide in Patients With Fibromyalgia. *Journal of Clinical Neuromuscular Disease*, *20*(3), 103–110. https://doi.org/10.1097/CND.0000000000000236

Martin, L., Stratton, H. J., Gomez, K., le Duy, D., Loya-Lopez, S., Tang, C., Calderon-Rivera, A., Ran, D., Nunna, V., Bellampalli, S. S., François-Moutal, L., Dumaire, N., Salih, L., Luo, S., Porreca, F., Ibrahim, M., Rogemond, V., Honnorat, J., Khanna, R., & Moutal, A. (2024). Mechanism, and treatment of anti-CV2/CRMP5 autoimmune pain. *BioRxiv : The Preprint Server for Biology*. https://doi.org/10.1101/2024.05.04.592533

Meacham, K., Shepherd, A., Mohapatra, D. P., & Haroutounian, S. (2017). Neuropathic Pain: Central vs. Peripheral Mechanisms. *Current Pain and Headache Reports*, *21*(6), 28. https://doi.org/10.1007/s11916-017-0629-5

Mischkowski, D., Palacios-Barrios, E. E., Banker, L., Dildine, T. C., & Atlas, L. Y. (2018). Pain or nociception? Subjective experience mediates the effects of acute noxious heat on autonomic responses. *Pain*, *159*(4), 699–711. https://doi.org/10.1097/j.pain.0000000000001132

Morelli, L., Serra, L., Ricciardiello, F., Gligora, I., Donadio, V., Caprini, M., Liguori, R., & Giannoccaro, M. P. (2024). The role of antibodies in small fiber neuropathy: a review of currently available evidence. *Reviews in the Neurosciences*, *35*(8), 877–893. https://doi.org/10.1515/revneuro-2024-0027

Murin, P. J., Massabki, I., & Kafaie, J. (2024). Anti–Plexin-D1 Seropositive Small Fiber Neuropathy: Clinical Phenotype, Demographics, and Literature Review. *Journal of Clinical Neuromuscular Disease*, *25*(3), 132–140. https://doi.org/10.1097/CND.0000000000000472

Nagarajan, E., Kang, S. A., Holmes, C., & Govindarajan, R. (2021). Clinical features with anti fibroblast growth factor receptor 3 (FGFR3) antibody-related polyneuropathy: a retrospective study. *BMC Neurology*, *21*(1), 74. https://doi.org/10.1186/s12883-021-02090-2

Nolano, M., Manganelli, F., Provitera, V., Pisciotta, C., Stancanelli, A., Caporaso, G., Iodice, R., Shy, M. E., & Santoro, L. (2015). Small nerve fiber involvement in CMT1A. *Neurology*, *84*(4), 407–414. https://doi.org/10.1212/WNL.0000000000001188

Obaid, A. H., Zografou, C., Vadysirisack, D. D., Munro-Sheldon, B., Fichtner, M. L., Roy, B., Philbrick, W. M., Bennett, J. L., Nowak, R. J., & O'Connor, K. C. (2021). *Heterogeneity of acetylcholine receptor autoantibody-mediated complement activity in patients with myasthenia gravis*. https://doi.org/10.1101/2021.10.05.21264566

Parisien, M., Lima, L. v., Dagostino, C., El-Hachem, N., Drury, G. L., Grant, A. v., Huising, J., Verma, V., Meloto, C. B., Silva, J. R., Dutra, G. G. S., Markova, T., Dang, H., Tessier, P. A., Slade, G. D., Nackley, A. G., Ghasemlou, N., Mogil, J. S., Allegri, M., & Diatchenko, L. (2022). Acute inflammatory response via neutrophil activation protects against the development of chronic pain. *Science Translational Medicine*, *14*(644). https://doi.org/10.1126/scitranslmed.abj9954

Pascal, M. M. V., Themistocleous, A. C., Baron, R., Binder, A., Bouhassira, D., Crombez, G., Finnerup, N. B., Gierthmühlen, J., Granovsky, Y., Groop, L., Hebert, H. L., Jensen, T. S., Johnsen, K., McCarthy, M. I., Meng, W., Palmer, C. N. A., Rice, A. S. C., Serra, J., Solà, R., … Bennett, D. L. H. (2018). DOLORisk: study protocol for a multi-centre observational study to understand the risk factors and determinants of neuropathic pain. *Wellcome Open Research*, *3*, 63. https://doi.org/10.12688/wellcomeopenres.14576.1

Raasing, L., Veltkamp, M., Datema, M., Korenromp, I., Grutters, J. C., & Vogels, O. J. M. (2025). Sarcoidosis-related small fiber neuropathy: Focus on fatigue, pain, restless legs syndrome, and cognitive function. *Sarcoidosis, Vasculitis, and Diffuse Lung Diseases: Official Journal of WASOG*, *42*(1), 16214. https://doi.org/10.36141/svdld.v42i1.16214

Salih, L. Y., Dumaire, N. la, Gieré, C., Vest, E., Alkhateeb, H., Moritz, C. P., Tholance, Y., Camdessanché, J.-P., Antoine, J.-C., Honnorat, J., Kafaie, J., François-Moutal, L., & Moutal, A. (2025). Pathogenic Role of FGFR3 Autoantibodies in Small Fiber Neuropathy. *bioRxiv*. https://doi.org/10.1101/2025.06.01.657230

Sanmarco, L. M., Polonio, C. M., Wheeler, M. A., & Quintana, F. J. (2021). Functional immune cell–astrocyte interactions. *Journal of Experimental Medicine*, *218*(9). https://doi.org/10.1084/jem.20202715

Seefried, S., Barcic, A., Grijalva Yepez, M. F., Reinhardt, L., Appeltshauser, L., Doppler, K., Üçeyler, N., & Sommer, C. (2025). Autoantibodies in patients with fibromyalgia syndrome. *Pain*, *166*(8), 1922–1933. https://doi.org/10.1097/j.pain.0000000000003535

Seeliger, T., Dreyer, H. N., Siemer, J. M., Bönig, L., Gingele, S., Dohrn, M. F., Prenzler, N., Ernst, D., Witte, T., & Skripuletz, T. (2023). Clinical and paraclinical features of small fiber neuropathy in Sjögren's syndrome. *Journal of Neurology*, *270*(2), 1004–1010. https://doi.org/10.1007/s00415-022-11431-1

Siracusa, R., Paola, R. di, Cuzzocrea, S., & Impellizzeri, D. (2021). Fibromyalgia: Pathogenesis, Mechanisms, Diagnosis and Treatment Options Update. *International Journal of Molecular Sciences*, *22*(8). https://doi.org/10.3390/ijms22083891

Sneddon, L. U. (2018). Comparative Physiology of Nociception and Pain. *Physiology*, *33*(1), 63–73. https://doi.org/10.1152/physiol.00022.2017

Soleimani, B., Board, C., Yu, T., Tracey, I., Irani, S. R., & Foley, P. (2023). Immunotherapy-Responsive Neuropathic Pain and Allodynia in a Patient With Glycine Receptor Autoantibodies. *Neurology Neuroimmunology & Neuroinflammation*, *10*(6). https://doi.org/10.1212/NXI.0000000000200160

Terkelsen, A. J., Karlsson, P., Lauria, G., Freeman, R., Finnerup, N. B., & Jensen, T. S. (2017). The diagnostic challenge of small fibre neuropathy: clinical presentations, evaluations, and causes. *The Lancet Neurology*, *16*(11), 934–944. https://doi.org/10.1016/S1474-4422(17)30329-0

Tholance, Y., Moritz, C. P., Rosier, C., Ferraud, K., Lassablière, F., Reynaud-Federspiel, E., França Jr, M. C., Martinez, A. R. M., Camdessanché, J.-P., & Antoine, J.-C. (2020). Clinical characterisation of sensory neuropathy with anti-FGFR3 autoantibodies. *Journal of Neurology, Neurosurgery & Psychiatry*, *91*(1), 49–57. https://doi.org/10.1136/jnnp-2019-321849

Thouaye, M., & Yalcin, I. (2023). Neuropathic pain: From actual pharmacological treatments to new therapeutic horizons. *Pharmacology & Therapeutics*, *251*, 108546. https://doi.org/10.1016/j.pharmthera.2023.108546

van de Mortel, J. P. M., Budding, K., Dijkxhoorn, K., Minnema, M. C., Vrancken, A. F. J. E., Notermans, N. C., van der Pol, W. L., Attarian, S., Basta, I., van den Bergh, P. Y. K., Bianco, M., Briani, C., Cauquil, C., Carr, A. S., Cornblath, D. R., Cutellè, C., D'Sa, S., Delmont, E., van Doormaal, P. T. C., … Thomas, S. (2025). The Role of Complement Activation in IgM M-Protein–Associated Neuropathies. *Neurology Neuroimmunology & Neuroinflammation*, *12*(1). https://doi.org/10.1212/NXI.0000000000200339

van Gorkom, T., van Arkel, G. H. J., Voet, W., Thijsen, S. F. T., & Kremer, K. (2021). Consequences of the Edge Effect in a Commercial Enzyme-Linked Immunosorbent Assay for the Diagnosis of Lyme Neuroborreliosis. *Journal of Clinical Microbiology*, *59*(8). https://doi.org/10.1128/JCM.03280-20

van Hecke, O., Austin, S. K., Khan, R. A., Smith, B. H., & Torrance, N. (2014). Neuropathic pain in the general population: A systematic review of epidemiological studies. *Pain*, *155*(4), 654–662. https://doi.org/10.1016/j.pain.2013.11.013

Wolfe, F., & Rasker, J. J. (2021). The Evolution of Fibromyalgia, Its Concepts, and Criteria. *Cureus*. https://doi.org/10.7759/cureus.20010

Woodhall, M., Mgbachi, V., Fox, H., Irani, S., & Waters, P. (2022). Utility of Live Cell-Based Assays for Autoimmune Neurology Diagnostics. *The Journal of Applied Laboratory Medicine*, *7*(1), 391–393. https://doi.org/10.1093/jalm/jfab133

Zeidman, L. A., Levine, T., & Cangelosi, J. (2024). Small-Vessel Vasculitis or Perifolliculitis in Small-Fiber Neuropathy With TS-HDS, FGFR-3, or Plexin D1 Antibodies. *Journal of Clinical Neuromuscular Disease*, *26*(2), 63–69. https://doi.org/10.1097/CND.0000000000000492